ACTIVATION OF GASES BY ELECTRON COLLISION
FOR
REACTION WITH CARBON

A Thesis submitted for the degree of

DOCTOR OF PHILOSOPHY

in the Faculty of Science

of the

University of London

by

DENNIS KEITH WICKENDEN, B.Sc.

Department of Chemical Engineering and Chemical Technology,
Imperial College of Science and Technology,
London S.W.7

August, 1965.

ABSTRACT

A study has been made of the radiation induced reactions in the systems CO_2/carbon and CO/carbon at low pressures using low voltage electrons emitted from an oxide coated cathode. It has been shown that in the absence of radiation CO_2 is reduced to CO both by reaction with the free metal in the oxide surface and by its thermal decomposition on striking the heated cathode. Using constant currents in a static system of CO, it has been shown that the threshold energy of the electrons required to promote decomposition of CO is approximately 14 eV. in the presence of carbon and approximately 25 eV. in its absence. The upper threshold has been confirmed by experiments performed in flowing CO, where it was found that the currents obtainable from the cathode were significantly greater when decomposition occurred than when it did not. It is concluded from these results that CO decomposes by an ionic mechanism which can be catalysed by a carbon surface. Using a carbon-14 tracer technique, it has been shown that the primary radiolysis product responsible for carbon gasification in the CO_2/carbon system is electrically neutral and that only a slight increase in gasification rate is observed when positive ions are present. It has been shown that these species are present mainly in the region of the glow discharge produced by the electrons. Spectroscopic studies of this discharge tend to favour an excited

form of CO_2 as being the neutral species responsible for gasification. When comparing the results obtained with sooty carbon and pyrolytic carbon it is apparent that sooty carbon gives rise to much greater electrical currents and carbon gasification rates. Differences in experimental conditions would explain some of the discrepancy but it is probable that sooty carbon is fundamentally more reactive and that this increased reactivity leads to the greater currents.

ACKNOWLEDGEMENTS

The author would like to express his special thanks to Dr. R. F. Strickland-Constable for his invaluable guidance throughout this research, and to thank Professor K. G. Denbigh, in whose department this work was carried out.

This research was made possible by the generous financial support provided by the United Kingdom Atomic Energy Authority at Harwell. The author is very much obliged to the Chemistry Division of this group, and in particular to Mr. J. Wright, with whom useful discussions have been held and to Mr. R. S. Sach, who kindly prepared the carbon-14 samples employed in this research.

CONTENTS

TITLE 1

ABSTRACT 2

ACKNOWLEDGEMENTS 4

CONTENTS 5

CHAPTER 1 - GENERAL INTRODUCTION 9

CHAPTER 2 - REVIEW OF EXISTING KNOWLEDGE IN THIS FIELD

A. Radio-chemical reactions in pure CO_2

2.1 Ionisation processes 14

2.2 Radical formation 17

2.5 Overall effect of radiation on CO_2 18

B. Radio-chemical reactions in pure CO

2.4 Ionisation processes 22

2.5 Radical formation 23

2.6 Overall effect of radiation on CO 24

C. Radiation induced reactions in the system CO_2/CO/C

2.7 General summary 26

CHAPTER 3 - APPARATUS AND SUMMARY OF CLAXTON'S RESULTS

3.1 General description of the apparatus 33

3.2 Summary of Claxton's studies 39

3.3 Carbon weight loss 39

3.4 Protective effect of carbon upon an oxide cathode . 41

3.4 Static charges of CO and CO_2 42

CHAPTER 4 - STATIC EXPERIMENTS WITH CARBON DI-OXIDE

4.1 Introduction 43

4.2 Experimental procedure 44

4.3 Results and discussion 46

4.4 Thermal reactions with filament 52

4.5 Weight-loss experiments 56

4.6 Temperature of carbon surface 58

4.7 Summary 61

CHAPTER 5 - EXPERIMENTS WITH CARBON MONOXIDE

A. Static experiments

5.1 Introduction 63

5.2 Experimental procedure 64

5.3 Results 68

5.4 Conclusions from static runs 73

B. Flow experiments

5.5 Experimental procedure 73

5.6 Results 76

5.7 Discussion of results 79

5.8 Summary 86

CHAPTER 6 - SPECTROSCOPIC STUDY OF THE GLOW DISCHARGE

6.1 Introduction 87

6.2 Experimental procedure and results 87

CHAPTER 7 - CARBON-14 TRACER TECHNIQUES

7.1 Introduction 95
7.2 Internal Geiger counting technique 98
7.3 Gas scintillation technique 104

CHAPTER 8 - EXPERIMENTS WITH CARBON-14

A. Carbon-14 on silica

8.1 Carbon-14 sample 113
8.2.1 Static experiments at 0, 15, and 20 volts 113
8.2.2 Results 114
8.3 Effect of geometry 117
8.4 Effect of surface condition 118
8.5.1 Flow experiments at 25 volts 120
8.5.2 Results 121
8.6 Distribution of carbon-14 in the gas phase 126
8.7 Summary 129

B. Carbon-14 on molybdenum

8.8 Carbon-14 sample 130
8.9.1 Flow experiments 130
8.9.2 Results 132
8.10 Summary 138
8.11 Comparison of carbon-14 and carbon soot results . . 139

CHAPTER 9 - GENERAL SUMMARY

9.1 Experimental results 144
9.2 Application to reactor conditions 146

APPENDICES

A. EXPERIMENTAL RESULTS 153

B. Rate of reaction $CO_2 = CO + O$ on striking the heated filament 174

C. References cited in the text 176

CHAPTER 1

GENERAL INTRODUCTION

In the pressure-vessel design of nuclear reactor adopted in the early stages of the British nuclear power programme graphite was chosen as the neutron moderator and carbon dioxide as the coolant gas. Graphite is an attractive material for use in nuclear reactors because of its favourable nuclear properties, its ease of manufacture into the shapes and sizes required and in a relatively pure state, and its good mechanical properties which improve with temperature and enable it to serve as a structural material as well as a moderator. Carbon dioxide was chosen as the coolant gas since it is readily available in a pure form, has a low neutron capture cross-section and physical properties which confer good heat-transfer and pumping characteristics.

In the early reactors the coolant gas is in contact with the graphite and must therefore be compatible with it, producing no deleterious effects within the projected life of the reactor. In the absence of radiation carbon dioxide does not react with graphite to a significant extent at temperatures below 650°C. However, it does react with graphite under the influence of radiation and therefore the use of carbon dioxide as a coolant sets limits to the temperature, pressure and power density at which a reactor may be operated. Much research has been carried out on the radiation induced reactions occurring in the $CO_2/CO/C$ systems to determine the limits of these parameters in order that the behaviour of new reactors may be reliably predicted by extrapolation of the results obtained from those already in existence.

Basically, two requirements are necessary for the extrapolation of the results:

1) a knowledge of the effects of the parameters for which extrapolations are required, and
2) a quantitative understanding of the radiolytic processes taking place in the $CO_2/CO/C$ system.

The first requirement has motivated most of the work performed in in-pile experiments. Data from experiments performed in the Harwell reactor B.E.P.O. have shown that the radiation induced reaction between carbon dioxide and graphite may be interpreted in terms of the decomposition of the carbon dioxide in the gas phase producing active species which are carried downstream to where they can react with the graphite surface to produce carbon monoxide. In view of the known stability of pure carbon dioxide under reactor radiation it was concluded that the graphite acts as an inhibitor of recombination processes and also as a vehicle for attack by the chemically active species produced by the radiolysis.

In any reaction between a solid and a gas the accessibility of the solid surface to the gas is important and for graphite there are two features of special relevance:

i) graphite has a much greater surface area in its pores than it has superficially, so that the gas within the pores has better access to a carbon surface than has the gas in the larger spaces outside the bulk;

ii) the reaction between the graphite surface and the chemically active species produced in the radiolysis is not controlled by the transport of normal carbon dioxide molecules to the interior of the bulk as is required in the high temperature thermal oxidation.

The importance of this pore reaction rules out the possibility of obtaining quantitative information on the basic radiolytic processes from the in-pile experiments owing to the difficulty in controlling the conditions inside the pores. An additional complication in in-pile experiments is the complex nature of the reactor radiation which is made up of neutrons, electrons and gamma-rays, each having a complex energy spectrum ranging from zero to several Mev. These high energies result in the formation of all possible excited and ionised species in the radiolysis of the carbon dioxide and carbon monoxide and makes the identification of those responsible for the carbon gasification impossible. In order that the basic kinetics of the reactions occurring may be elucidated laboratory experiments have to be performed in which the energy and flux of the incident radiation may be carefully controlled at values comparable with the primary excitation and ionisation potentials of carbon dioxide and carbon monoxide. For these experiments two types of low-energy radiation may be used - either vacuum ultra-violet photons or low energy electrons.

The present work has served to further develop apparatus in which gases at low pressures can be bombarded by electrons emitted from an oxide coated cathode and accelerated to energies in the range of 10 to 40 electron-volts. A carbon-14 tracer technique has been developed whereby the gasification of very small amounts of carbon by the excited gas may be measured easily and accurately.

These studies are intended to elucidate some of the basic processes which occur in the radiation induced reaction between carbon dioxide and graphite. In particular it is intended to assess the relative importance of ionic and neutral excited species in the reaction mechanism. The effect of using low pressures is to increase the lifetime of the active species and to reduce the effect of secondary processes occurring in the gas phase. It is interesting to note that the product of pressure and radius of the carbon sample is of the same order of magnitude for the system used in this work and that occurring in the pores of a graphite sample in a reactor ; this means that the results obtained here may be more readily applied to the conditions of a nuclear reactor.

CHAPTER 2

REVIEW OF EXISTING KNOWLEDGE IN THIS FIELD

A. Radio chemical reactions in pure CO_2.

2.1. Ionisation processes.

The first ionisation potential of CO_2 has been studied by various workers using the well established electron or photon impact or spectrographic techniques. A summary of the results obtained by them is shown in Table I.

TABLE I

First Ionisation Potential of CO_2

Method	Ionisation Potential (eV)	Reference
Electron impact	14.4	1
" "	13.9 ± 0.1	2
" "	13.85 ± 0.01	3
" "	13.88 ± 0.03	4
" "	13.78	5
Photon impact	14.0 ± 0.3	6
" "	13.6 ± 0.2	7
Spectroscopic	13.79 ± 0.06	8
"	14.4	9
"	13.78	10

From these results it can be concluded that the first ionisation potential of CO_2 is 13.8 ± 0.1 eV.

Higher ionisation potentials for CO_2, corresponding to different electronic energy levels of the $CO_2{}^+$ ion, have been reported by workers using vacuum ultra-violet absorption[10,11] or direct photo-ionisation[7] methods. The results are essentially in agreement with each other and give values of 17.1, 18.1 and 19.4 eV.

The appearance potentials of other ion fragments have been measured by Smyth and Stueckelberg[1], Kallmann and Rosen[12] and Kambara[2] using different types of mass-spectrometers. The results of these workers are summarised in Table II and can be seen to be in agreement with each other.

TABLE II

Appearance potentials of ion fragments in CO_2

	Product	Ref 1.	Ref 12.	Ref 2.	Calculated Min. Energy
1.	CO_2^+	14	(14.4)	13.9 ± 0.1	--
2.	O^+	17	19.6 ± 0.4	20.3 ± 0.2	19.0
3.	CO^+	18	20.4 ± 0.7	20.5 ± 0.2	19.7
4.	C^+	29.	28.3 ± 1.5	26.6 ± 0.2	26.6
5.	O_2^+	--	20.0 ± 1.0	--	18.7

The values of the minimum energy given in the last column of Table II were calculated by Smyth from the heats of dissociation and ionisation potentials relevant to the process.

The presence of the O_2^+ ion, reported by Smyth and Stueckelberg, was observed at higher pressures only and was attributed to a secondary reaction between ionised and neutral CO_2 : i.e. $CO_2^+ + CO_2 = 2CO + O_2^+$. The relative abundances of the ions varied with the gas pressure in their ionisation tube but, at a pressure of 0.8 uHg and with an accelerating voltage of 40 V, the ratios of $CO_2^+ : CO^+ : O^+ : C^+$ were found to be 100:20:7:3. Similar values were obtained in more recent studies by Hayawaka and Suguira[13] and by Lorquet[14]. The latter's values of 100 : 8 : 6.5 : 4 compared favourably with the theoretical values of 100 : 5.5 : 6.5 : 4 computed from known data on the ionisation cross-sections.

Smyth and Stueckelberg also observed that, at CO_2 pressures greater than 5 µHg, the intensity of the CO^+ ion decreased with increasing CO_2 pressure. They attributed this phenomenon to the ion-exchange reaction $CO^+ + CO_2 \rightarrow CO_2^+ + C$ - a reaction now known to be 80% efficient.

Kambara obtained similar results for the appearance of the O_2^+ ion at higher pressures and found that, while the relative abundances of the ions was constant at low pressures, at high pressures the ratios of CO^+, O^+ and C^+ to CO_2^+ increased.

2.2. Radical Formation

The ultra-violet absorption spectrum of CO_2 has been studied by Leifson[15] and by Lyman[16]. From the data collected Bonhoffer and Harteck[17] were able to conclude that the observed continuous absorption spectrum corresponded to a dissociation of CO_2 into neutral CO and a normal oxygen atom occurring at 2250 A° or 5.5 eV. This value of 5.5 eV has been confirmed by Gaydon who employed a calculation based on thermo-chemical data together with a spectroscopically determined value for the heat of dissociation of CO. For the complete dissociation of CO_2 into one carbon and two oxygen atoms he obtained a value of 16.5 eV.

Measurements of the absorption spectrum of CO_2 in the vacuum ultra-violet by Inn et al.[19] enabled values to be computed for the upper limits of the energy necessary for the dissociation of CO_2 into excited radicals. These values are given in Table III together with values cited by Weekes[20] from other spectral data.

TABLE III

Appearance potentials of various radical products

	Products	Energy[19] (eV)	Energy[20] (eV)
1)	$CO('\Sigma) + O(^3P)$	6.8	5.4
2)	$CO('\Sigma) + O(^1D)$	7.7	7.4
3)	$CO('\Sigma) + C(^1S)$	10.3	9.7

TABLE III (continued)

	Products	Energy[19] (eV)	Energy[20] (eV)
4)	$CO(a\,^3\Pi) + O(^3P)$	--	11.4
5)	$CO(d\,^3\Pi) + O(^3P)$	--	13.1

Since the ground state of the CO_2 molecule is a singlet state $(^1\Sigma)$, process 1) cannot take place directly due to spin conservation rules. Wilde et al.[21] suggest that an intermediate excited state of CO_2 is involved and that it is probably the $CO_2(^3\Pi)$ state predicted earlier by Mulliken[22]. They suggest also that the formation of $O(^1D)$ goes via the intermediary of an excited $CO_2(^1\Pi)$ state. The $CO_2(^1\Sigma) \rightarrow CO_2(^3\Pi) \rightarrow CO(^1\Sigma) + O(^3P)$ reaction has been postulated also by Brabbs et al.[23] in their study of the dissociation of CO_2 induced by shockwaves.

2.3. Overall Effect of Radiation on CO_2

The behaviour of pure CO_2 when subjected to radiation bombardment depends on the nature of the radiation and the dose rate involved. When subjected to electrical discharges, vacuum ultra-violet bombardment or high dose-rate reactor (high-energy) radiation it decomposes to form carbon monoxide and oxygen but when subjected to low dose-rates of high energy radiation it is apparently stable.

In vacuum ultra-violet radiation studies Groth[24] found the quantum yield of CO at 1470 A° to be near unity and suggested that oxygen atoms are formed in the primary process. Jucker and Rideal[25] stated, however, that the quantum yield was close to two and that no oxygen atoms are involved in the photolysis of CO_2. They proposed that the carbon monoxide and oxygen are formed by the reaction $CO_2^* + CO_2 \rightarrow 2CO + O_2$. To resolve these differences Mahan[26] repeated the experiment. He rigourously excluded mercury from his system since a mercury photosensitised reaction could promote decomposition by a stepwise accumulation of energy in CO_2 such as:

$$Hg + h\nu \rightarrow Hg^*$$

$$Hg^* + CO_2 \rightarrow CO_2^* + Hg$$

$$CO_2^* + Hg^* \rightarrow CO + O + Hg$$

Mahan found that oxygen atoms appear as a primary product with unit quantum efficiency, thus confirming Groth's value. Mahan concluded also that the oxygen atoms involved were electronically excited, possibly to the $O(^1D)$ state, since he could not detect $O(^3P)$ atoms by the chemi-luminescent reaction with nitric oxide.

The decomposition of CO_2 into carbon monoxide and oxygen proceeds rapidly when subjected to electrical discharges induced by micro-wave generators or radio-frequency arcs. In such discharges excited forms of CO_2,

CO_2^+, CO, CO^+, C, C^+ and O have been identified definitely by spectrographic analysis and, therefore, it is unreasonable to exclude any possible product from the reaction analysis. Working with a radio-frequency arc, Wilde et al.[21] found that the CO and O_2 yields decreased exponentially with increasing flow rate, increased linearly with current but depended little on pressure. They were able to explain the dependence of the yields on the pressure and current by proposing the following reaction scheme:-

$$CO_2 \rightsquigarrow CO + O \text{ and } O^*$$
$$CO_2 \rightsquigarrow CO_2^+ + e^-$$
$$CO_2^+ + e^- \longrightarrow CO + O \text{ and } O^*$$
$$CO + O^* \longrightarrow CO_2$$
$$CO + O \longrightarrow CO_2^* \longrightarrow CO_2 + hv$$
$$CO_2 + O^* \longrightarrow CO + O_2$$
$$O + O^* \longrightarrow O_2^* \longrightarrow O_2 + hv$$
$$O + O \longrightarrow O_2$$

At low dose-rates pure CO_2 is stable when bombarded with x-rays, γ-rays or reactor radiation although in the presence of traces of oxygen acceptors such as sulfur dioxide, nitrogen dioxide or mercury it decomposes readily to form carbon monoxide and oxygen. Therefore this apparent stability is almost certainly due to a very rapid recombination of the primary radiolysis products, but the exact nature of the recombination process remains in doubt.

Hirschfelder and Taylor[27], from a survey of then existing data on the decomposition of CO_2, the oxidation of CO and the formation of ozone, concluded that the back reaction was due to the oxidation of CO by ozone. However, Harteck and Dondes[28] have shown that the reaction $CO + O_3 \longrightarrow CO_2 + O_2$ requires an activation energy of approximately 22 k cals/mole. They proposed a new reaction mechanism making use of a chain reaction involving carbon atoms and the carbon sub-oxides C_2O and C_3O_2. There is no direct evidence for the presence of these molecules in the radiolysis of CO_2 and polymeric solids, which would be expected to be formed when these sub-oxides are present, have been reported only in systems containing an appreciable amount of CO. In addition Sutton et al[30] have shown that C_3O_2 actually increases the rate of formation of CO.

More recently, Dominey[31] while working on the exchange of carbon-14 between ^{14}CO and $^{12}CO_2$ has attempted to explain the apparent stability of CO_2 in terms of both ionic and excited species while Anbar[32a] has suggested that CO_3 may be an important intermediate in the recombination process. The CO_3 hypothesis has received further support from the recent experimental evidence of Warneck[32b] working on the photolysis of CO_2 by vacuum ultra-violet radiation.

B. Radio-chemical reactions in pure CO

2.4. Ionisation processes

The appearance potentials of the possible ion fragments in CO have been the object of study by various workers for many years in an attempt to find a decisive value for the dissociation energy of CO. The results of the four most recent determinations are summarised in Table IV.

TABLE IV

Appearance potentials of ion fragments in CO

Product	Ref 33	Ref 34	Ref 35	Ref 36
1. CO^+	14.1 ± 0.1	--	14.10	14.01
2. C^+	20.9 ± 0.2	20.9 ± 0.2	20.95 ± 0.05	20.89 ± 0.09
3.	22.8 ± 0.2	22.8 ± 0.2	22.69 ± 0.05	22.57 ± 0.20
4. C^-	--	--	23.65 ± 0.10	22.97 ± 0.05
5. O^+	23.3 ± 0.2	23.2 ± 0.3	23.7 ± 0.2	23.41 ± 0.17
6.	--	--	25.8 ± 0.2	24.78 ± 0.17
7. O^-	9.5 ± 0.2	9.6 ± 0.2	9.5 ± 0.2	9.39 ± 0.05
8.	20.9 ± 0.2	21.1 ± 0.2	20.95 ± 0.05	20.92 ± 0.05

Fineman and Petrocelli[36] identified the dissociation products as follows:-

7 $CO \rightsquigarrow C(^3P) + O^-(^2P)$ at 9.4 eV

1 $\rightsquigarrow CO^+ + e$ at 14.1 eV

2 and 8 $\rightsquigarrow C^+(^2P) + O^-(^2P)$ at 20.9 eV

3	$\rightsquigarrow C^+(^2P) + O(^3P) + e$	at	22.6 eV
4 and 5	$\rightsquigarrow C^-(^4S) + O^+(^4S)$	at	23.6 eV
6a	$\rightsquigarrow C(^3P) + O^+(^4S)$	at	24.8 eV
6b	$\rightsquigarrow C(^1D) + O^+(^4S)$	at	25.8 eV

Hayawaka and Suguira[13] found the relative abundance of the ions CO$^+$, C$^+$ and O$^+$ to be 100, 5.5 and 3. Lorquet[14] found the relative abundances to be 94 : 4 : 2 which were in relatively good agreement with the theoretically determined values of 89 : 9 : 3.

Using a direct photo-ionisation method Weissler et al.[7] observed higher appearance potentials of the CO$^+$ ion at 16.6, 18.4, 20.1 and 25.7 eV which are in good agreement with spectroscopic measurements.

2.5. Radical Formation

The dissociation energy of CO and the latent heat of sublimation of carbon have been frequently investigated in an effort to evaluate them accurately. If a reliable determination of one is made the other follows through a relationship involving the standard heat of formation of CO.

Values for the dissociation energy of CO ranging from 6.92 to 11.11 eV have been proposed to explain the data collected from various studies. Gaydon[37] strongly criticised the electron impact work and from spectroscopic data deduced that 11.11 eV was the correct value for the dissociation energy.

In fact, electron impact data failed to yield a decisive value for the dissociation energy, D(CO), prior to 1958. Hagstrum[37] originally concluded from his data that D(CO) was 9.60 eV, but this result depended on the existence of an excited state of the O^- ion of about the same energy as the electron affinity of oxygen, EA(O). In 1955, Branscomb and Smith[38] published an accurate determination of the electron affinity of oxygen atoms of 1.45 ± 0.10 eV and found no evidence of stable excited states of O^- by the photo-detachment of electrons from O_2^- ions. In 1958, Hagstrum[39] demonstrated that his data could be explained using D(CO) of 11.11 eV and EA(O) of 1.45 eV without using his previous assumption of an excited O^- ion. Since then Lagergren[35] and Fineman and Petrocelli[36] have shown that their results support these values and thus it is fairly certain that the dissociation energy of carbon monoxide into normal carbon and oxygen atoms is 11.11 eV.

2.6. Overall effect of radiation on pure CO

Unlike CO_2, carbon monoxide is readily decomposed by all energetic radiation and the ultimate product of the decomposition is a brown or black solid.

Working with α-radiation Cameron and Ramsey[40] and Lind and Bardwell[41] described two solids, a black one which settled on the bottom of the reaction vessel and brownish yellow film which distributed itself evenly over the walls of the reaction vessel. On heating these solids in vacuo CO_2 and CO were formed and if the solids were re-irradiated in the presence of CO_2 they rapidly disappeared with the formation of CO. From stoichlometric considerations Lind and Bardwell proposed an initial reaction scheme of

$$6CO \rightsquigarrow 2CO_2 + C + C_3O_2$$

suggesting that the carbon would fall to the bottom of the reaction vessel and that carbon sub-oxide would polymerise on the walls.

In recent experiments in the Harwell reactor D.I.D.O. Marsh has followed the radiolysis of CO to 75% completion and the empirical formula for the solid has been found to be $C_{1.9}O$. This suggests that the reaction scheme is best fitted by the empirical equation

$$3CO \rightsquigarrow CO_2 + C_2O \ .$$

The addition of metals such as Au, Pt or of colloidal graphite to act as possible scavengers of oxygen atoms had little effect on the rate of CO decomposition. The physical appearance and distribution of the deposits were, however, different and the solid was no longer particulate. In the presence of graphite the gas composition changed towards a constant CO : CO_2 ratio depending on the gas pressure and geometrical arrangement used. The empirical formula of the solid varied from C_3O_2 at room temperature to C_3O at 350° C.

Rudolph and Lind[63] concluded from the x-radiolysis of carbon monoxide that both CO* and CO^+ are concerned when pure carbon monoxide is used but that with CO/CO_2 mixtures the CO^+ ion is de-activated by the reaction $CO^+ + CO_2 = CO_2^+ + CO$ and only CO* reacts. They suggested the following fates for the ions detected by mass spectrometry:

$$CO^+ + CO \longrightarrow CO_2^+ + C$$
$$O^+ + CO \longrightarrow CO_2^+$$
$$C^+ + CO \longrightarrow C_2O^+ \longrightarrow C_3O_2^+ \longrightarrow \text{solids}$$

C. Radiation Induced Reactions in the System $CO_2/CO/C$

2.7. General summary

From the studies of the decomposition of pure CO_2 under radiation bombardment it would seem easy to conclude what would happen when carbon is added to the system. As when other oxygen acceptors, such as mercury, are added the CO_2 should decompose to form carbon monoxide and the carbon should be oxidised to form further carbon monoxide. If the carbon monoxide builds up to a sufficiently high level it would be expected to decompose also, with the formation of carbon rich solid polymers. These general conclusions have been confirmed experimentally but the results obtained have shown that the precise nature of the reactions is far more complicated and is not fully understood. Much work has been undertaken at Harwell and elsewhere in an attempt to gather information on the reaction mechanism and in particular on the nature of the chemically active species which causes the gasification of the solid carbon. Thorough reviews of the experimental results and of the ideas on the reaction mechanisms involved have been presented in 1958[43], 1960[44] and 1963[45] and will be dealt with rather briefly here.

Since the problem is directly concerned with the compatibility of carbon and CO_2 under reactor conditions many of the experiments have been performed in pile at Harwell, where the radiation consists mainly of fast neutrons. Under these conditions the energy absorbed by an atom is a function of its atomic number but dosiometric studies have shown that the rates of energy absorption by carbon and oxygen atoms are approximately equal and, therefore, that the energy absorbed per unit mass is the same for CO_2, CO and carbon.

In a gas-cooled reactor the mass of the graphite moderator greatly exceeds the mass of the CO_2 coolant and therefore the majority of the energy is absorbed in the solid phase. The results obtained by Davidge and Marsh[46] have shown that the energy absorbed in the gas phase is the more important in the radiation induced reaction. In their apparatus the gas was circulated over a graphite specimen contained in a temperature controlled furnace in the core of a reactor. A large silica vessel was incorporated in the system close to the graphite specimen so that the volume of gas irradiated before reaching the graphite depended on the direction of flow. They found that the rate of CO formation was considerably greater when the large volume was upstream of the graphite than when it was downstream.

Copestake and Corney[47] have performed an extensive series of sealed-tube experiments at 80°C and 500°C in the Harwell reactor B.E.P.O. and at 30°C in a gamma-ray source. They have shown that, under the conditions employed, the production of CO from CO_2 and graphite mixtures is not very dependent on the nature of the graphite but that very big changes can be produced by changing the gas pressure, the solid to gas mass ratio, and the geometrical arrangement. Tomlinson and Walker[48] also have shown that within a factor of two the rate of attack on the graphite is independent of the physical structure of the carbon and appears to be unaffected by the presence of chemical impurities which catalyse the thermal oxidation reaction.

The experimental results of Gow and Marsh[49] on the effect of temperature on the radiation induced reaction have shown that between 100°C and 600°C the rate of CO formation is increased by a factor less than three. This corresponds to an 'activation energy" of about 1.5 k cals/mole but it is difficult to attach a real significance to this quantity. However, it is consistent with the idea of a reaction controlled by both the radiation production of active species and the gaseous diffusion of these species to the carbon surface - a diffusion in which many are lost by de-activation or recombination processes which are likely to have small activation energies. Above 600°C there is a marked increase in the rate of CO production due to the thermal oxidation taking place.

Using a radio-active tracer technique in which graphite samples containing carbon-14 were used, Feates and Waites[50] have shown that the condition of the surface of the graphite appears to have a small but significant effect on the nature of the molecules (CO_2 or CO) which transport the carbon-14 from the solid to the gas phase. Evidence of the effect of the carbon surface on the rate of CO production has been demonstrated in gas flow experiments by Sach[51], who found that at constant dose rates the rate of CO production decreases over the early periods of irradiation before settling down to a constant value.

The results may be broadly summarised by saying that the radiation induced reaction between CO_2 and graphite is initiated by a process taking place in the gas phase and that it depends little on the physical structure of the carbon but that the oxidation state of the carbon surface has a significant effect. To explain the fact that in carbon-14 experiments the species CO, ^{14}CO and $^{14}CO_2$ are observed the following tentative mechanism has been proposed by Wright and in which the species enclosed in brackets represent surface states:-

$$CO_2 \rightsquigarrow CO + O \quad \ldots\ldots 1)$$

$$(^{14}C) + O \longrightarrow (^{14}CO) \quad \ldots\ldots 2)$$

$$(^{14}CO) \longrightarrow {}^{14}CO \quad \ldots\ldots 3)$$

$$(^{14}CO) + O \longrightarrow {}^{14}CO_2 \quad \ldots\ldots 4)$$

If, in the early stages of irradiation, there is a deficit of adsorbed oxygen reaction 4) would be relatively insignificant and a higher rate of CO production would follow via reactions 2) and 3). The above mechanism is written for oxygen atoms being the reactive species but they could be written equally well for an excited CO_2 molecule being the reactive species.

An overall reaction mechanism proposed by Wright[52], which fits all the observations on carbon gasification and on exchange (or recombination) and which seems to give the proper relationship between the reaction steps controlling these two processes, is as follows:-

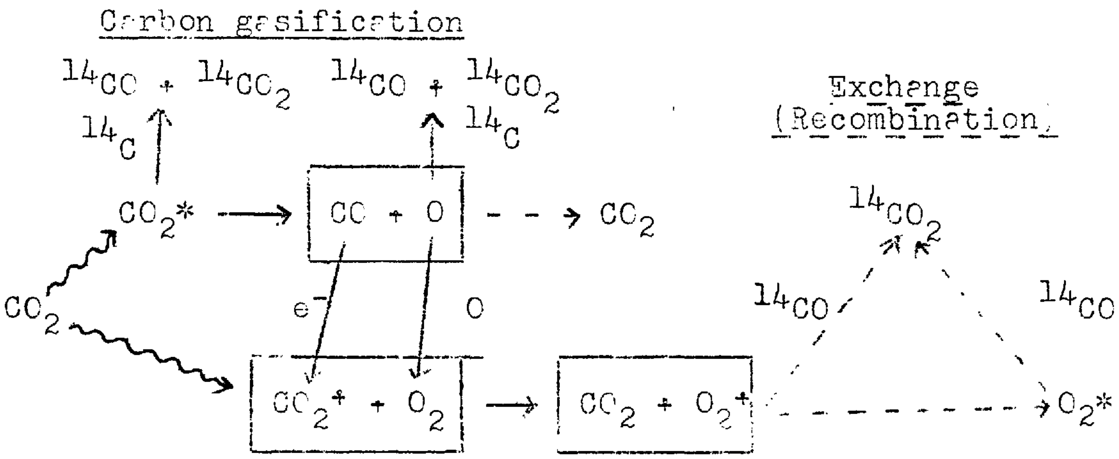
Carbon gasification
$^{14}CO + {}^{14}CO_2$
^{14}C
$^{14}CO + {}^{14}CO_2$
^{14}C
CO_2^*
$CO + O$
CO_2
CO_2
e^-
O
$CO_2^+ + O_2$
$CO_2 + O_2^+$
Exchange
(Recombination)
$^{14}CO_2$
^{14}CO
^{14}CO
O_2^*

This mechanism takes in all possible routes and does not distinguish between the individual steps. It must be emphasised that more experimental evidence is required before a scheme such as this could be considered as established, but it can provide a reasonable working hypothesis.

FIGURE 1

LAYOUT OF GAS STORAGE SECTION AND REACTION VESSEL

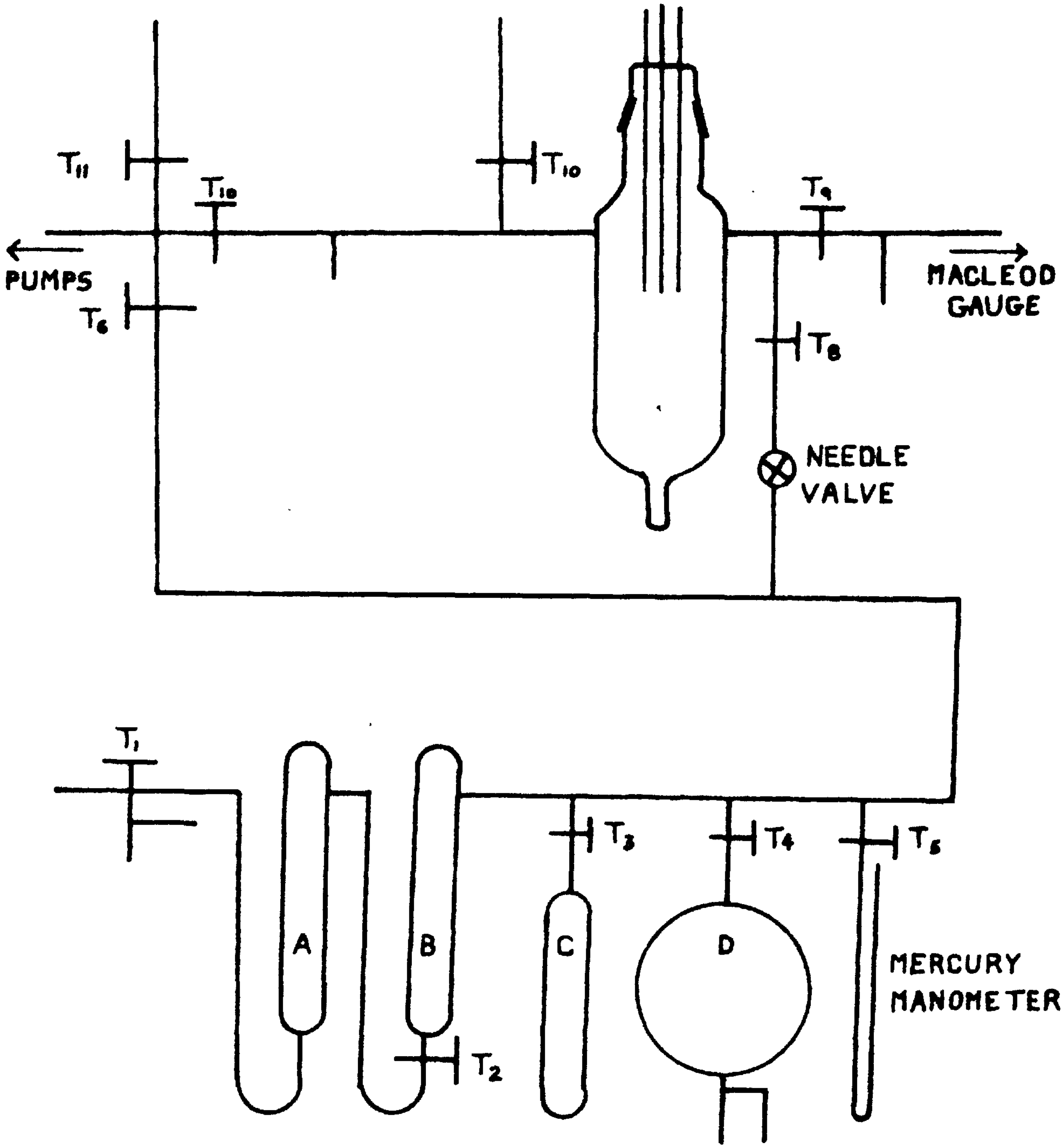

T_{11}
T_{10}
T_{10}
T_9
PUMPS
MACLEOD GAUGE
T_6
T_8
NEEDLE VALVE
T_1
A
B
T_2
T_3
C
T_4
D
T_5
MERCURY MANOMETER

CHAPTER 3

APPARATUS AND SUMMARY OF CLAXTON'S RESULTS

Since Claxton's apparatus and method were used in the present research a general description of the apparatus will be given in this chapter together with a summary of the results obtained by Claxton[53].

3.1. General Description of the Apparatus

The apparatus was constructed of Pyrex glass and consisted of three sections - one designed for the purification and storage of the gases used, a low pressure section containing the reaction vessel assembly and a section for the analysis of the gaseous products for carbon-14 content. A diagram giving the general layout of the first two sections is reproduced in figure 1.

Carbon dioxide and carbon monoxide were obtained from commercial cylinders and entered the system via tap T_1 and were dried by passing through tubes A and B which contained calcium chloride ($CaCl_2$) and magnesium perchlorate ($Mg(ClO_4)_2$) respectively. The carbon dioxide was purified by alternately freezing it out with liquid nitrogen in tube C and the liquid air appendage at the bottom of vessel D and pumping away the top and bottom fractions via tap T6. This was done a number of times and the gas was finally stored in the gas reservoir D. The carbon monoxide was dried by passing through tubes A and B and was stored in the reservoir. The gases were kept dry by having an appendage containing magnesium perchlorate in the reservoir. When carbon monoxide was used the liquid air appendage was immersed in liquid nitrogen to retain any impurities condensible at $77^{\circ}K$. The different components of the storage section were connected with capillary tubing and a mercury manometer was included to measure the gas pressure in the reservoir.

The low pressure section consisted of the reaction vessel and a Macleod gauge with a liquid air trap in between them to reduce the mercury contamination in the reaction vessel when necessary. The Macleod gauge was of the bench type supplied by Edwards High Vacuum Ltd. and could measure pressures in the range 10^{-2} to 10^{2} μHg. The gauge was modified by replacing the fixed reservoir with a movable one connected to the gauge by thick walled P.V.C. tubing. Pressures were read by suspending the reservoir from a hook whose position could be adjusted by a screw thread - a method which enabled pressures to be read quickly and accurately. Additional air traps were included to prevent air being swept into the system by the flowing mercury and a non-return valve was installed just above the gauge to prevent mercury being let over into the reaction vessel. The mercury was triple-distilled grade A mercury and was replaced

FIGURE 2

REACTION VESSEL

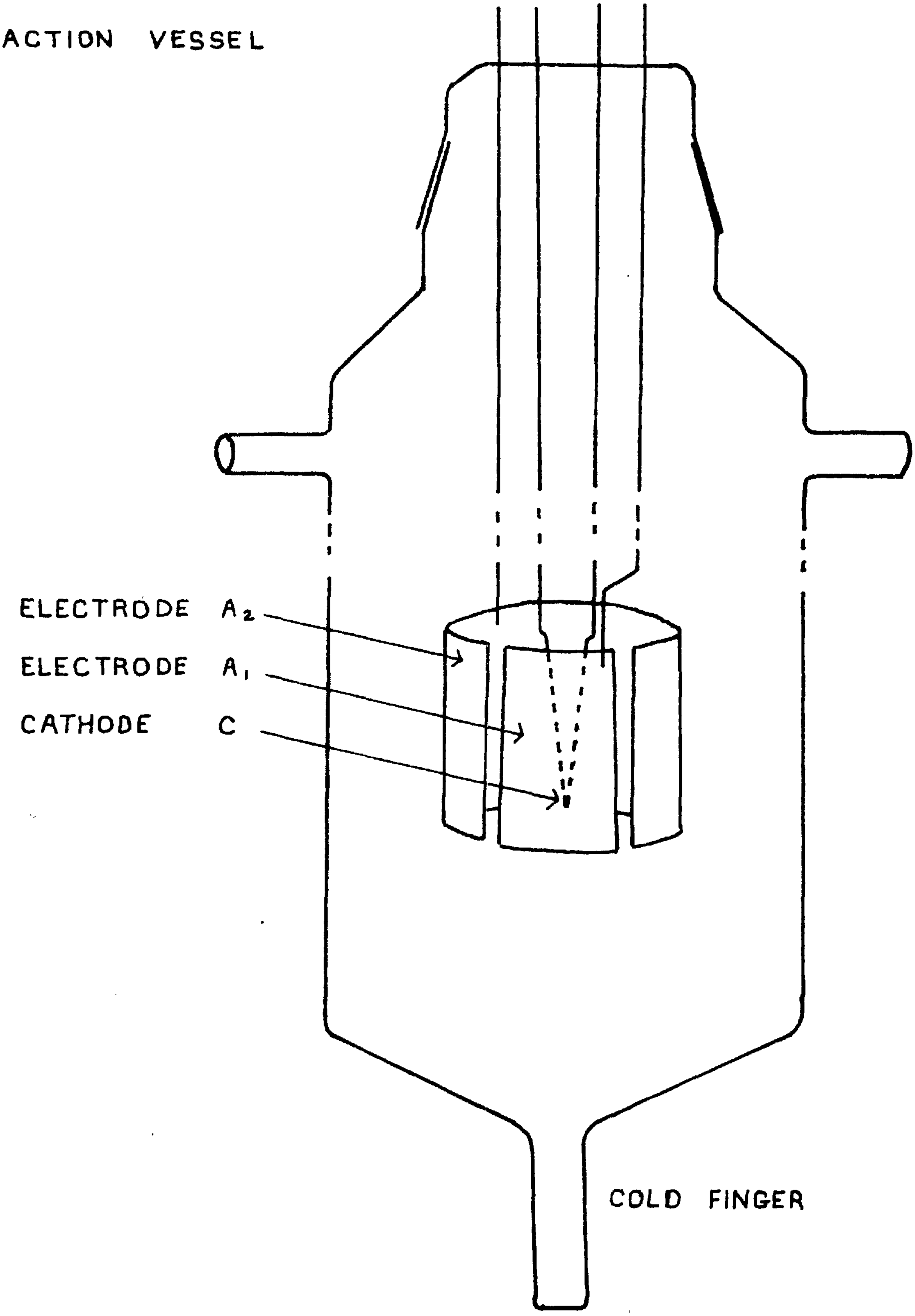
ELECTRODE A_2
ELECTRODE A_1
CATHODE C
COLD FINGER

periodically to decrease contamination risks.

A diagram of the reaction vessel is reproduced in figure 2; its dimensions were body length 25 cms. and internal diameter 8 cms. Attached to the body were a B 45 cone and socket, with the socket containing 5 tungsten leads which supported the various electrodes used in the researches. Beneath the reaction vessel was a small liquid air appendage used in the analysis of the reaction products. The electrodes consisted of a small anode A_1, a larger electrode A_2 used for supporting the carbon deposit and a cathode C. The electrodes A_1 and A_2 were made of aluminium foil 0.01 inches thick. The cathode consisted of a composite oxide layer coated onto a nickel base and was supplied by the Marconi and Osram Valve Co. The nickel base was 99.9% pure with traces of silicone and magnesium and the coating was supplied as a mixture of barium, strontium and calcium carbonates in the proportions 5 : 4 : 1 . The filament was inserted into the reaction vessel as supplied and was formed in situ by heating in vacuo. The carbonates are decomposed to their respective oxides and the oxides are then partially reduced to the pure metals which provide the electron emission. Each electrode was connected to a tungsten lead by a short stainless steel rod and connection.

The gas was admitted from the storage section to the reaction vessel through an Edwards spindle-seated needle-valve type OSIC. This provided a very fine control and flow pressures of as low as 1 μHg could be maintained accurately and easily.

The taps T_6 and T_7 enabled either section to be evacuated independently. Evacuation was provided by a 3-stage mercury diffusion pump, type 2M3A, backed by a rotary high-vacuum oil pump, type 1SP30, both being supplied by Edwards High Vacuum. With liquid nitrogen surrounding the cold trap between the diffusion pump and the system pressures below 0.01 μHg could be obtained easily and quickly.

All taps in the two sections were lubricated with Apiezon M grease and all cone and socket connections were greased with Apiezon L grease.

The glass walls of the body of the reaction vessel were degassed by heating them to approximately 300°C while pumping at pressures below 1 uHg. When the system had cooled down to room temperature the filament was formed and the electrodes were degassed by electron bombardment from the filament.

The electrical circuit diagram is reproduced in figure 3. The filament was heated with an alternating current obtained from a step-down transformer fed by a Berco rotary regavolt transformer to give a continuous

FIGURE 3

ELECTRICAL CIRCUIT DIAGRAM

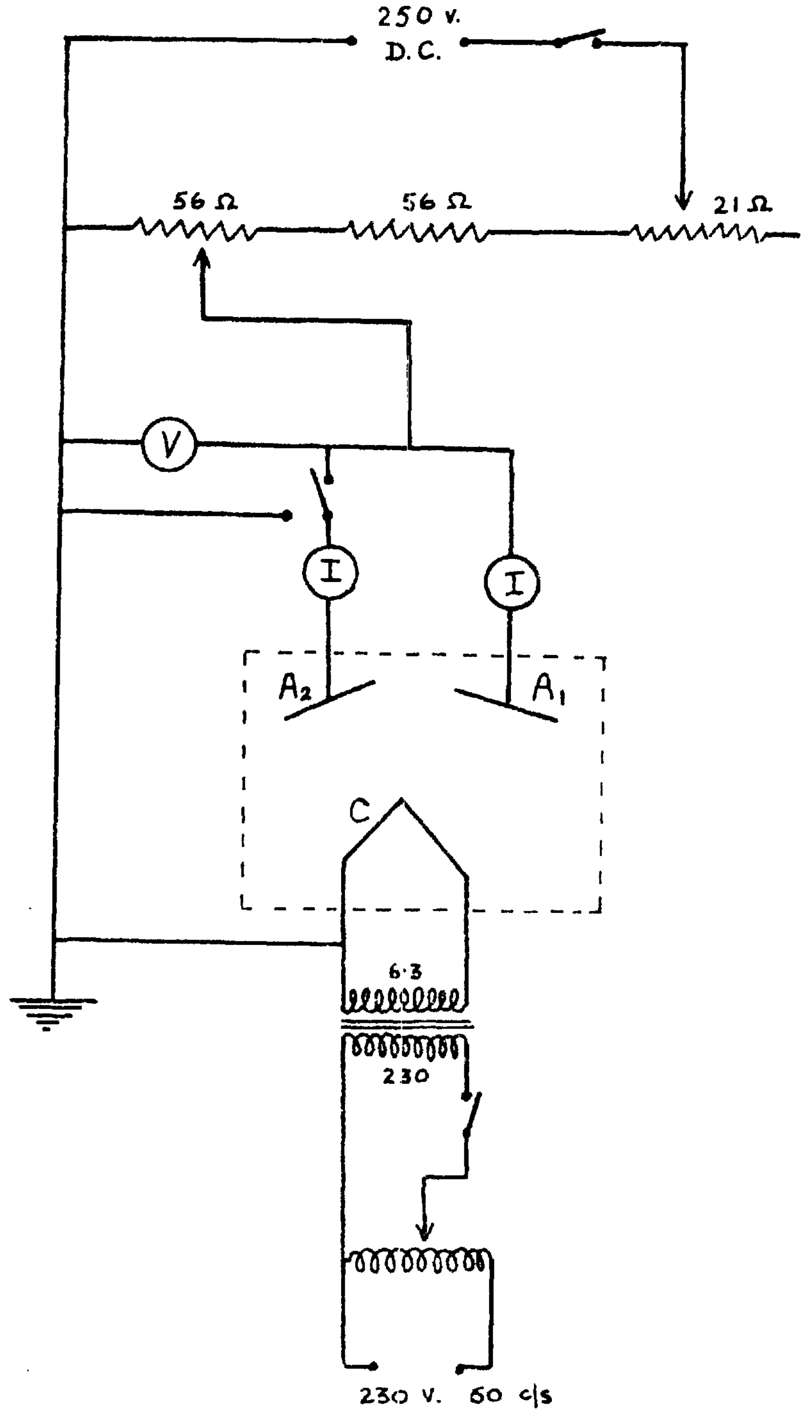

250 V.
D.C.
56 Ω
56 Ω
21 Ω
V
I
I
A_2
A_1
C
6·3
230
230 V. 60 c/s

variation of filament temperature up to 1200°C. The accelerating potential applied between the cathode and electrode A_1 was obtained from a variable resistance connected across a D.C. supply. The electrode A_2 could be maintained at the potential of electrode A_1, at the potential of the cathode or electrically isolated from either one. The currents and voltages were measured by Mark 8 AVO-meters.

A description of the carbon-14 analysis section will be given in chapter 7.

3.2. Summary of Claxton's Studies

Using the apparatus described in the previous section Claxton performed three series of experiments on the effect of the radiolysis of CO_2 in the presence of carbon. The carbon was prepared by burning napthalene in air and depositing the soot onto the aluminium foil which formed electrode A_2. This was then heated to about 500°C for about 30 minutes in a stream of nitrogen before being weighed and inserted into the reaction vessel.

3.3. Carbon weight loss

This series of experiments was performed in a single pass flow system of CO_2 at pressures of 70 μHg and 20 μHg and was intended to show whether the active species attacking the carbon was electrically charged or neutral. For this purpose the anode A_1 was held 25 volts positive with respect to the cathode and the electrode A_2 was held in one of the following conditions:

a) 25 volts positive with respect to the cathode

b) at the same potential as the cathode

c) suspended in the reaction vessel and so isolated from the other electrodes.

The effect of having the carbon in these three conditions was determined by comparing the measured carbon weight losses for a given milli-amp minutes - a measure of the total charge passing through the gas. It was found that the extent of the attack on the carbon was independent of the electrical condition of the carbon and therefore led to the conclusion that the attacking species was electrically neutral. Entirely similar results were obtained when mercury vapour was excluded from the reaction vessel and so ruled out the possibility of a mercury photo-sensitised reaction taking place. From a consideration of the different ionisation and excitation processes occurring in CO_2 at energies less than 25 eV it suggests that the primary process responsible for the attack on carbon is

$$CO_2 + e \rightsquigarrow CO + O^{(*)} + e$$

The reaction was accompanied by a quite intense, pale blue glow, present mainly between the electrodes and attributed to the presence of excited states of a number of unknown species.

3.4. Protective effect of carbon upon an oxide coated cathode

The presence or absence of carbon from the reaction vessel had a marked effect on the current drawn from the oxide-coated cathode. It was found that in the absence of carbon - electrode A_2 in position but with no carbon film on it - the current fell off rapidly with time, whereas in the presence of carbon the current was relatively stable. This effect was noted with electrode A_2 in all three conditions specified above and was due, therefore, to the presence or absence of carbon only. It was explained by assuming that the active species which react with carbon, when present, are capable, in its absence, of attacking the cathode. This attack would presumably involve the oxidation of the free metals present on the cathode surface and which are responsible for the thermionic emission. This interpretation was supported further by the fact that the CO_2 decomposed readily in the absence of the carbon film.

3.5. Static charges of CO and CO_2

When static charges of CO and CO_2 were bombarded with 25 eV electrons the system came rapidly to a steady state of approximately 80% CO which was maintained for long reaction times. A correct mass balance between reactants and reaction products was not obtained owing to electrical "clean-up" processes taking place. Starting with pure CO_2 the yields of oxygen atoms in the product gases were of the order of 70 - 90% of the oxygen atoms in the reactant, while when starting with pure CO the yields were lower and varied over wide limits from 10% to 85%.

CHAPTER 4

STATIC EXPERIMENTS WITH CARBON-DI-OXIDE

4.1 Introduction

Using electrons of 25eV energy only, Claxton was able to conclude that the species causing the gasification of carbon was electrically neutral and probably atomic oxygen. The most convincing method of determining the exact nature of the reactive species would be to determine the rate of carbon gasification as a function of the energy of the bombarding electrons and to correlate any thresholds in the resulting curve with the known excitation and ionisation processes summarised in Chapter 2. The reaction could be measured by directly computing the rate of removal of carbon from the solid phase to the gas phase or, alternatively, by monitoring the change in gas composition and calculating back from a simple stoichiometric relationship such as $CO_2 + C \rightsquigarrow 2CO$.

Unfortunately the current between the electrodes in the reaction vessel decreases sharply with decreasing voltage below 20 volts and the carbon weight loss method used successfuly by Claxton becomes impractical owing to the excessively long reaction times that would be involved. Therefore, in the present work a radio-active tracer technique using a carbon -14 surface has been developed:

but before this some experiments were performed in a static system of CO_2 to study further the possibility of using the change in gas composition as a means of measuring the carbon gasification reaction.

4.2 Experimental Procedure

In this series of experiments the apparatus was set up as described in Section 3.1 with a carbon surface deposited on electrode A_2. After the electrodes had been degassed the system was shut off from the pumps and pure CO_2 was admitted to the reaction vessel via the needle-valve until the pressure measured on the Macleod gauge was approximately 60 μHg. The relevant potential was applied between the filament and the anode - with electrode A_2 connected so that it was at the same potential as the anode. The filament was then switched on for a short period of time and the current was noted at regular intervals. After the filament had been switched off the apparatus was left to stand for approximately five minutes so that it could cool down to room temperature. The gas mixture was then analysed for fractions condensible and non-condensible at 77^{o} K by immersing the liquid air appendage in liquid nitrogen - the fractions were assumed to be carbon di-oxide and carbon monoxide respectively. The reaction was then allowed to proceed for a further short period of time before

FIGURE 4

% CO AS FUNCTION OF REACTION TIME

CARBON PRESENT

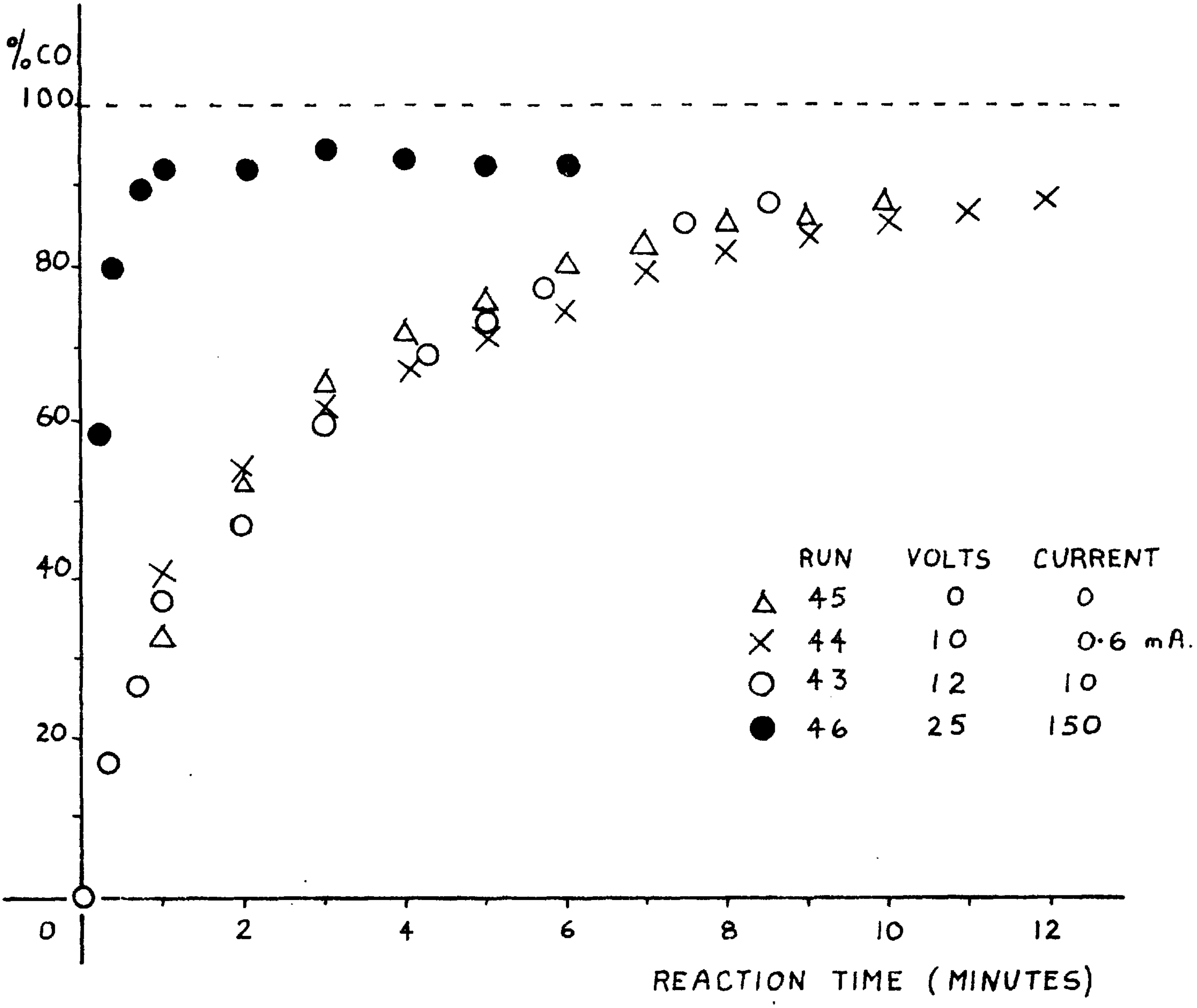

a further analysis was carried out. This was repeated several times so that the complete reaction could be followed using a single charge of gas.

The disadvantage of using this method is that the reaction had to be halted while analysis was carried out and any concentrations of free radicals or excited species formed during the reaction would be destroyed by re-combination or de-excitation processes at each stoppage. However, the results did give considerably less scatter than previous methods and could be used for a more sensible analysis.

4.3 Results and Discussion

Runs were carried out using accelerating voltages of 0,10 and 12 volts and the results obtained are given in tables 1, 2 and 3 respectively of the appendix. The results are plotted in figure 4 as the percentage carbon monoxide as a function of reaction time. It can be seen from these plots that the conversion of carbon di-oxide to carbon monoxide is the same for all three potentials and, since one of these potentials is zero, the conversion must be due to a non-radiolytic process. It will be shown that this "thermal" conversion can be attributed to the reaction of CO_2 with the filament.

A run was then performed with the anode and carbon at 25 volts to determine the effect of using a higher electronic

FIGURE 5

CO AND CO_2 PARTIAL PRESSURES AS FUNCTION OF TIME FOR $V = 0$ AND $V = 25$ v.

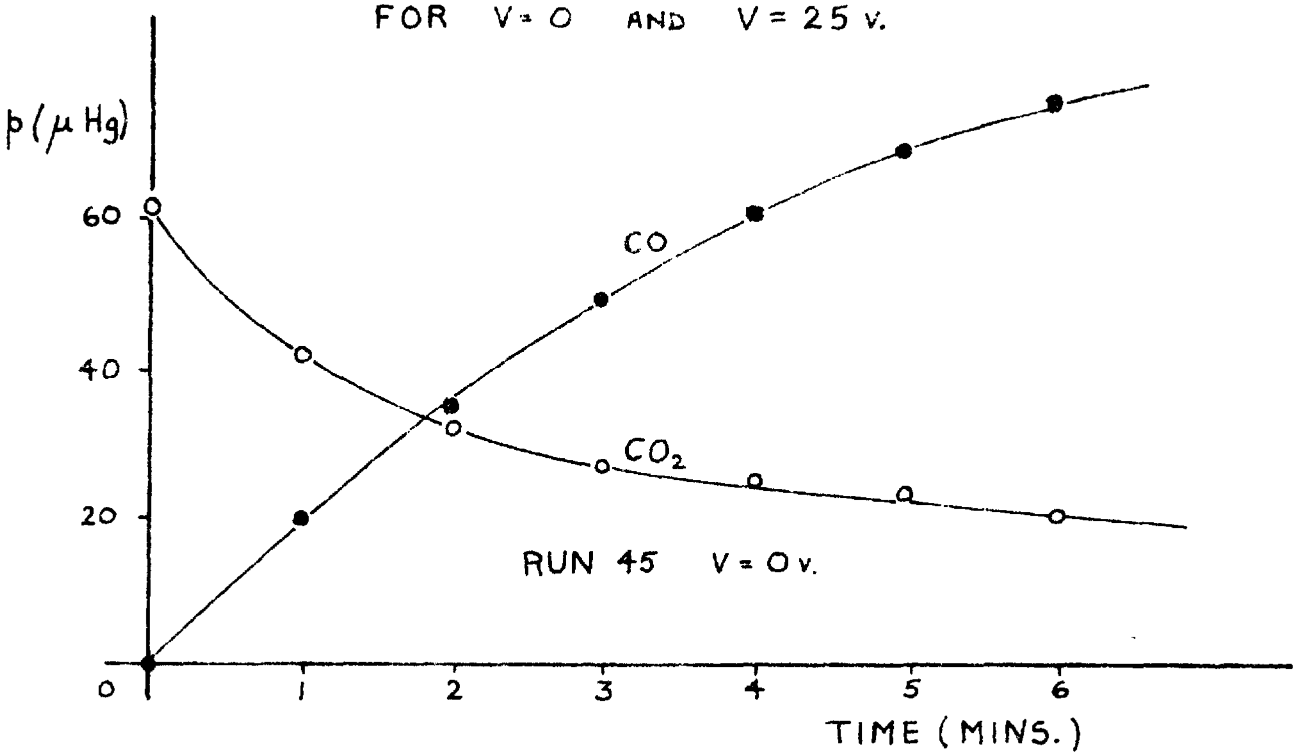

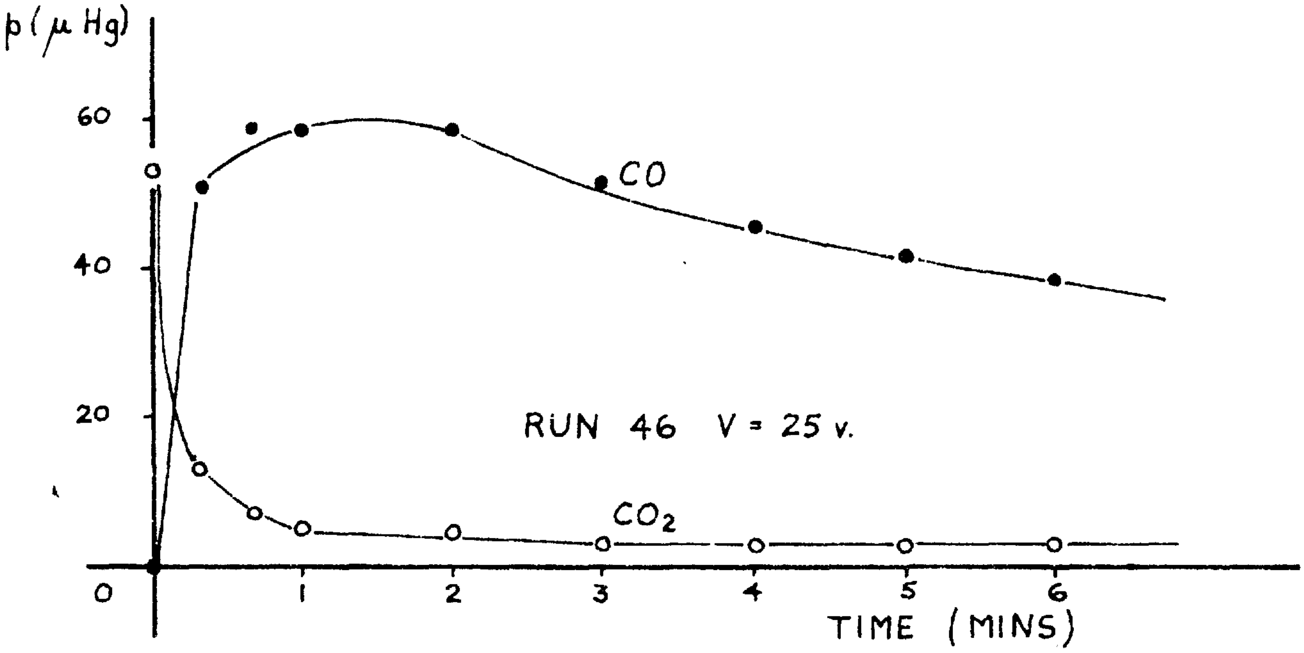

energy. The results obtained are given in table 4 and the percentage carbon monoxide as a function of reaction time is shown in figure 4 with the other results. It can be seen that there is a much more rapid conversion to carbon monoxide in this case and this demonstrates the effect of a radiolytic process.

The differences between the runs at 0 and 25 volts are even more pronounced when the actual partial pressures of carbon di-oxide and carbon monoxide are plotted as functions of reaction time - as shown in figure 5. The rate of decrease of carbon di-oxide is much more rapid for the 25 volt case as would be expected, as is the initial carbon monoxide increase.

It will furthermore be seen that, in the 25 volt case, the carbon monoxide partial pressure after reaching a maximum in one minute thereafter starts to decrease: this may be attributed to the radiolytic decomposition of the carbon monoxide into carbon sub-oxide polymers. This cannot be attributed to a reaction of carbon monoxide with the filament since the effect is absent in the 0 volt case.

Similar experiments were performed using 25 volt and 0 volt electrons in the absence of the carbon film. The electrode A_2 was inserted bare of carbon and, as before, it was connected to the anode. The results obtained are given in tables 5 and 6 respectively. Plots of the

FIGURE 6

% CO AS FUNCTION OF REACTION TIME

CARBON ABSENT

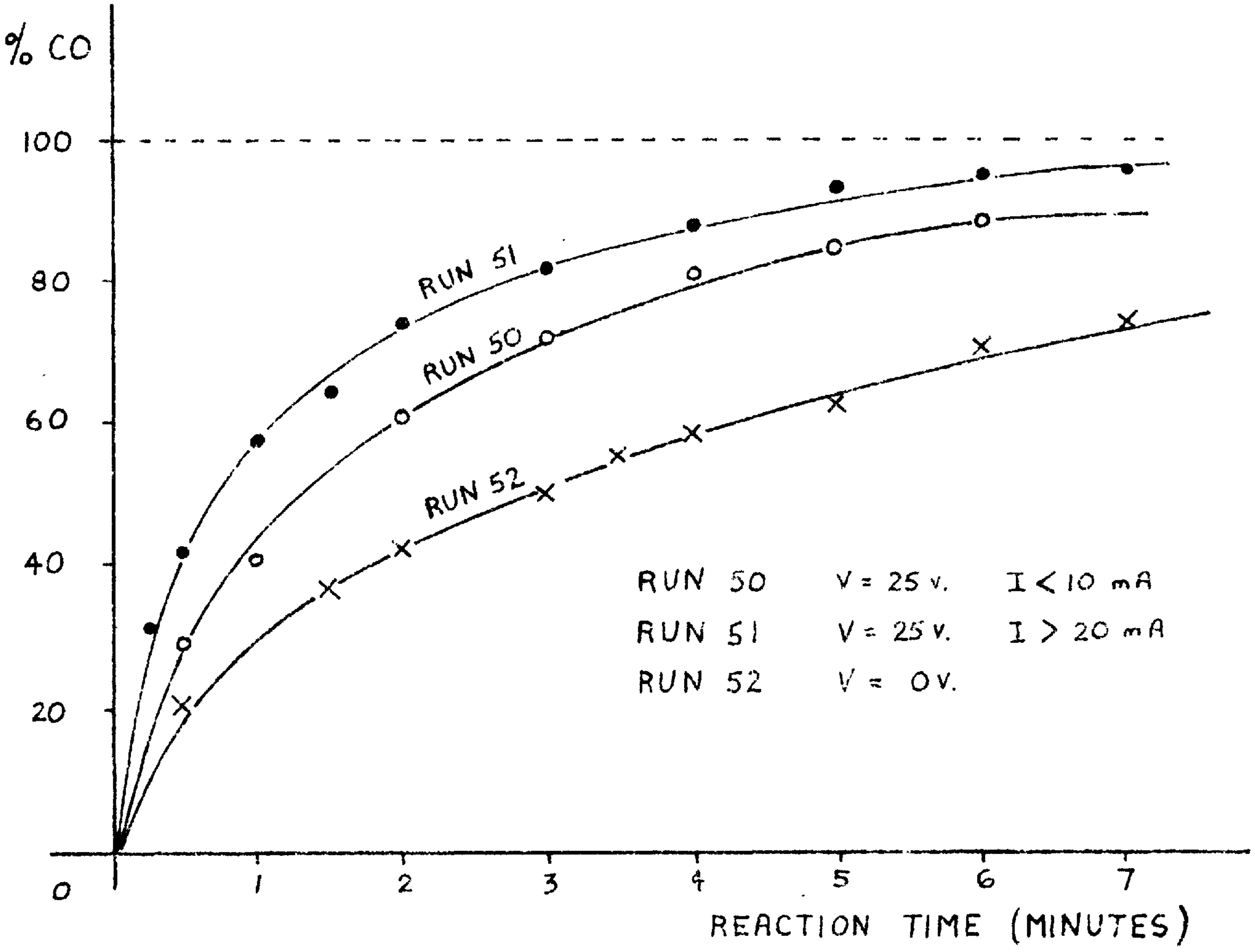

percentages of carbon monoxide as functions of reaction time are given in figure 6. It can be seen that the conversion to carbon monoxide occurs in all three runs shown. By comparing the runs for zero accelerating field in figures 4 and 6 it is seen that the zero volts conversion is largely independent of the presence of carbon.

The runs at 25 volts show that in the absence of carbon the carbon dioxide is undergoing radiolytic decomposition as would be expected. The differences between runs 50 and 51 may be attributed to the different currents obtained from the filament in the two runs - less than 10mA in run 50 and greater than 30mA in run 51. It should be noted that, as demonstrated in run 50, a current of approximately 8mA is enough to show a significant difference between the radiation induced reaction and the thermal reaction in the absence of carbon. In run 43 (figure 4) in which a current of approximately 10mA was obtained for 12 volt electrons in the presence of carbon there was no significant difference from the thermal reaction. This may indicate that no radiation induced reaction was taking place in this case.

It should be noted also that in runs 50 and 51 (table 5) the actual partial pressure of carbon monoxide continued to increase throughout the runs and exhibited no decrease as observed in run 45 when carbon was present and 25 volt electrons were used. An explanation of this phenomenon

FIGURE 7

CO_2 AND CO PARTIAL PRESSURES AS FUNCTIONS OF TIME IN ZERO ACCELERATING FIELDS

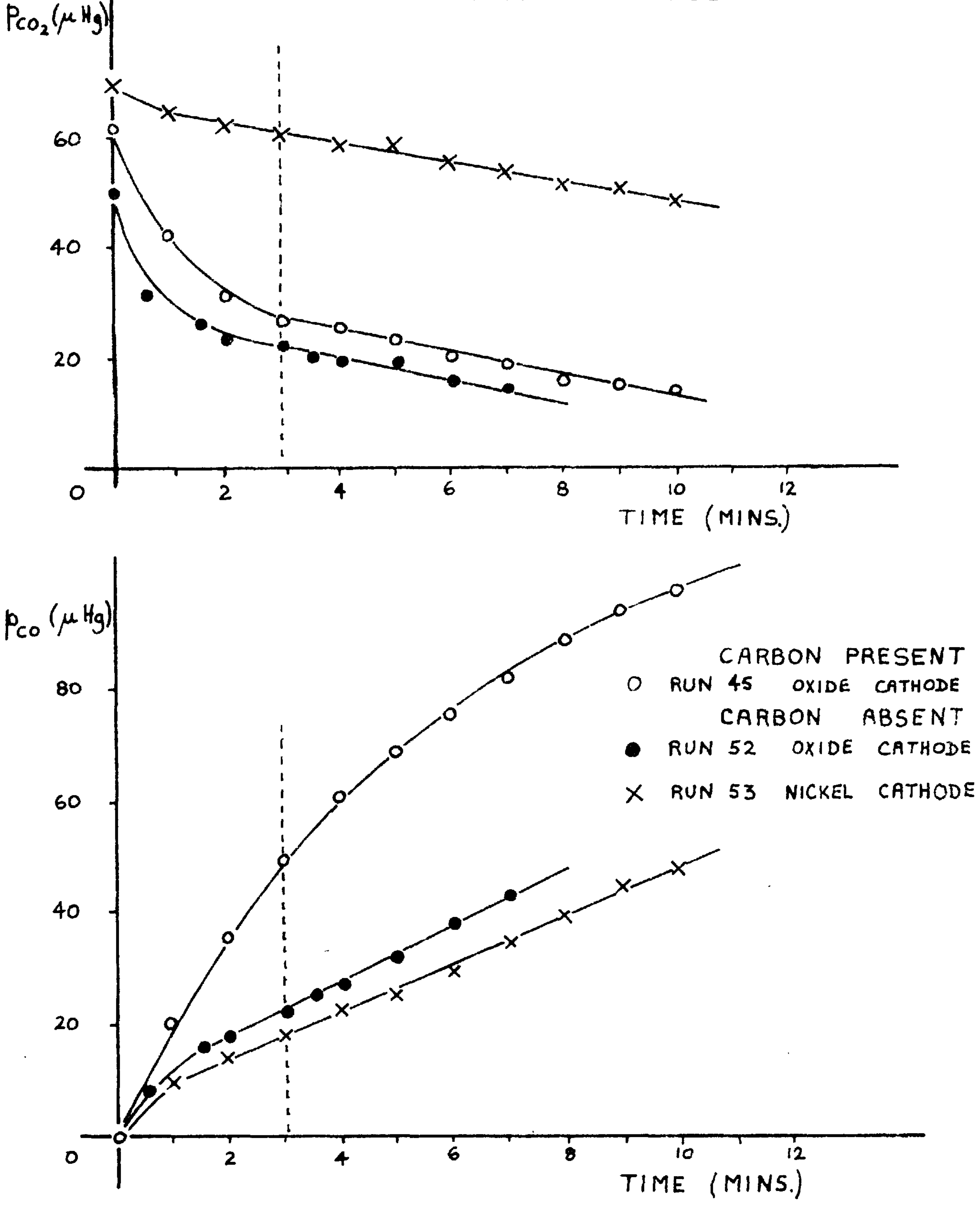

will be given in section 5.7 dealing with experiments performed with carbon monoxide.

4.4 Thermal reactions with filament

To determine whether the reactions observed in zero accelerating fields could be attributed to the thermal dissociation of carbon dioxide into carbon monoxide and oxygen atoms on striking the filament a run was performed with a heated nickel strip in place of the oxide-coated filament. The nickel strip was prepared by removing all traces of the carbonate layer from a normal cathode and it was heated with the same voltage (5 volts a.c.) as the other runs. The results obtained in this run are given in table 7. It can be seen that appreciable decomposition of carbon dioxide into carbon monoxide does take place although to a smaller extent than with a normal filament.

Plots of the carbon dioxide and carbon monoxide partial pressures as functions of reaction time in which zero accelerating fields were used for the normal filament in the presence and absence of carbon-runs 45 and 52 - and for the nickel strip in the absence of carbon-run 53- are shown in figure 7. By comparing the plots of the carbon dioxide partial pressure the following conclusions may be drawn:

1) In the first three minutes of reaction time there is a rapid removal of carbon dioxide in the runs with the

oxide cathode and this must be due to a chemical reaction of the carbon dioxide with the oxide surface.

2) After the first three minutes the carbon dioxide pressure decrease is constant for all three runs and equal to 1.8 $\pm$ 0.2 μHg/min. This suggests that a similar process is occurring in all three cases and is due to the presence of a heated surface and is most probably the thermal dissociation of carbon dioxide on striking the filament. An approximate calculation based on kinetic theory data does, in fact, give an answer of the right order of magnitude for this rate of thermal dissociation. The calculation is given in the appendix.

The chemical reactions which can occur between carbon dioxide and an oxide-coated filament have been fully described by Herrman and Krieg.[54] Their conclusions were that at temperatures below 800°C the carbon dioxide would react with the metal oxide to form a stable carbonate compound.

$$MO + CO_2 = MCO_3 \quad \ldots\ldots\ldots \quad 1)$$

and at temperatures above 800°C the carbon dioxide would react with the free metal to form the corresponding oxide

$$M + CO_2 = MO + CO \quad \ldots\ldots \quad 2)$$

To verify their findings the following experiment was carried out:-

a) With an initial gas pressure of 71 μHg pure CO_2, the filament was heated to approximately 500°C for 60 seconds. At the end of the reaction the pressure had been reduced to 7 μHg and the gas remaining contained 94% carbon dioxide. This is consistent with reaction 1) taking place.

b) The filament was then heated to 1000°C for 60 seconds with the liquid air appendage immersed in liquid nitrogen to freeze out any carbon dioxide as it was produced. At the end of this reaction the pressure had risen to 75 μHg and contained 96% carbon dioxide. This is consistent with the decomposition of the carbonate formed in step a).

c) The filament was then heated to 1000°C for 60 seconds without the liquid nitrogen. The pressure remained constant at 75 μHg but the carbon dioxide concentration decreased from 96% to 60%. This is consistent with reaction 2) taking place at this temperature.

Thus, the conversion of carbon dioxide to carbon monoxide in the absence of an accelerating field may be attributed to the oxidation of the free metals on the filament surface and to the thermal dissociation of carbon dioxide on striking the heated surface. Owing to this thermal conversion the method of monitoring the change in gas composition as a means of detecting the radiolytic reaction between carbon dioxide and carbon was abandoned.

Experiments were next performed using different filament

FIGURE 8

CO$_2$ AND CO PARTIAL PRESSURES AS FUNCTION OF TIME

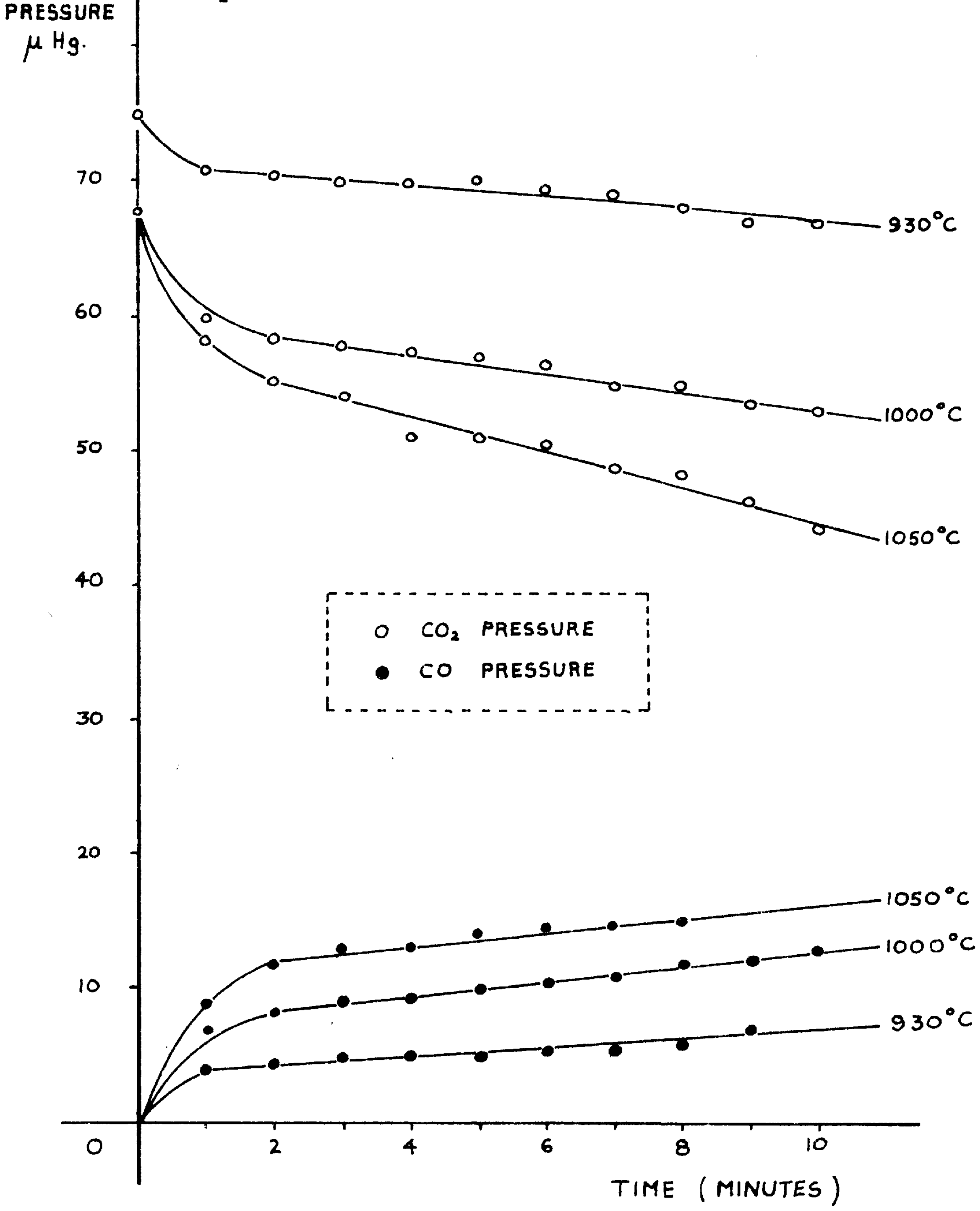

temperatures to determine the best working conditions at voltages in excess of 10 volts with regard to the current drawn from the filament and the carbon monoxide formation. The temperature of the filament was measured using a Pye Disappearing Filament Pyrometer. The experiments were performed in a static system of carbon dioxide in the presence of a carbon film. The results obtained in zero accelerating field are shown in figure 8. No results are shown for temperatures below 900°C for at this temperature there was a marked decrease in the current for all accelerating voltages and these temperatures could not be considered. From these results it was decided to use filament temperatures of the order of 930°C for future work.

4.5 Weight-loss experiments

The fact that some of the carbon monoxide formation in zero accelerating field could be attributed to the thermal decomposition of carbon dioxide on striking the heated filament led to the performance of runs in flowing carbon dioxide to determine whether this thermal decomposition had a measurable effect on the carbon weight loss experiments performed by Claxton.

The runs were performed using a flow pressure of approximately 60 μ Hg and using reaction times of 60 and 90 minutes. The results obtained are given in table 8a and it

FIGURE 8 A.

CARBON WEIGHT LOSS AS FUNCTION OF MILLIAMP-MINUTES

CARBON AT SAME POTENTIAL AS ANODE

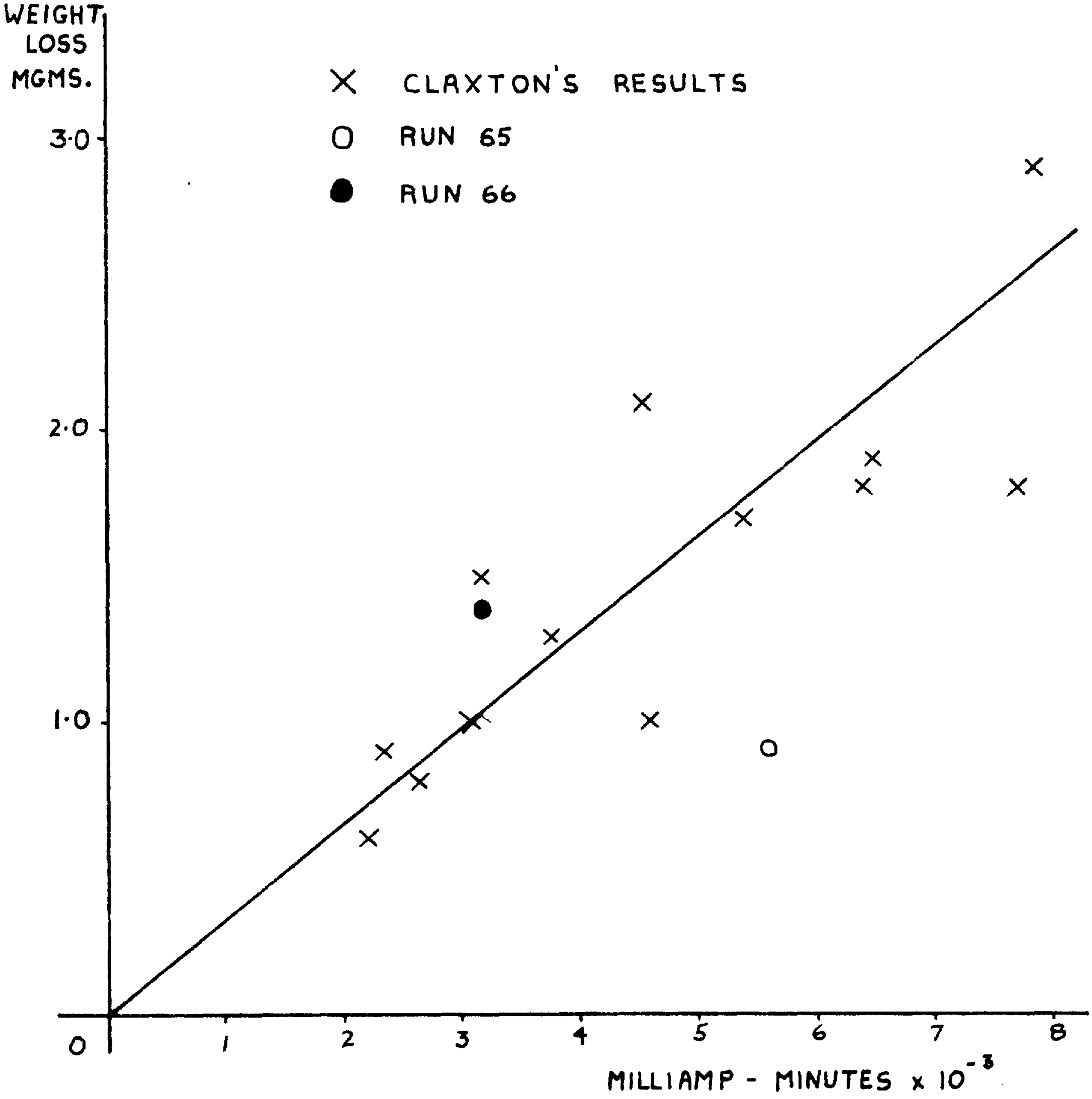

can be seen that there were no significant changes in the weights of the carbon films. From this one can conclude that the thermal decomposition of carbon dioxide has no significant effect on the weight loss results.

The runs at 25 volts, whose results are given in table 8b), were performed as a repeat of Claxton's results. The fact that the result of run 65 is significantly lower than that of run 66 can be attributed to the fact that at the end of the run it was noticed that the carbon film had completely disappeared from two large segments of the supporting aluminium backing and, thus, reduced the area of attack possible. It is interesting to note that the two bare patches corresponded to the positions of the electrode closest to the filament and demonstrated that the chemical attack on the carbon observed might be temperature dependent. The result of run 66 agreed well with Claxton's results as can be seen in figure 8a).

4.6. Temperature of carbon surface

The observation made in the last section that the radiolytic reaction might be temperature dependent led to the performance of a series of experiments in which the temperature of electrode A_2 was measured using a variety of different gas pressures and electrical currents flowing through the system.

FIGURE 9

THERMO-ELECTRIC E.M.F. AS FUNCTION OF TIME

CORRESPONDING TEMPERATURES FROM KAYE AND LABY

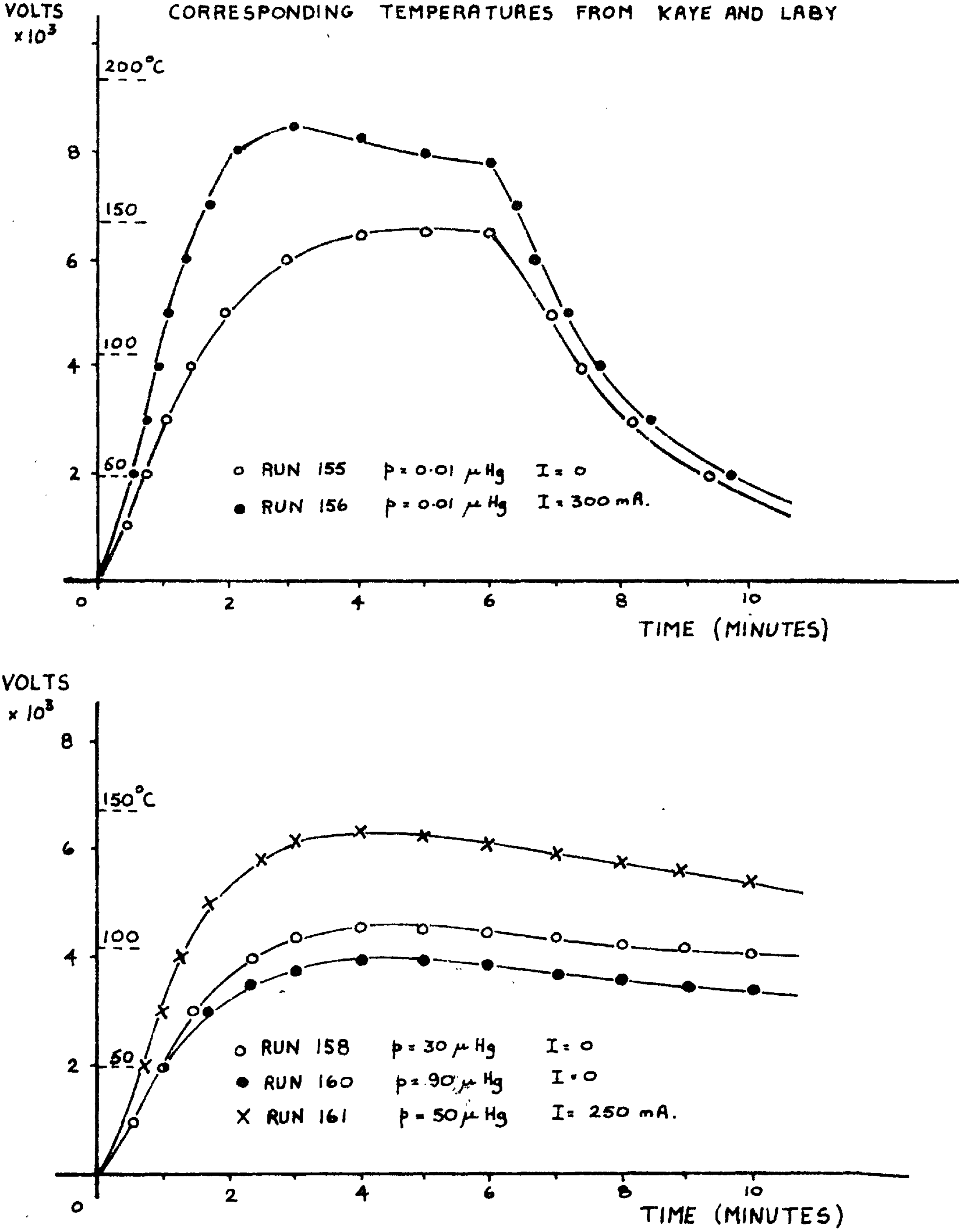

The temperature of the electrode was measured by placing a copper-constantan thermo-couple in the reaction vessel. The thermo-couple was assembled by soldering together two lengths of 30 s.w.g. copper and constantan wire. The free ends were soldered to two lengths of 18 s.w.g. copper wire which, in turn, were connected to two of the tungsten leads of the reaction vessel. The junction was fixed to the centre of the reverse side of electrode A_2 with an epoxy resin - copper filings mixture. With this arrangement the hot and cold were both inside the reaction vessel but any stray emf's generated at the tungsten connections were eliminated.

The results obtained are reproduced in graphical form in figure 9 for runs 155 and 156 in which low pressures were used and runs 158, 160 and 161 in which high pressures were used. In all cases the temperature rose rapidly and then levelled off to a steady value between 100 and 200°C depending on the gas pressure and current employed during the run. The slight decreases in the thermo-elect ic emf noted after the maxima may be attributed to the heating up of the cold junction by conduction of heat along the constantan wire. In runs 155 and 156 the filament was switched off after 3 minutes and it can be seen that the electrode cooled down to room temperature fairly rapidly.

The thermodynamic equilibrium data for the thermal reaction $CO_2 + C = 2CO$ are given in table IV. The partial pressures of carbon dioxide and carbon monoxide are computed for a total pressure of 60 μHg.

TABLE IV

Equilibrium data for the reaction $CO_2 + C = 2CO$

T°C	$\log_{10}K_p$	PCO_2	PCO	% CO
127	-13.324	60	0	0.0
227	- 8.792	58.5	1.5	2.5
327	- 5.760	26	34	56.8
427	- 3.614	1	59	98.4

From this table it can be seen that, at the temperatures of the electrode measured, the equilibrium pressure of carbon monoxide is very low and this indicates very little attack on the carbon. Thus, the results of measuring the temperature of the carbon surface confirm the weight loss experiments in zero accelerating fields described in the previous section in which no significant thermal attack on the carbon surface could be detected.

4.7 Summary

It has been shown that under conditions unfavourable for a radiolytic reaction taking place there is a rapid conversion of carbon dioxide to carbon monoxide owing to the occurence of a chemical reaction between the carbon dioxide and the free metal in the oxide layer of the filament. Carbon monoxide formation occurs also from the thermal decomposition of carbon dioxide on striking the heated filament. These thermal effects rule out the possibility of utilising the change in gas composition as a means of monitoring the radiolytic reaction.

The thermal decomposition has been shown to have no significant effect on the carbon weight loss experiments performed at 25 volts.

Measurements of the temperature of the carbon surface have shown that there is no significant thermal reaction between the carbon dioxide and carbon.

Experiments performed at 25 volts have shown that carbon dioxide undergoes a radiolytic decomposition both in the presence and the absence of a carbon surface. The decomposition of the carbon monoxide produced depends on the presence of a carbon surface since it apparently remains stable in its absence.

CHAPTER 5

EXPERIMENTS WITH CARBON MONOXIDE

A. Static experiments

5.1. Introduction.

Owing to the absence of a chemical reaction between carbon monoxide and the oxide coated cathode, as noted in section 4.3, it was possible to perform a series of experiments with carbon monoxide based on the experimental method developed by Caress and Rideal[55]. In this method the decomposition of carbon monoxide was determined as a function of electron energy while the electron current was maintained constant by varying the temperature of the cathode. Their reaction vessel was totally immersed in liquid nitrogen, and therefore, and CO_2 was frozen out as produced and the reaction could be followed by measuring the carbon monoxide pressure as a function of reaction time. They found that when pure carbon monoxide was used no decomposition occurred below the ionisation potential of 14 volts, followed by a very slight reaction until a very large increase in the decomposition rate occurred at 19 volts. Further thresholds in the reaction were determined at 32 and 40 volts. They attributed the 19 volt threshold to the formation and subsequent reaction of an excited state of the carbon monoxide ion.

This seemed a sensitive method of detecting thresholds and therefore it was used in this work to determine the effect of the presence or the absence of a carbon film on the decomposition of carbon monoxide. Besides this, it was important to determine the nature of the carbon monoxide - carbon reaction in this apparatus due to the large proportion of carbon monoxide produced when working with carbon dioxide owing to the reaction with the filament.

5.2. Experimental Procedure.

The electrode assembly used in this series of experiments consisted of an oxide coated cathode surrounded by a single aluminium anode of linear dimensions 8 x 8 cms. For runs in the presence of carbon a carbon film was deposited on the inside surface of the aluminium by burning napthalene in air. Prior to placing the anode in the reaction vessel it was heated to 500°C for thirty minutes in a stream of nitrogen to remove any impurities such as water vapour or hydrogen.

When the apparatus had been assembled it was degassed by pumping at a pressure of below 10^{-5}mm Hg for at least thirty minutes while the walls of the reaction vessel were heated to approximately 150°C. After the apparatus had cooled down to room temperature the oxide cathode was formed and the anode was degassed by allowing a current of over 500 milli-amps to pass between the electrodes for a few minutes.

The reaction vessel was then switched off from the pumps and was left to stand for at least 10 minutes while periodic checks were made on the pressure to ensure that no air was leaking in or that any gas was desorbing from the electrodes or glass walls. The reaction vessel was then filled with carbon monoxide from the resevoir, via the needle-valve, to a pressure of approximately 75μHg. The appendage at the bottom of the reaction vessel was immersed in liquid nitrogen in order to freeze out any condensible gases if and when formed. The level of liquid nitrogen was kept topped up throughout the course of a single run. The cathode -anode potential difference was then adjusted to the relevant value and the filament was switched on for periods of 60 seconds each. The filament - transformer feed variac was adjusted until the current measured on the Avometor was 5.0 milli-amps. A steady current was set up well within the first 5 seconds and could be controlled to within ± 0.1 milli-amps for the remainder of each period. After each period of 60 seconds the reaction vessel was allowed to stand and cool for a period of 5 minutes before the carbon monoxide pressure was read on the Macleod gauge. The pressure of the gas collected in the appendage during the course of the run was also measured.

FIGURE 10

STATIC CHARGES OF CARBON MONOXIDE

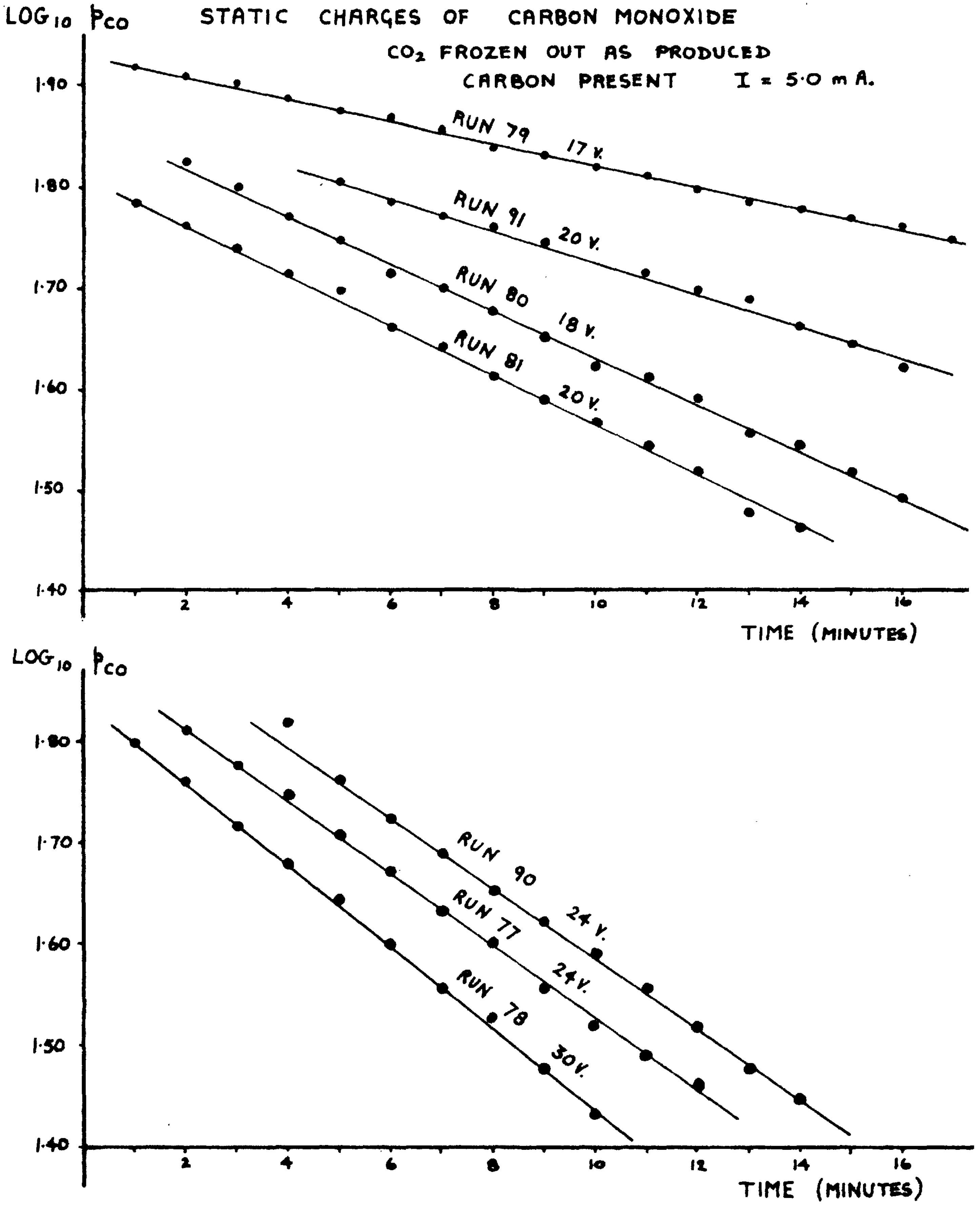

CO$_2$ FROZEN OUT AS PRODUCED

CARBON PRESENT $I = 5{\cdot}0$ mA.

FIGURE 11

STATIC CHARGES OF CARBON MONOXIDE

CO_2 FROZEN OUT AS PRODUCED

CARBON ABSENT $I = 5{\cdot}0$ mA.

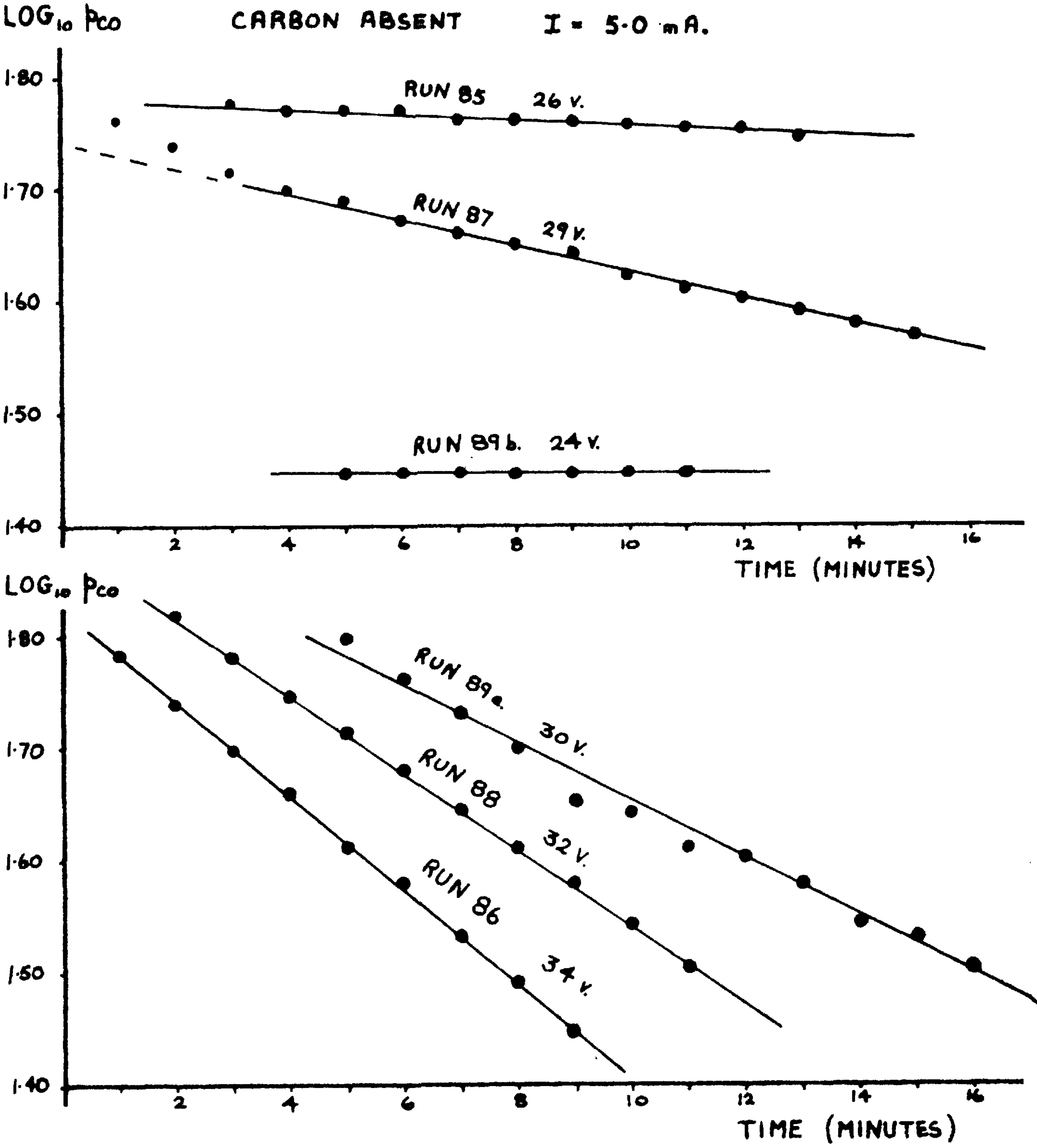

For the majority of runs the total reaction time was such that the carbon monoxide pressure fell to less than 30μHg. For runs 77 to 81 inclusive the mercury vapour in the reaction vessel was reduced appreciably by immersing the trap between the reaction vessel and the Macleod gauge in a solid CO_2 - acetone mixture.

5.3. Results.

The results obtained are reproduced in figure 10 for the runs performed in the presence of carbon and in figure 11 for the runs performed in the absence of carbon. They are shown as plots of the carbon monoxide pressure in microns Hg on a logarithmic scale as functions of reaction time. It can be seen that in each case there is a reasonable straight line fit indicating that the rate of carbon monoxide decomposition is proportional to the carbon monoxide pressure.

The exponential constant obtained from each plot is given in table 9 and reproduced as a function of electron energy in figure 12. The fourth column in table 9 gives the ratio of carbon dioxide formed to carbon monoxide destroyed; theoretically this ratio would be 0.33 for the reaction $3CO \rightsquigarrow CO_2$ + solids and would be 0.50 for the reaction $2CO \rightsquigarrow CO_2 + C$. The fifth column in table 9 gives the filament heating voltage required to maintain a total current of 5 mA

FIGURE 12

STATIC CHARGES OF CARBON MONOXIDE

$I = 5.0$ mA. $p = p_0 e^{-\alpha t}$

α AS A FUNCTION OF ELECTRON ENERGY

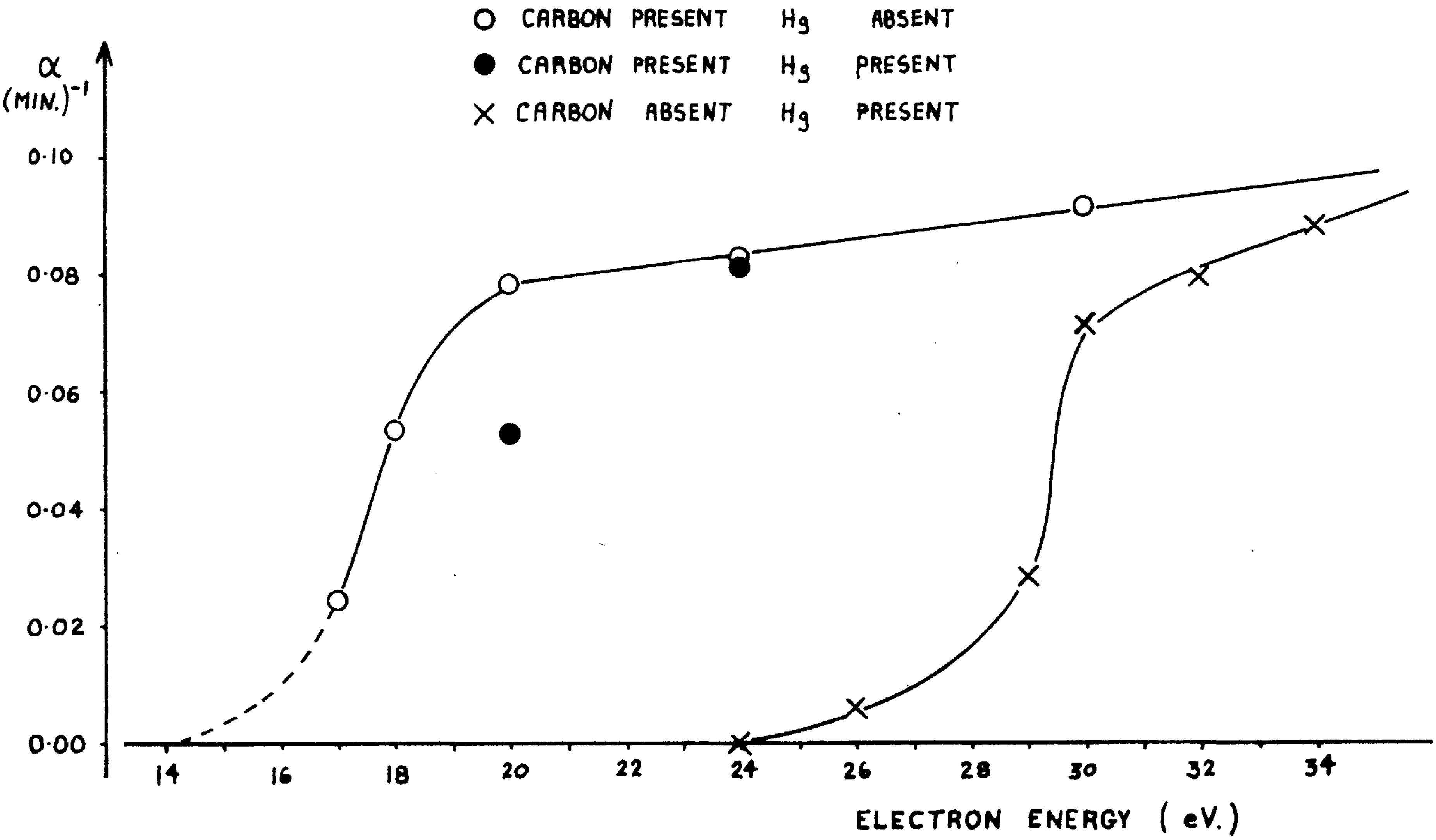

during the course of a run. This total current is composed of molecular or atomic ions in addition to the primary and secondary electrons and the heating voltage serves as a qualitative indication of the primary electron current.

Inspection of figure 12 shows that there is a remarkable difference in behaviour of the reaction rate for the decomposition of carbon monoxide as a function of electron energy depending on whether carbon is present or absent. When carbon is present the threshold voltage is certainly less than 17 volts and when carbon is absent the threshold voltage is between 24 and 26 volts. This phenomenon had been hinted at earlier, in section 4.3, when discussing the difference in behaviour of the carbon monoxide partial pressure when carbon dioxide was irradicated with electrons of 25 eV energy in the presence and in the absence of carbon.

When comparing the results obtained in the presence and in the absence of mercury vapour it can be seen that mercury seems to have little effect, if any, on the decomposition rate. The runs at 24 volts gave identical results while the runs at 20 volts gave a lower value for the decomposition rate in the presence of mercury than in it's absence. If mercury is to have a significant effect on the decomposition of carbon monoxide one would expect the presence of mercury to

FIGURE 13

CURRENT OBTAINED AS FUNCTION OF VOLTAGE

FILAMENT HEATING VOLTAGE 6·9 v.
CO PRESSURE 60 μHg. — CARBON PRESENT

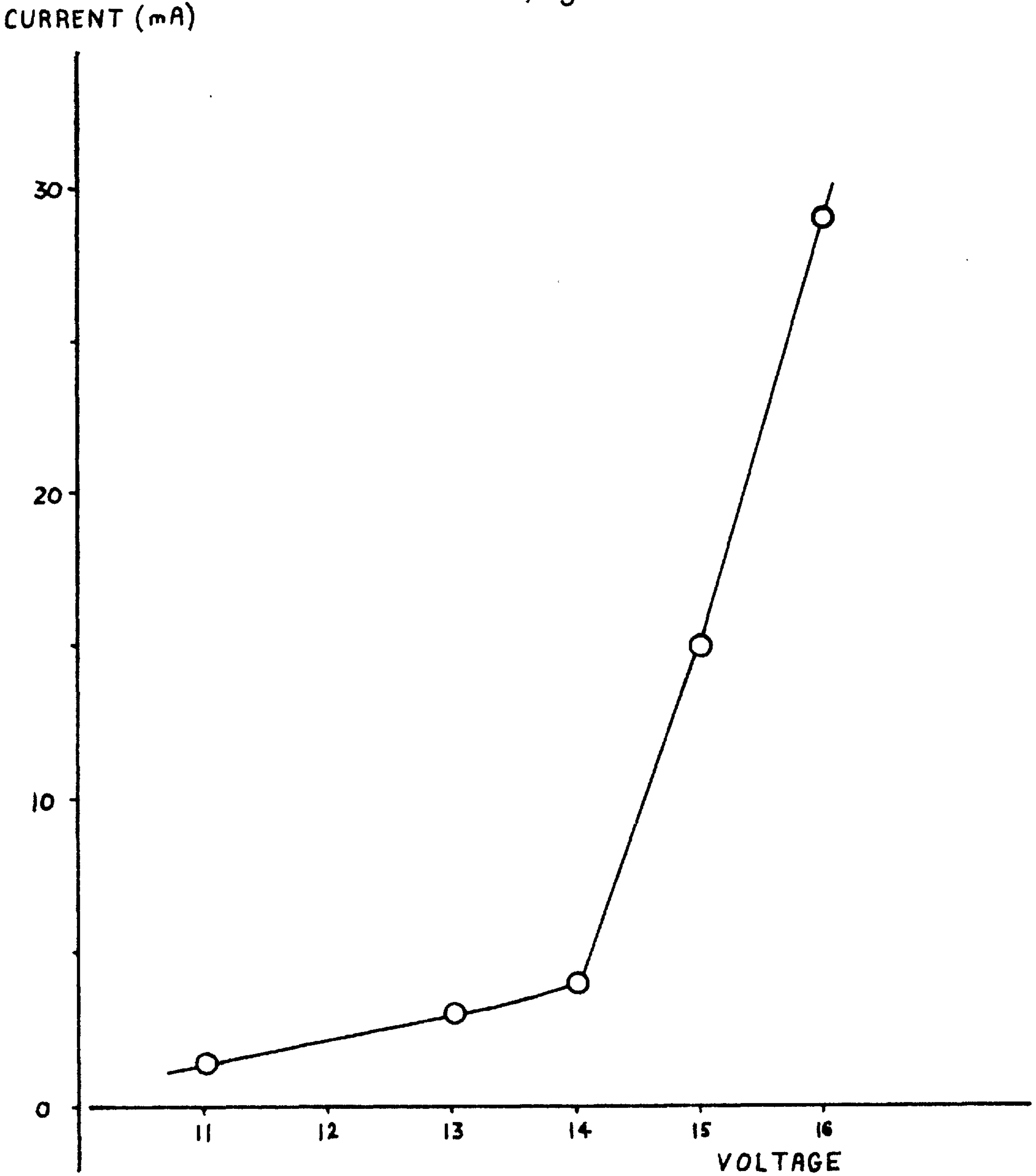

enhance the decomposition rate either by a mercury photosensitised reaction or by being an oxygen scavenger.

A reasonable approximation to the thresholds may be obtained from studying the filament heating voltage required to maintain a total current of 5mA in the reaction vessel. This follows from the fifth column of table 9 where it can be seen that a heating voltage of 6.9 volts was required in run 89b where decomposition did not occur whereas the heating voltage was significantly lower in the remainder of the runs in which decomposition did occur. Therefore a run (Run 92) was performed in which the current was measured as a function of accelorating voltage using a constant heating voltage of 6.9 volts. The results obtained are reproduced in figure 13 and it can be seen that a large increase in current is observed at approximately 14 volts. If a similar reaction is occuring in the presence and in the absence of carbon these results would support the conclusion that the threshold for decomposition of carbon monoxide in the presence of carbon occurs at approximately 14 volts.

This observed difference in current with applied voltage, especially near the thresholds for decomposition, led to the performance of a series of experiments in a flowing system of carbon monoxide in which the current was measured as a function of applied voltage for constant filament temperature.

5.4. Conclusions from Static Runs.

1) At constant currents the rate of carbon monoxide decomposition is proportional to the carbon monoxide pressure.

2) In the presence of carbon the threshold for decomposition to commence is probably 14 volts.

3) In the absence of carbon the threshold for decomposition to commence is between 24 and 26 volts.

B. Flow experiments.

5.5. Experimental procedure.

The electrode assembly used in this series of experiments was the same as in the static experiments. A fresh filament was used for each run and a fresh carbon film was used for each run in the presence of carbon.

After the system had been degassed and the filament formed the system was pumped for thirty minutes under the highest vacuum obtainable. Carbon monoxide was them pumped through the system at such a rate that the pressure on the Macleod gauge was approximately 20μHg. The relevant potential was applied between the filament and the anode and the filament was then switched on and adjusted until it was at a temperature of 850°C. The current was noted at half minute intervals and each run was performed for a total time of 27 minutes. The pressure in the system was measured periodically and,

FIGURE 14

CURRENT FROM FILAMENT AT 850°C AS FUNCTION OF TIME

CARBON PRESENT CO FLOW PRESSURE 20 μ Hg.

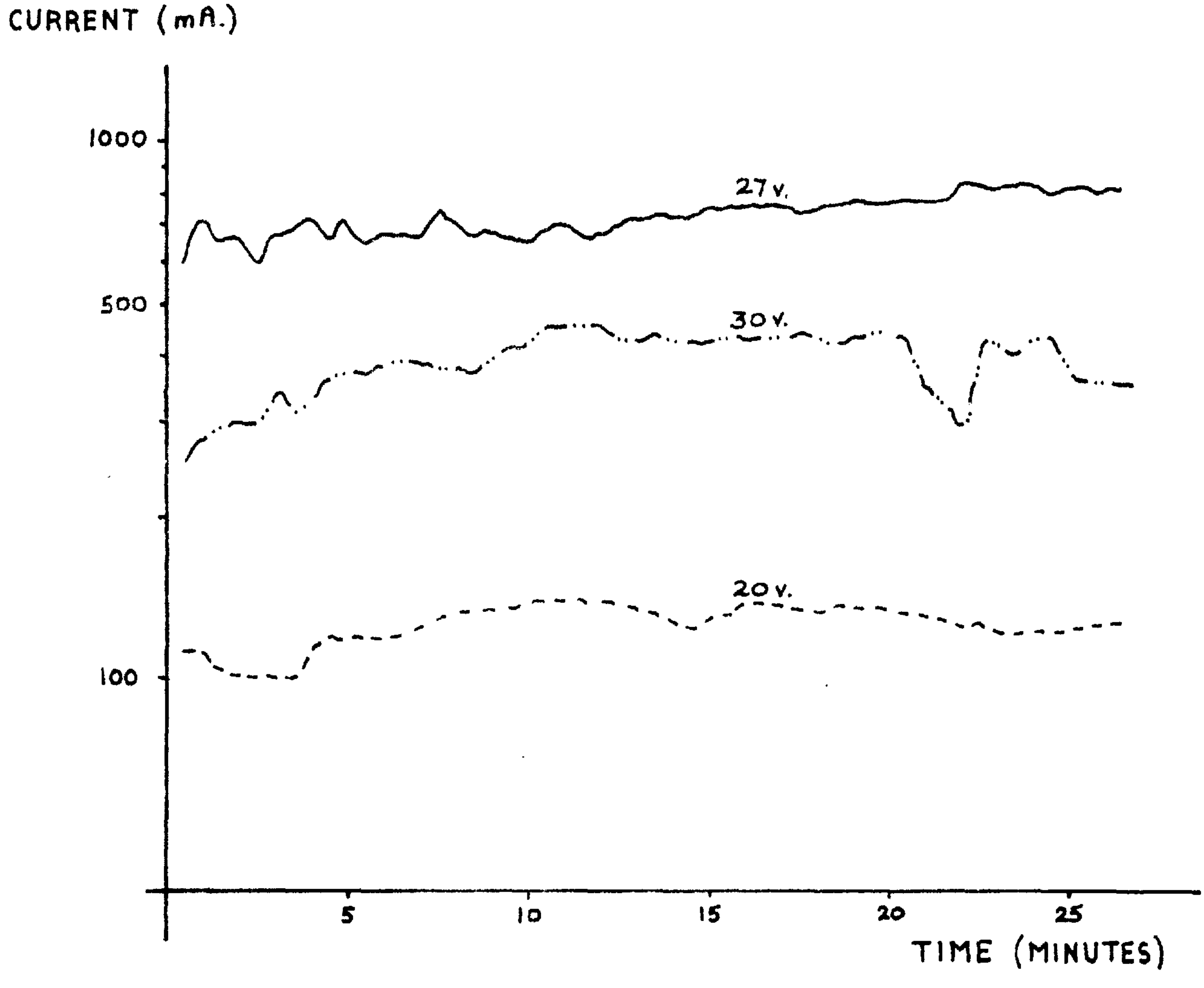

FIGURE 15

CURRENT FROM FILAMENT AT 850°C AS FUNCTION OF TIM

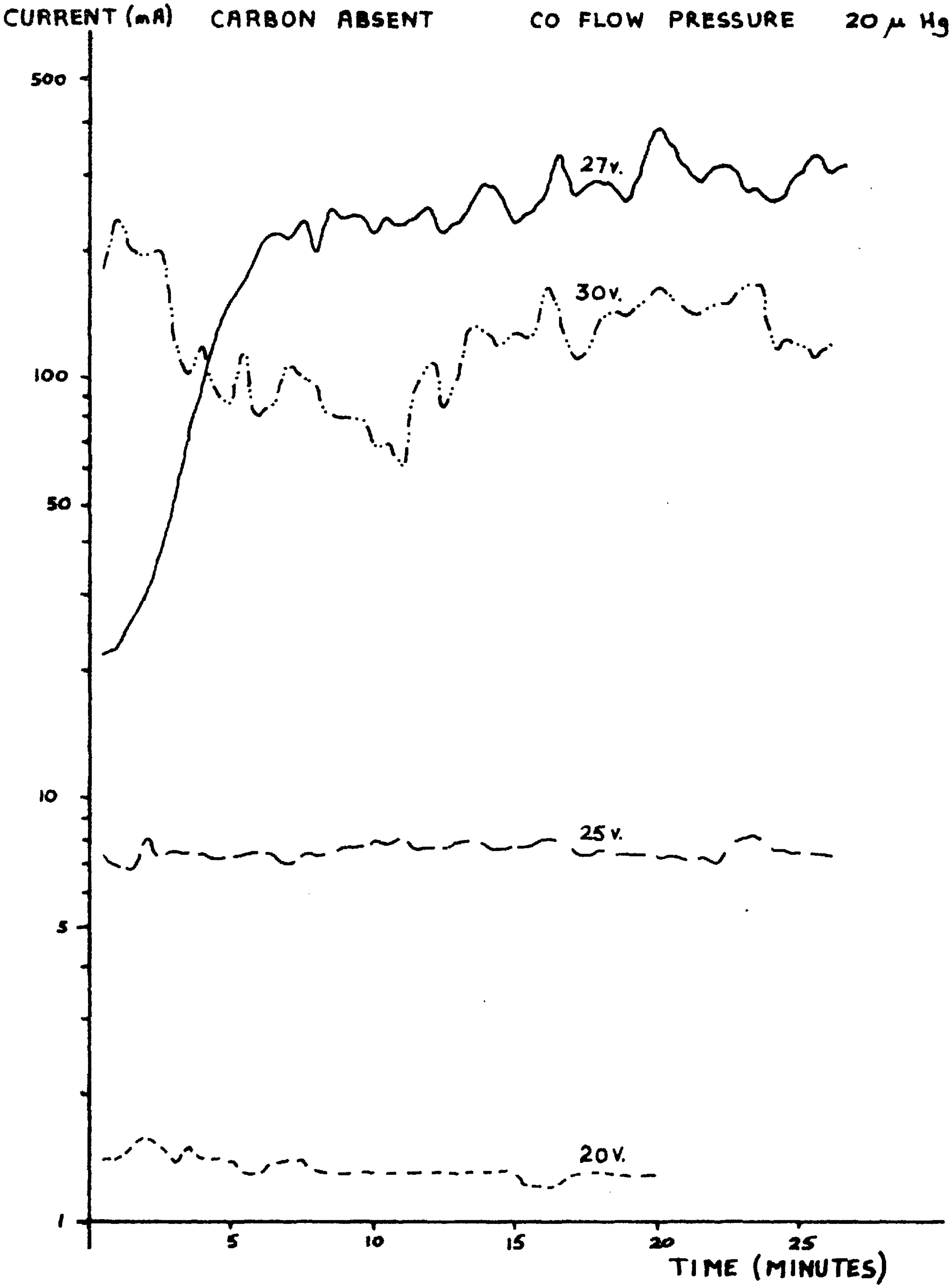

if necessary, the needle-valve was adjusted to maintain as constant a pressure as possible.

5.6. Results.

The results obtained in this series of experiments are reproduced in graphical form in figure 14 for the runs performed in the presence of carbon and in figure 15 for the runs performed in the absence of carbon. The current is plotted on a logarithmic scale as a function of time. As with the experiments in a static system the results of these experiments in a flowing system show a remarkable difference in behaviour depending on the presence or on the absence of carbon in the reaction vessel.

For all three runs performed in the presence of carbon the currents were very steady and at values greater than 100 mA. and they were accompanied by an intense pale blue glow discharge.

For the runs performed in the absence of carbon there was a much greater spread in values of the current obtainable. For the runs performed at 20 and 25 volts the currents were again very steady, but at very low values, and there was no glow present in the system. The run at 30 volts had an erratic current characteristic and was accompanied by an intense pale blue glow discharge. The run at 27 volts proved the

FIGURE 16

RATIO OF $\frac{\text{CURRENT WITH CARBON ABSENT } (I_1)}{\text{CURRENT WITH CARBON PRESENT } (I_2)}$

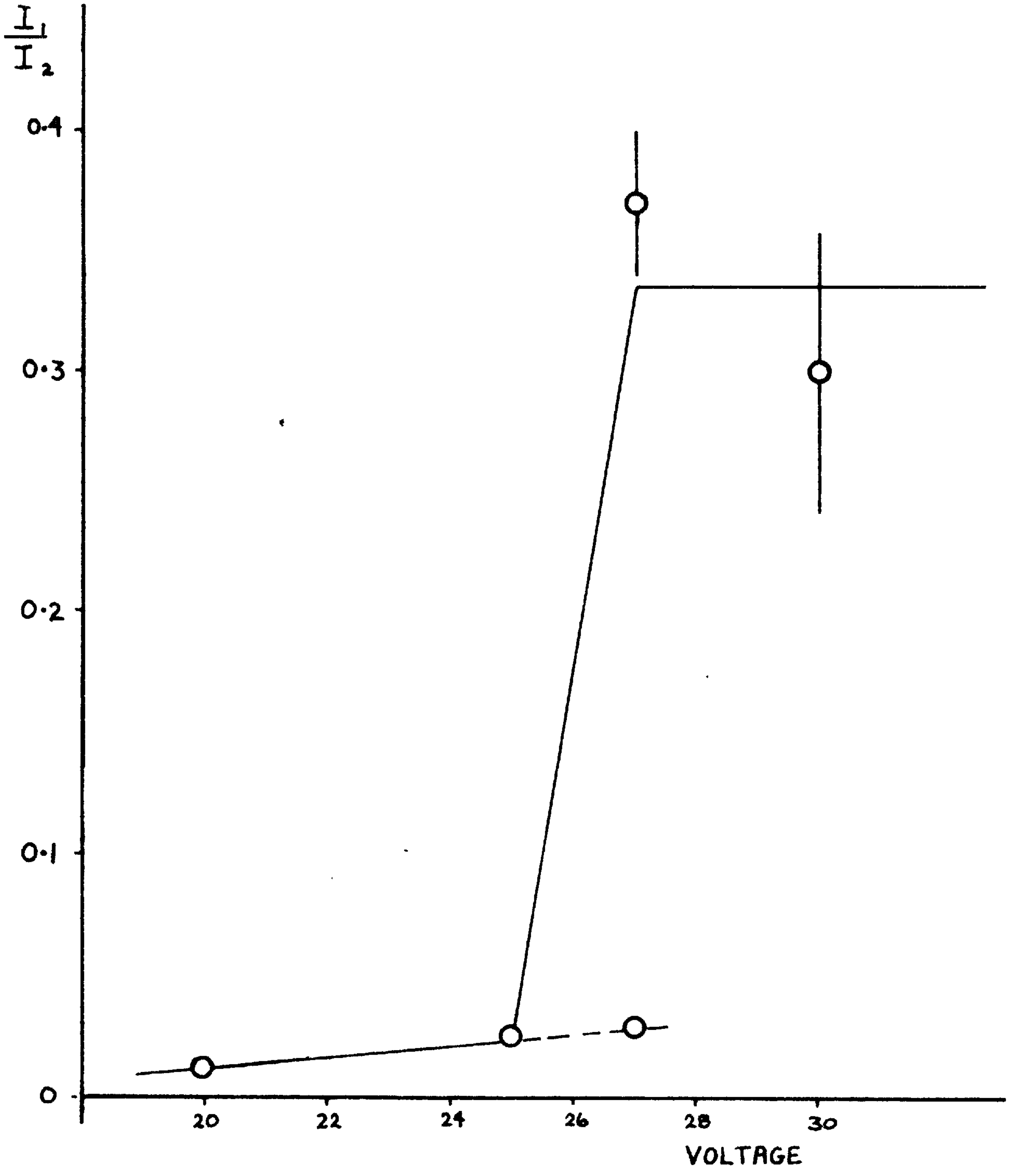

most interesting. At the start of the run the current was fairly low and the discharge was faintly visible but as time progressed the current increased rapidly and the discharge increased in intensity until a seemingly steady state was reached. It should be noted, also, that when the apparatus was dismantled at the end of the runs at 27 and 30 volts a brownish deposit was noticed on the aluminium anode and indicated that some form of deposition had taken place. No such deposits were present at the end of the runs at 20 and 25 volts.

The ratios of currents obtained in the absence of carbon to those obtained in the presence of carbon are given in table 10. It is assumed that the current obtainable in the presence of carbon and at an applied voltage of 25 volts would be of the order of 300 ± 100 mA. The values of these ratios are reproduced in figure 16 as a function of applied voltage. Once again there is a definite sharp increase occurring between 25 and 27 volts which is in agreement with the runs in a static system.

It should be remembered that all these runs in a flowing system were performed using a constant filament temperature and, therefore, an approximately constant primary electron current. This would mean that the large currents recorded would contain a great proportion of ions and secondary electrons.

5.7. Discussion of results.

It has been shown that in both the static and the flow experiments the behaviour of carbon monoxide under bombardment of low energy electrons is significantly different in the presence of a carbon surface than in its absence.

It was concluded from the static experiments that, when a constant current is used, the threshold energy of the electrons required to promote decomposition is approximately 14eV in the presence of carbon and approximatley 25eV in the absence of carbon. It was concluded also that when the decomposition was at a minimum the contribution to the total current by the primary electrons from the filament was at a maximum. This suggests that ions play a major role in the decomposition mechanism.

It was concluded from the flow experiments, in which a constant filament temperature was used, that the ratio of the current obtained in the absence of carbon to the current obtained in the presence of carbon underwent a marked transition at between 25 and 27 volts. This transition point marked also the appearance of an intense pale blue glow discharge and the appearance of solid deposits in the reaction vessel. Owing to the close agreement of this transition point with the upper threshold value from the static experiments it is reasonable to conclude that the same phenomenon is being observed in the two cases when a carbon surface is absent from the reaction vessel. That the current was considerably higher in the cases where decomposition was known to occur supports the hypothesis that ionic species are important in the decomposition mechanism.

A qualitative idea on the difference in behaviour of carbon monoxide decomposition in the presence and in the absence of a carbon surface may be obtained from the work of Bromley and Strickland-Constable[56] who postulated that the rate of a reaction which produces a solid and a gaseous product, such as $2CO=CO_2+C$, must be proportional to the amount of solid product present. Their argument was as follows: consider a vessel with inert walls and containing carbon in equilibrium with CO and CO_2. In this system the rate of the reverse reaction

$$CO_2 + C = 2CO$$

must certainly be proportional to the surface area of solid carbon present since the carbon is in this case one of the reactants. But, since the gase are in equilibrium it must be assumed that the forward and back reactions are proceeding at equal rates in opposite directions: therefore, the rate of the forward reaction must also be proportional to the surface area of carbon present; and this will apply, at any rate approximately, even when the system is not in equilibrium.

They concluded, therefore, that the rate of the reaction of CO with CO will be proportional to the surface area of carbon present. Physically this must be explained by assuming that the reaction proceeds as a catalytic reaction on the carbon surface. In the absence of any free carbon the initiation of the reaction $2CO = CO_2 + C$ may be expected to be attended with special difficulty.

This argument was developed to explain the normal thermal reaction but, if it can be applied also to the radiation induced reaction, it does give a qualitative explanation of why more energy is required to initiate the decomposition of carbon monoxide in the absence of a carbon surface.

What is now needed is a quantitive explanation of the energy difference and an idea of the reactions involved in the two cases. If the assumption that the threshold energy in the presence of carbon is approximately 14 eV is correct then the primary step in the decomposition mechanism will be

$$CO + e \rightsquigarrow CO^+ + 2e \quad ..... \ 14.1eV.$$

The ion may then react in one of three possible ways:

1) by recombination with an electron leading to dissociation into carbon and oxygen atoms and the subsequent reaction with the carbon surface.

i.e. $$CO^+ + e \rightarrow CO^* \rightarrow C + O$$

$$C_s + O \rightarrow C(O)$$

$$C(O) + O \rightarrow CO_2$$

$$C(O) + CO \rightarrow CO_2 + C_s$$

The reaction $CO + O \rightarrow CO_2$ is ruled out since this would be independent of the carbon surface.

2) by direct reaction of the ion with a surface oxide already present

$$CO^+ + C(O) \rightarrow CO_2^+ + C_s$$

and subsequent neutralisation of the dioxide ion. This reaction could take another form wherin the CO^+ ion is adsorbed on the carbon surface and subsequently reacts with a further adsorbed ion or with a CO molecule coming from the gas phase.

or 3) by reaction with a neutral CO molecule in the gas phase to form a metastable ionic complex which reacts with the carbon surface to form carbon dioxide

$$CO^+ + CO \rightarrow CO.CO^+$$

$$CO.CO^+ + C_s \rightarrow CO_2^+ + 2C_s$$

In the last two alternatives proposed a positive ion is assumed to react with or be adsorbed by the carbon surface which is positively charged. This is feasible since a discharge is present in all cases where decomposition takes place. Under discharge conditions most of the potential drop takes place close to the cathode and thus there is only a slight potential gradient near the anode which the positive ions would have to overcome.

An alternative mechanism which could explain the results is the ionisation of a carbon dioxide surface complex and the subsequent break-away of this ion from the surface:

$$\mathrm{CO} \rightsquigarrow \mathrm{C} + \mathrm{O}$$

$$\mathrm{C_s} + 2\mathrm{O} \longrightarrow \mathrm{C(O_2)}$$

$$\mathrm{C(O_2)} + e \longrightarrow \mathrm{C(O_2)}^+ + 2e$$

$$\mathrm{C(O_2)}^+ \longrightarrow \mathrm{CO_2}^+$$

Possible support for this last mechanism comes from the third step enumerated which is a current multiplication process. Such a process must occur in order that the large currents noted in section 5.6 may be obtained. Furthermore, in the runs performed in the absence of carbon these large currents were obtainable only in the cases where carbon deposits were formed and this finding may indicate that the current multiplication process does take place on the carbon surface.

When carbon is absent from the reaction vessel the threshold for decomposition to commence is between 24 and 26 eV. The possible excitation processes known to occur in this region are as follows:-

$$\mathrm{CO} \rightsquigarrow \mathrm{C}^-(^4\mathrm{S}) + \mathrm{O}^+\ (^4\mathrm{S}) \quad \ldots\ldots \quad 23.6\,\mathrm{eV}$$

$$\rightsquigarrow \mathrm{C}(^3\mathrm{P}) + \mathrm{O}^+\ (^4\mathrm{S}) \quad \ldots\ldots \quad 24.8\,\mathrm{eV}$$

$$\rightsquigarrow C(^1D) + O^+ (^4S) \quad \ldots\ldots \; 25.8\,\text{eV}$$

$$\rightsquigarrow CO^{+*} \quad \ldots\ldots \; 25.7\,\text{eV}$$

If one of these excitation processes leads to the decomposition of carbon monoxide in the absence of carbon it should be possible to use it to explain how the carbon monoxide decomposes purely in the gas phase.

The first process involves a negative ion and would not be expected to play a major role in the decomposition owing to its difficulty of production and also owing to the rapid recombination reaction expected to occur. However, the oxygen ion could react with a CO molecule and the carbon ion could be electrically attracted to the aluminium anode where it would form a carbon deposit

i.e. $CO \rightsquigarrow C^- + O^+$

$$CO + O^+ \longrightarrow CO_2{}^+$$

$$C^- + \text{Anode} \longrightarrow C_s$$

Once the carbon deposit formation reaches a critical rate or size one would expect the overall reaction to be consistent with the "carbon present" case. This would explain the fact that the rates of decomposition in the "carbon present" and the "carbon absent" cases appear to approach one another at electron energies greater than 30 eV, as shown in figure 12.

The middle two processes, occurring at 24.8 and 25.8 eV, involve an oxygen ion only and the reaction scheme in these cases could lead to the gaseous formation of CO_2 in a similar manner to above.

$$
\begin{aligned}
&CO \rightsquigarrow C^{(*)} + O^{+} + e \\
&CO + O^{+} \rightarrow CO_2^{+} \\
&C^{(*)} + C^{(*)} \rightarrow C_2
\end{aligned}
$$

The last reaction in this scheme would be the initiation of the carbon deposit formation.

The process leading to the formation of an excited carbon monoxide ion occurring at 25.7eV could possibly promote the gaseous decomposition to CO_2 in the following scheme:-

$$
\begin{aligned}
&CO \rightsquigarrow CO^{+*} + e \\
&CO^{+*} + CO \rightarrow (CO.CO^{+})^{*} \\
&(CO.CO^{+})^{*} \rightarrow CO_2^{+} + C \\
&C + C \rightarrow C_2
\end{aligned}
$$

This reaction scheme is made feasible when one considers the fact that the excitation energy of the carbon monoxide ion is 11.6eV above the ground state and, therefore, it has sufficient energy to dissociate a neutral carbon monoxide molecule.

In this discussion various reaction schemes have been suggested for the decomposition of carbon monoxide both in the presence and absence of free carbon. There is no conclusive evidence to support any single one of these but they may lead some light on the mechanism of carbon monoxide decomposition. However, it is apparent that ions do play a major role in this decomposition.

5.8. Summary

It has been shown that the threshold energy of the bombarding electrons required to promote decomposition of carbon monoxide depends on the presence or absence of a carbon surface in the reaction vessel. In its presence the threshold energy has been found to be 14eV, while in its absence the threshold energy has been found to be approximately 25eV.

In a static system, in which constant currents were used, the rate of decomposition has been found to obey a first-order law.

In a flow system, in which constant filament temperatures were used, it has been found that under conditions where carbon monoxide decomposes much greater currents were obtainable than under conditions where carbon monoxide remains stable.

The threshold obtained at 25eV in the absence of a carbon surface has been shown to be the appearance potential of a pale blue glow discharge and also the appearance potential for the formation of carbonaceous deposits.

From the excitation and ionisation thresholds known to occur in carbon monoxide it has been possible to construct several reaction mechanisms which could possibly explain the observed phenomena but there is no conclusive evidence to support any single one of them.

CHAPTER 6

SPECTROGRAPHIC STUDY OF THE GLOW DISCHARGE.

6.1. Introduction.

A constant feature of the work carried on with this apparatus was the presence of a glow discharge in the reaction vessel when currents greater than approximately 10 milli-amps were employed. A discharge could be produced in mercury vapour, carbon monoxide or carbon dioxide and in all three cases it was pale blue in colour. Furthermore, it was noted in section 5.6 that the discharge was present only in the cases where carbon monoxide was found to decompose and this would tend to indicate that the species responsible for the decomposition could possibly make some contribution to the spectrum of the discharge. Therefore this spectroscopic study of the discharge was undertaken to determine the species responsible for its appearance.

6.2. Experimental Procedure and results.

The electrode assemly was set up as described in section 5.2. The aluminium anode had linear dimensions of 8x7 cms to enable a wide vertical slit to be included in the anode to give a reasonable radiation intensity at the spectrograph slit. The plane of the anode slit was focused onto the plane of the spectrograph slit to enable the discharge occurring near the carbon surface to be photographed. The instrument used was a Zeiss medium quartz spectrograph which had a working range of 2000 to 5600 A^o but the Pyrex walls of the reaction vessel set a lower limit of the spectra obtainable at 2900 A^o. The photographs were taken using Ilford HP3 plates.

The apparatus was set up as previously described and photographs were taken of the spectra of the discharge produced under the following conditions.

a) Evacuated vessel. This corresponded to pressures less than 10^{-5}mm Hg on the Macleod gauge and meant that the gas in the reaction vessel was predominantly mercury vapour.

b) Flowing CO with carbon present and with mercury vapour present or absent. The mercury vapour was excluded from the reaction vessel by shutting of the tap between the reaction vessel and the Macleod gauge.

c) Flowing CO_2 with carbon present and with mercury vapour present or absent.

d) Flowing CO_2 with carbon absent and with mercury vapour present.

In order to obtain reasonable exposure times - of the order of 30 minutes - currents of the order of 200 mA had to be employed in all cases.

FIGURE 17

Spectra obtained with flowing carbon monoxide - carbon present.

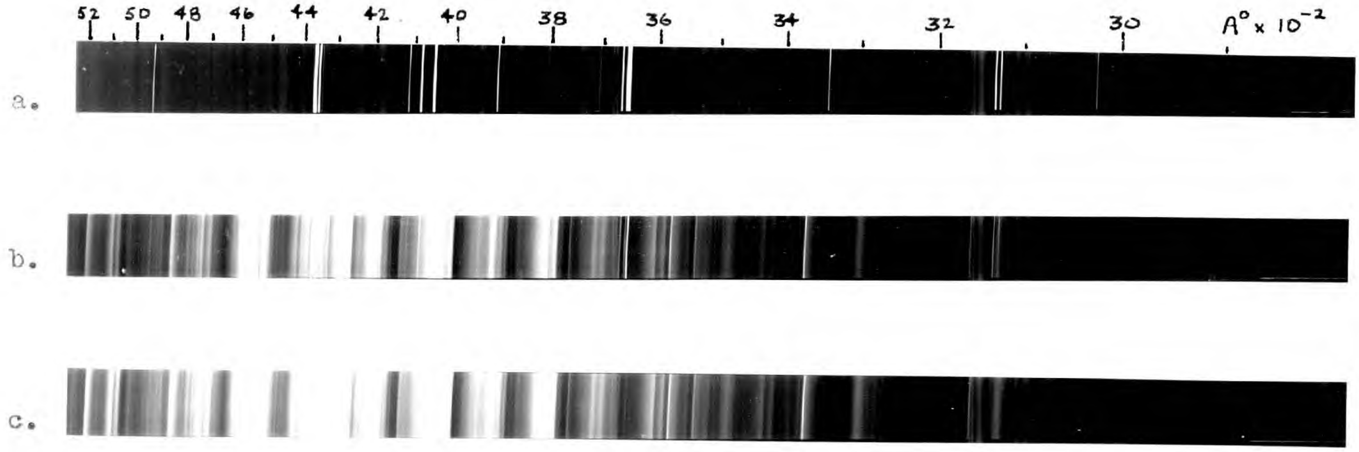
52
50
48
46
44
42
40
38
36
34
32
30
$A^\circ \times 10^{-2}$
a.
b.
c.

a. Evacuated discharge

b. Flowing carbon monoxide - mercury present

c. Flowing carbon monoxide - mercury absent

FIGURE 18

Spectra obtained with flowing carbon dioxide - carbon present

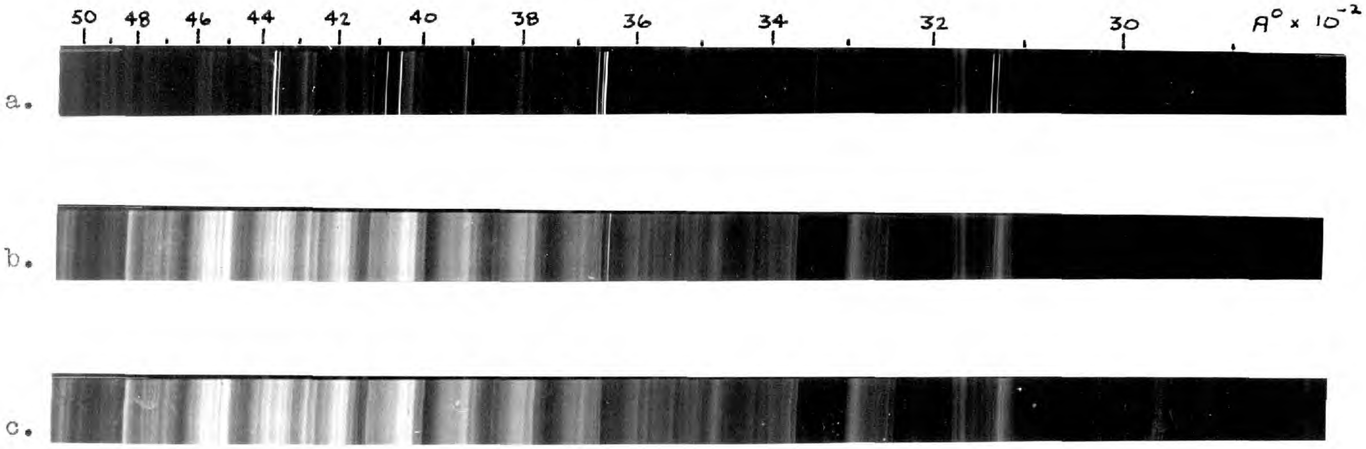
50
48
46
44
42
40
38
36
34
32
30
A° x 10⁻²
a.
b.
c.

a. Evacuated discharge

b. Flowing carbon dioxide - mercury present

c. Flowing carbon dioxide - mercury absent

Photographs of the spectra obtained for conditions a), b) and c) are reproduced in figures 17 and 18. The following features can be observed in the spectra:

1) In figure 17 the "evacuated" spectrum corresponds to the pure mercury discharge. In figure 18 the corresponding spectrum shows traces of the CO^+ comet-tail system.

2) The spectra obtained in the presence or absence of mercury vapour are identical except for the presence or absence of the mercury lines. This shows that the mercury has no effect on the main spectra and from this one could possibly conclude that mercury has no effect on the reactions of CO and CO_2 with the carbon surface.

3) The spectra obtained with CO and CO_2 are identical in so far as they have exactly the same band systems present although the relative intensities of the individual band systems are somewhat different in the two cases. The spectrum obtained with carbon absent and with flowing CO_2 (not shown in text) appeared to have exactly the same form as when carbon was present.

The analysis of the spectrum obtained with flowing CO in the presence of mercury vapour and carbon (figure 17b) is given in table 11 and the analysis of the spectrum obtained with flowing CO_2 in the presence of mercury vapour and carbon (figure 18b) is given in table 12. The band heads were measured to approximately 1 A^{o} by using a three constant formula for the wavelength scale and were identified using the tables compiled by Pearse and Gaydon[57]. The band systems definitely identified are given in table V.

TABLE V

Band systems identified in spectra

1)	CO^{+}	Comet - tail
2)	CO	Angstrom
3)	CO	3rd Positive
4)	CO	Triplet
5)	CO_2	Fox, Duffendack and Barker
6)	Hg	(line spectrum)
7)	N_2	2nd positive
8)	N_2^{+}	1st negative

The two nitrogen band systems were identified in the CO spectrum only and arose probably from being an impurity in the original supply cylinder. The absence of other band systems in the CO spectrum and the absence of any foreign band system in the CO_2 spectrum served to demonstrate the purity of the inlet gases.

The extremely crowded nature of the overlapping band systems identified may have masked the presence of weaker band systems or line spectra but it can be concluded that there was no evidence of appreciable concentrations of

FIGURE 19

ELECTRONIC ENERGY LEVELS AND BAND SYSTEMS FOR CO AND CO$^+$

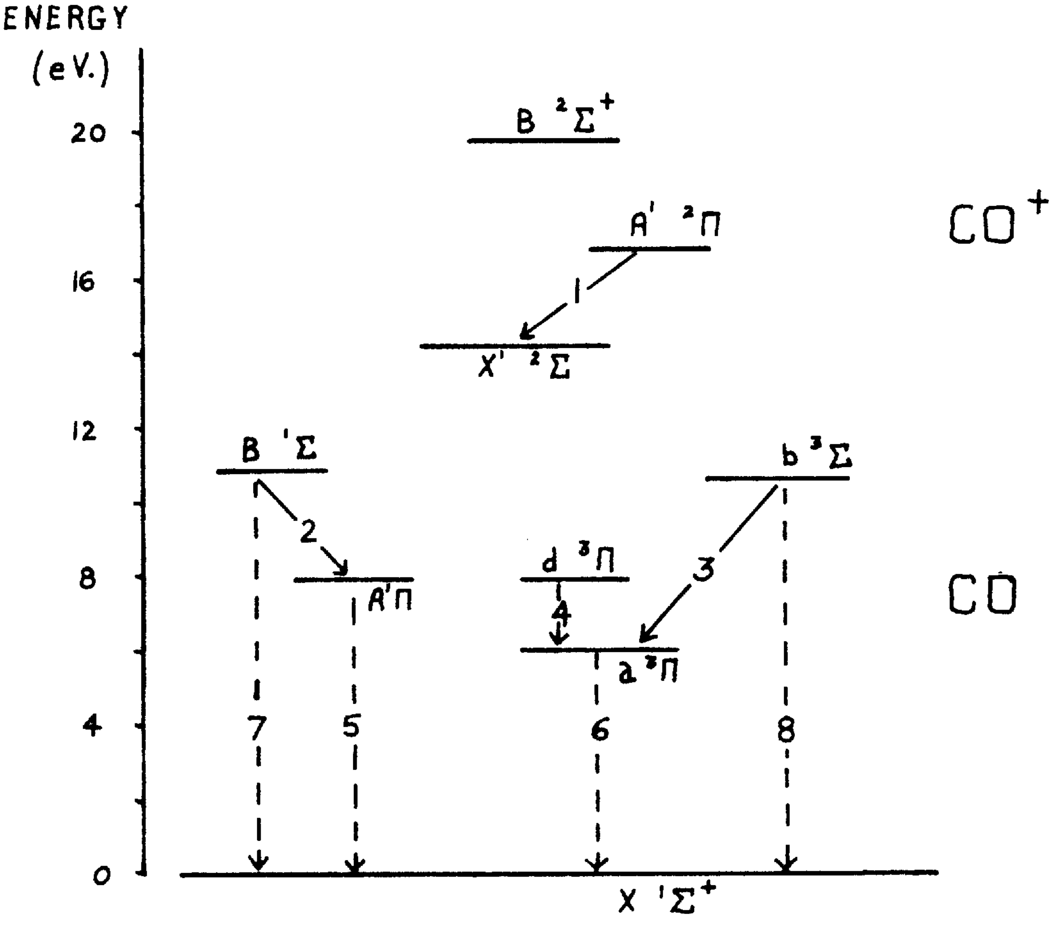
ENERGY
(eV.)
20
16
12
8
4
0
B $^2\Sigma^+$
A' $^2\Pi$
X' $^2\Sigma$
CO$^+$
B $^1\Sigma$
A'Π
d $^3\Pi$
a $^3\Pi$
b $^3\Sigma$
CO
1
2
3
4
5
6
7
8
X $^1\Sigma^+$

1.	CO$^+$	COMET-TAIL
2.	CO	ANGSTROM
3.	CO	3 RD. POSITIVE
4.	CO	TRIPLET
5.	CO	4 TH. POSITIVE (2800 - 1000 A°)
6.	CO	CAMERON
7. } 8. }	CO	HOPFIELD AND BIRGE

O, O^+, O_2, O_2^+ or C^+ in the discharge. This does not mean that such species are not present since their "free" life-time may be much shorter than their radiative life-time; i.e. they may undergo chemical reaction before they have a chance to be detected by the spectrograph.

A diagram of the electronic energy levels involved in the band systems identified for CO and CO^+ is reproduced in figure 19. In this diagram the full lines represent the band systems identified from the spectra and the broken lines represent systems probably present but undetected due to the lower limit of 2900 A^o imposed by absorbtion by the pyrex walls of the reaction vessel. The Cameron bands extend from 2600 to 2000 A^o, the 4th positive bands extend from 2800 to $1000A^o$ while the Hopfield and Birge extend down to less than $1000A^o$.

In table III of section 2.2 the values of the dissociation limits for CO_2 are given in electron volts. These values correspond to approximately 2,240 A^o for the production of $O(^3P)$ atoms, 1670 A^o for $O(^1D)$ atoms and 1,270 A^o for $O(^1S)$ atoms. This demonstrates that the far ultra-violet bands are energetic enough to photolyse the carbon dioxide. This may have a significant effect in all the reactions studied in the presence of the glow discharge.

CHAPTER 7

CARBON-14 TRACER TECHNIQUE

7.1. Introduction

When employing currents of the order of 200 milli-amps Claxton[53] was able to obtain carbon weight losses of approximately 3×10^{-4} milligrams per milli-amp minute. These currents were obtained with an accelerating voltage of 25 volts and could be maintained for periods of time of 60 minutes or longer. This meant that significant weight changes could be obtained in a reasonable reaction period. However, when lower accelerating voltages are employed with the electrode assembly used the current falls off drastically and to obtain the same weight losees the reaction times would become correspondingly longer. To overcome this difficulty a carbon-14 tracer technique has been developed to increase the sensitivity of the apparatus so that lower voltages and, more particularly, lower currents can be employed. The carbon surfaces prepared by burning napthalene in air and depositing the soot onto aluminium backings were replaced by carbon-14 doped surfaces prepared by cracking methane onto suitable backing materials. The reactions of gases with these surfaces could be monitored by following the transfer of carbon-14 from the solid phase into the gas phase.

Three possible methods of monitoring the carbon-14 were considered:-

1) the classical method of converting the carbon-14 to CO_2, absorption of this in sodium hydroxide solution and finally precipitation as $Ba^{14}CO_3$; the $Ba^{14}CO_3$ samples then being counted with a thin-window Geiger counter;

2) the use of $^{14}CO_2$ as part of the filling gas of a CO_2-CS_2 Geiger counter;

3) the use of a gas scintillation technique.

The first method has been used by many workers and has been found to be very reliable if somewhat cumbersome in application. Its main disadvantage is the low efficiency obtainable of a few percent and it was not considered further. The second method has an efficiency of 100% but trials to be described in section 7.2 have shown that reproducible and reliable filling mixtures for the Geiger tube are difficult to obtain. The third method of monitoring carbon-14 with a gas scintillation technique was finally adopted and has been found to be simple and reliable in operation with counting efficiencies of the order of 50%.

FIGURE 20

ANALYSIS SECTION FOR GAS GEIGER COUNTING

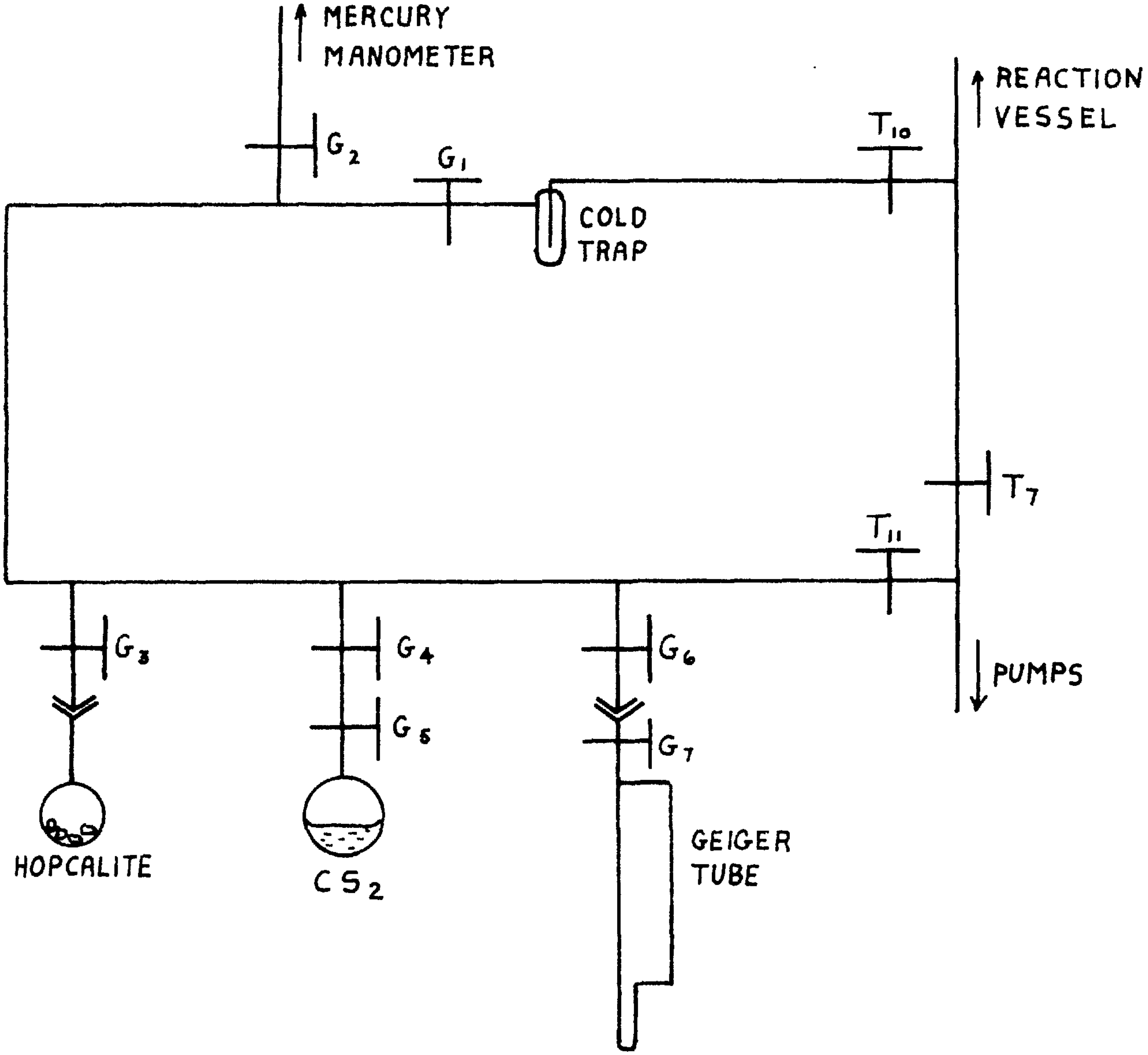
MERCURY MANOMETER
REACTION VESSEL
T_{10}
G_2
G_1
COLD TRAP
T_7
T_{11}
G_3
G_4
G_6
PUMPS
G_5
G_7
HOPCALITE
CS_2
GEIGER TUBE

7.2. Internal Geiger-counting technique

The use of an internal gas Geiger counter to monitor $^{14}CO_2$ was first reported by Brown and Miller[58,59]. They found that satisfactory counting characteristics could be obtained by filling a Geiger tube with CO_2 in the pressure range of 10 to 50 cms. Hg mixed with approximately 2 cms. Hg. pressure of CS_2 which acted as a carrier gas. They obtained good Geiger-Müller plateaus in the region between 2500 and 4500 volts, depending on the filling pressure, and the plateaus generally were between 200 and 300 volts wide. In this region the counter was 100% efficient and measured the absolute disintegration rate.

A diagram of the gas handling train for filling the Geiger tube employed in this work is reproduced in figure 20. In this train provisions are made for filling the tube with an inactive CO_2-CS_2 mixture and for converting CO to CO_2 to ensure that any gas entering the Geiger tube from the reaction vessel is CO_2 only. This latter provision is made necessary since it was shown in section 2-7 that the gasification of a carbon-14 surface leads to the appearance of ^{14}CO and $^{14}CO_2$ in the gas phase.

Madley and Strickland-Constable[60], among other workers, have shown that Hopcalite is an efficient oxidising agent for CO at low pressures. Hopcalite, supplied by Hopkin and Williams Ltd., is a commercial oxidising agent and is made up from a mixture of metallic oxides. Experiments were carried out on the oxidation of CO to CO_2 by Hopcalite under a variety of conditions in order to determine the best method of use. It was found that the most efficient and fastest way of oxidising very small quantities of CO was to use approximately 50 mgms. of Hopcalite heated to 100°C by an electric furnace and to collect the CO_2 in a liquid nitrogen cooled trap as soon as it was produced. Larger quantities of Hopcalite or dispensing with the liquid nitrogen cooled trap resulted in loss of gas by absorption on the Hopcalite which was difficult to recover. With this method efficiencies approaching 100% for converting CO to CO_2 could be obtained readily and reproducibly. Periodically the Hopcalite sample had to be renewed since with each charge of CO oxidised the rate of conversion would successively decrease. Attempts to re-activate spent Hopcalite samples by heating in an oxygen atmosphere proved inconsistent. Prior to use each fresh sample of Hopcalite was degassed by heating to 250°C while pumping at less than 10^{-5} mm. Hg. for several hours.

Analar grade carbon di-sulphide was stored in the bulb as shown in figure 20 and small quantities of vapour could be obtained by alternately opening and closing taps G_4 and G_5. The pure CO_2 filling gas for the Geiger tube was obtained from the storage section described in section 3.1.

The Geiger tube used was a GAIOM tube supplied by 20th Century Electronics Ltd. and it had cylindrical dimensions of radius 1.5 cms. and length 18 cms. The tube consisted of a cylindrical stainless steel cathode and a fine wire anode running down the axis. It could be attached to the vacuum system by means of a B10 cone and socket joint and had a cold finger attached to it for transfer of condensible gases. Prior to any run the tube was degassed to less than 10^{-5} mm. Hg. while being heated to 200°C.

It was decided that the filling mixture would be 20 cms. Hg. pressure of CO_2 and 2 cms. Hg. pressure of CS_2. At the start of any run this blank mixture was frozen out into the Geiger tube - the relevant pressures being measured on the mercury manometer.

In these trial experiments carbon-14 gas samples were obtained by reacting CO_2 with a carbon-14 containing surface deposited onto a cylindrical silica backing of radius 1.5 cms. and length 8.0 cms. The electrode arrangement in the reaction vessel was similar to that shown in figure 3 with the silica replacing electrodes A_1 and A_2. Static charges of CO_2 were irradiated for various lengths of time and at the end of each reaction the CO produced was oxidised to CO_2 and the total amount of CO_2 was then transferred to the filled Geiger tube. The Geiger tube

FIGURE 21

NEHER - HARPER QUENCHING CIRCUIT

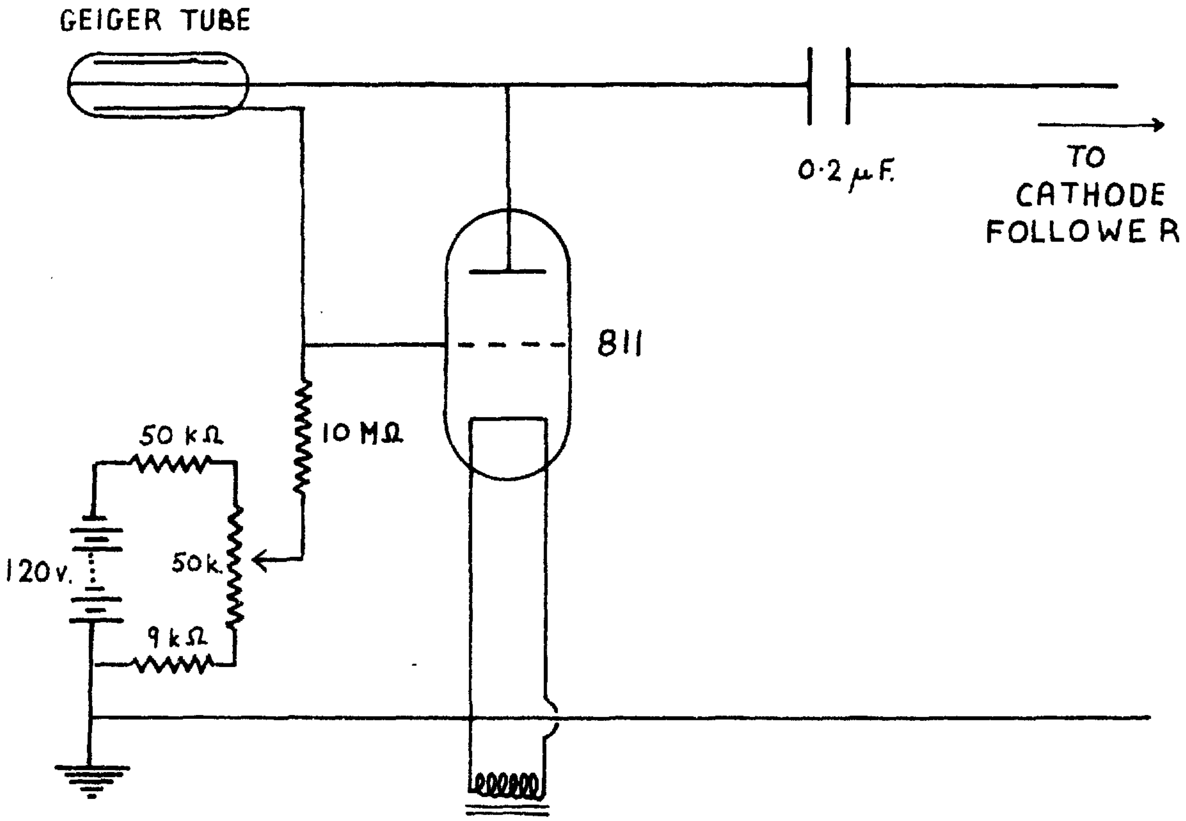
GEIGER TUBE
0·2 μF
TO CATHODE FOLLOWER
811
10 MΩ
50 kΩ
120 v.
50 k.
9 kΩ

was then isolated from the vacuum system by closing taps G_6 and G_7 and transferred to the counting system.

The use of counting equipment used to monitor the radio-activity in the gas mixture was kindly offered by Dr. D.W. Turner of the Chemistry Department and consisted of the following units:-

1) H.T. Unit working to 4000 Volts
2) I.D.L. Cathode Follower Type 658
3) I.D.L. Wide Band Amplifier Type 652
4) I.D.L. Scaler Type 1700

The first few samples measured showed no Geiger-Müller counting characteristics and the tube went into a continuous discharge at approximately 3000 volts. This indicated that the CO_2-CS_2 filling was not self quenching and that an electronic quenching circuit would have to be employed. Therefore, following Eidinoff[61], a Neher-Harper quenching circuit modified for use at high voltages was constructed.

The circuit diagram of this quenching circuit is shown in figure 21. The valve used is an R.C.A. transmitter triode type 811. This valve is biased to cut-off by the 50×10^3 ohm potentiometer so that in the quiescent state no current flows through the 10×10^6 ohm resistance. Once a negative pulse is developed in the Geiger tube the voltage at the anode drops and the valve becomes conducting and current flows in the grid circuit. This current causes a potential drop to develop across the 10 x 10^6 ohm resistance and therefore the potential of the cathode of the Geiger tube rises. This rise in cathode potential drops the potential across the Geiger tube to below its threshold value and thus prevents spurious discharges occurring and being counted on the scaler.

With this circuit installed the counting characteristics improved somewhat and the tube no longer went into a continuous discharge at 3000 volts. Of the twelve fillings investigated only one gave satisfactory counting behaviour with a reasonable plateau and single pulses. The remaining eleven samples each had a very short plateau and over this region each 'pulse' was recorded as a burst in the counts recorded of the order of 1000 events. This demonstrated that the quenching circuit was not functioning satisfactorily and that these spurious discharges were due probably to negative ion formation of some impurity in the tube.

Rather than develop this technique any further it was decided to go over to a gas scintillation technique which had been proved by other workers to be comparatively efficient and simple in operation.

7.3. Gas scintillation technique

A gas scintillation technique for monitoring the radiation from weak β-emitting gases was first reported by Stranks[62] and the method adopted here has been developed from his work by the Chemistry Division of AERE, Harwell. Essentially the method consists of transferring the radioactive gas to a glass cell whose walls are coated with a thin film of scintillator and counting the scintillations produced with a standard photo-multiplier assembly. In this method the counting is completely independent of the chemical form of the isotopic species and of the presence of trace impurities as long as the isotopic species and the impurities are in the gas phase. This leads to extremely simple gas handling techniques and to very accurate reproducibility.

In this work the chemical form of the isotopic species would be carbon-14 monoxide and carbon-14 dioxide and the gas handling techniques are to transfer these two components to the scintillation cell. Carbon dioxide was transferred by the use of liquid nitrogen. The carbon monoxide was transferred by absorption on silica gel. When cooled to 77°K silica gel is an efficient absorber of carbon monoxide and readily releases the absorbed gas when warmed up to room temperature.

FIGURE 22

ANALYSIS SECTION FOR GAS SCINTILLATION COUNTING

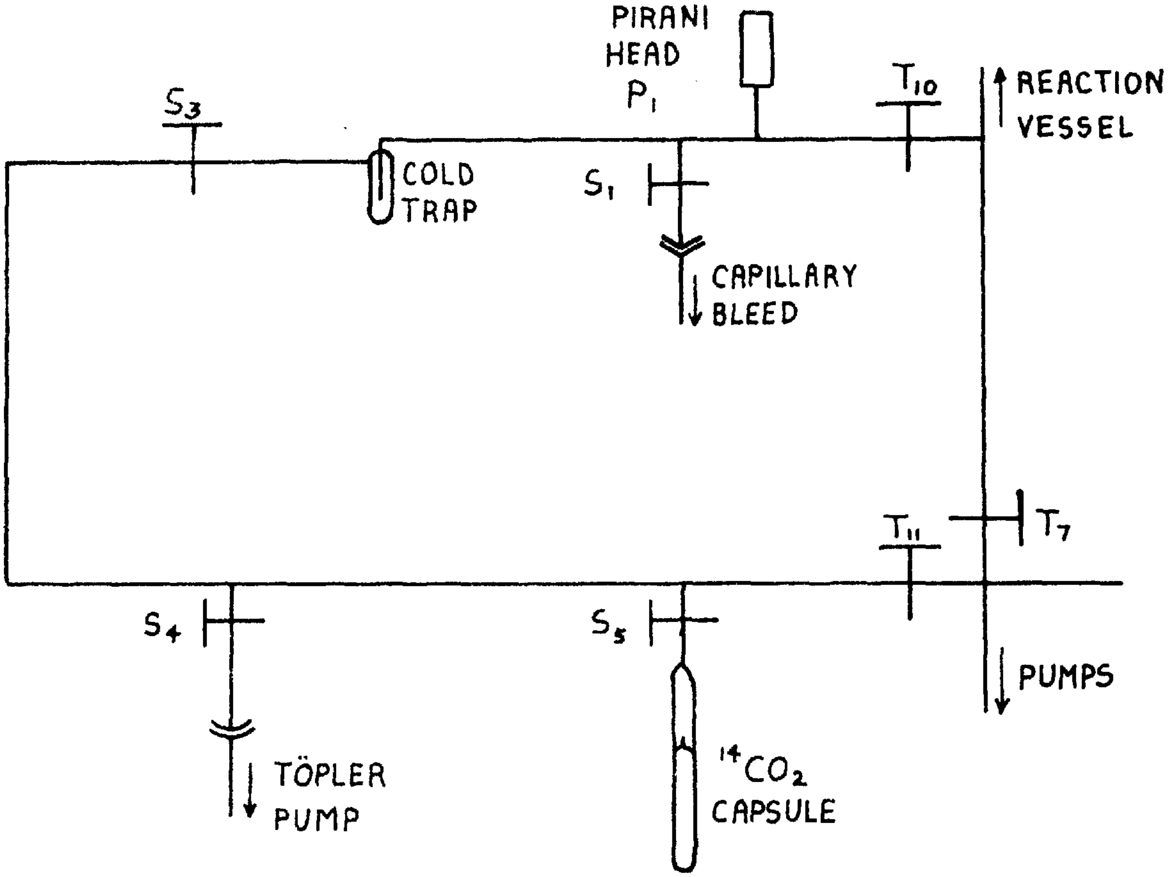
PIRANI HEAD P_1
S_3
COLD TRAP
S_1
CAPILLARY BLEED
T_{10}
REACTION VESSEL
T_7
T_{11}
S_4
S_5
PUMPS
TÖPLER PUMP
$^{14}CO_2$ CAPSULE

A diagram of the analysis section used for the gas scintillation counting is reproduced in figure 22. The Pirani head P_1 was connected to an Ionisation and Pirani Vacuum Gauge, Model I, supplied by Edwards High Vacuum Ltd., and served as a ready check on the gas pressure in the apparatus in the range between 1 and 200 µHg. The capillary bleed section served to collect all the gas employed in single pass flow runs in order that it could be analysed for carbon-14 content. At the end of a run this gas was transferred to the Töpler pump section to be transferred to the gas scintillation cell. A capsule containing 0.5 µC of $^{14}CO_2$ of specific activity 50 µC/mM was connected to the system below tap S_5 and served to determine the counting efficiency of the scintillation cell accurately and readily. The analysis section was connected to the reaction vessel via tap T_{10} and to the evacuating pumps via tap T_{11}.

Owing to the build-up of carbon monoxide from the thermal reaction of CO_2 with the filament, discussed in section 4.3, static runs could be performed for short reaction periods only. Flow runs reduce the concentration of carbon monoxide in the reaction vessel but in using carbon-14 all the gas employed in a reaction needs to be collected and with this in view the capillary bleed section was constructed. A diagram of this section is reproduced

FIGURE 23

CAPILLARY BLEED SECTION

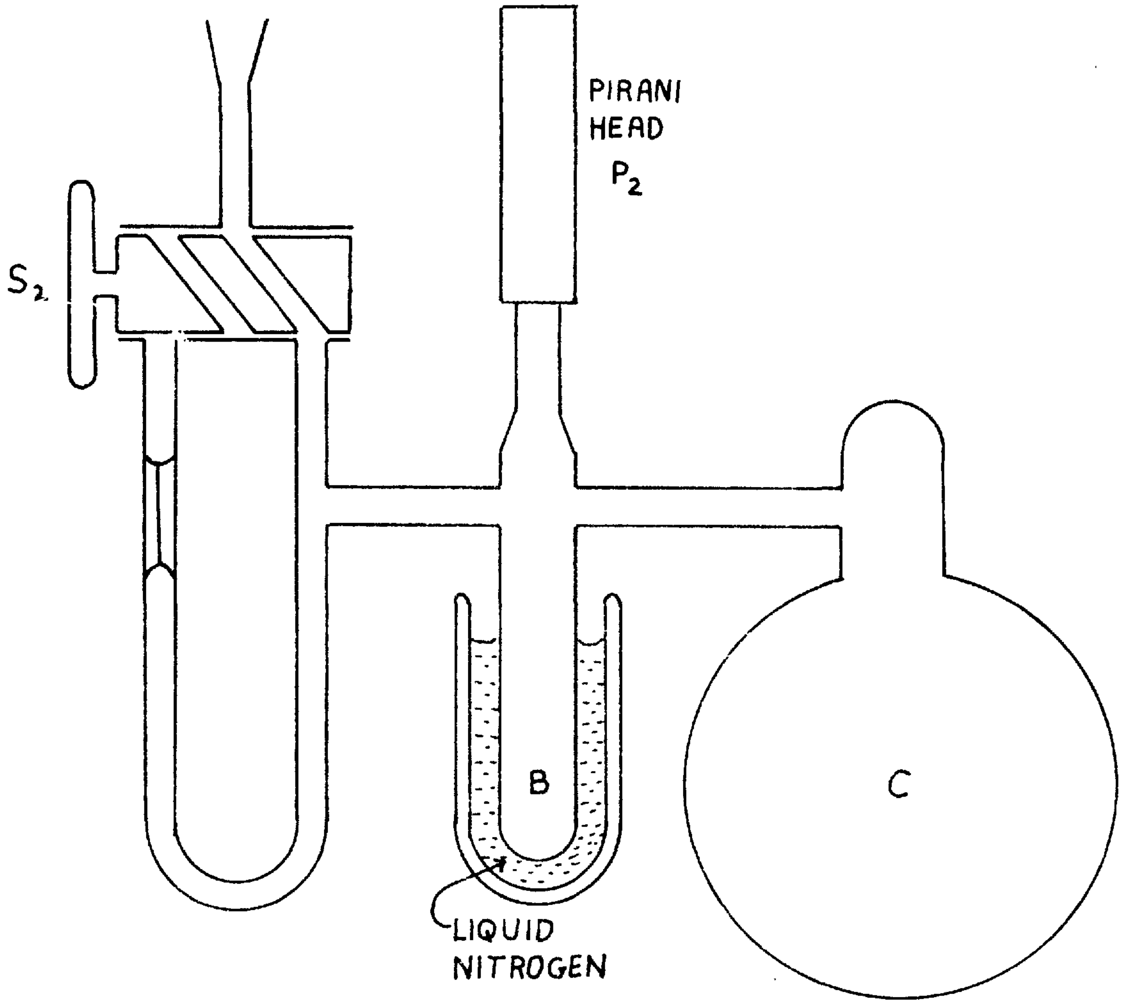
PIRANI
HEAD
P_2
S_2
B
C
LIQUID
NITROGEN

in figure 23. It consists of a large-bore two-way tap S_2 - in one arm of which was placed a short section of capillary tubing. During the course of a run gas would bleed through this capillary from the reaction vessel and the condensible fraction would be frozen out in the large liquid nitrogen trap (B) while the non-condensible fraction would collect in the large spherical vessel (C) of capacity 4 litres. The Pirani head P_2 served to monitor the pressure build-up of the non-condensible fraction. This bleed pump would work as long as the pressure inside it was lower than the pressure in the reaction vessel. The reaction times and currents in the reaction vessels were usually such that this pump worked satisfactorily and the carbon monoxide build-up was never great enough to affect the flow rate appreciably.

A diagram of the Töpler pump system finally employed for filling the scintillation cell is reproduced in figure 24. The scintillation cell is attached to the section with an S13 ball and socket joint above tap P_2 and the section is attached to the remainder of the system via two S19 ball and socket joints in the side-arm of tap P_1. The two T-bore taps P_1 and P_2 may be adjusted so that CO_2 may be frozen out on the cold finger in the main body of the pump, CO may be absorbed from the reaction vessel onto the silica gel in the tube below P_1 and subsequently

FIGURE 24

TÖPLER PUMP SYSTEM FOR FILLING SCINTILLATION CELL

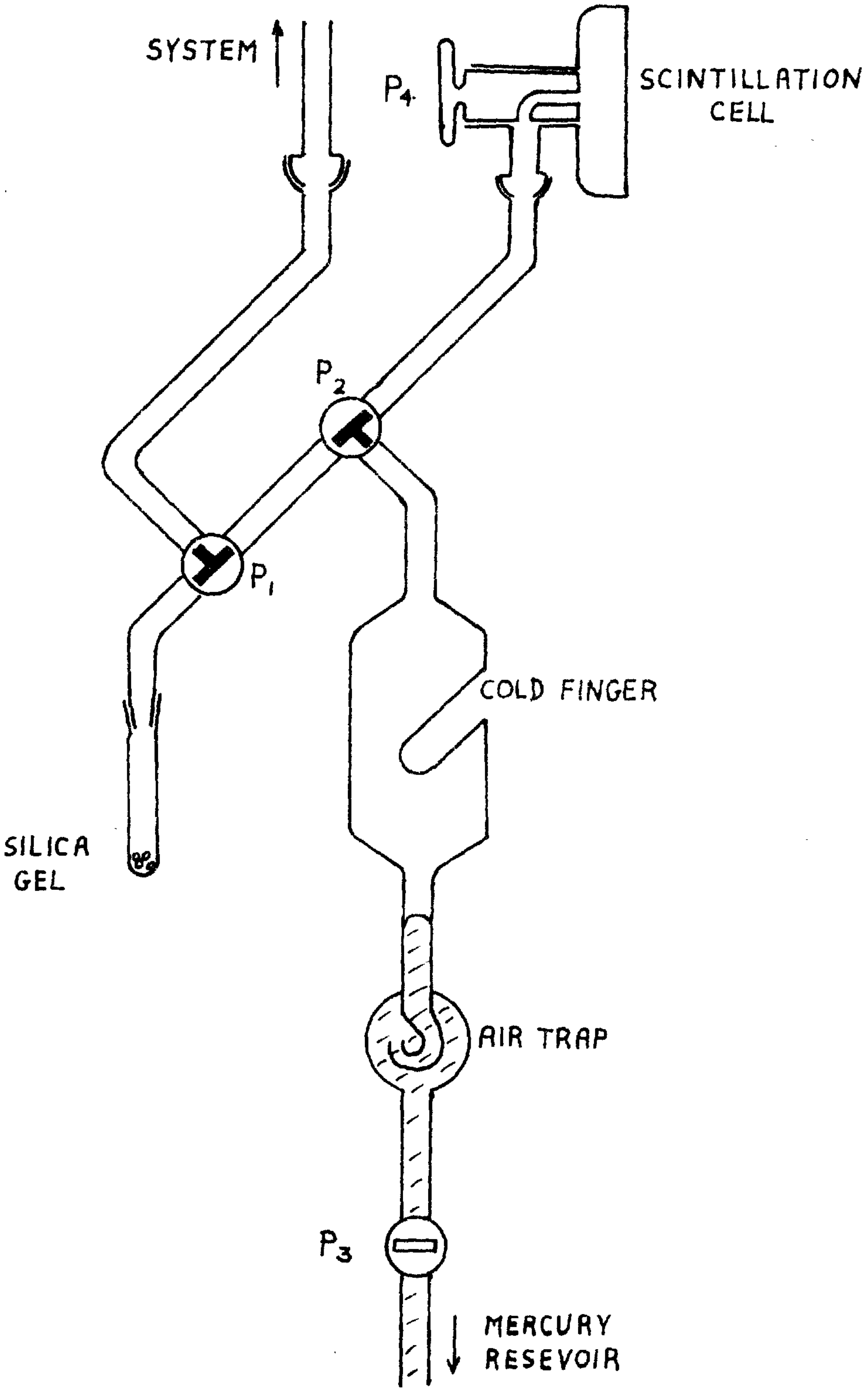
SYSTEM
P4
SCINTILLATION CELL
P2
P1
COLD FINGER
SILICA GEL
AIR TRAP
P3
MERCURY RESEVOIR

released into the main body of the pump and that the cell may be filled by flooding the main body of the pump with mercury from the reservoir below tap P_3 until the level of mercury is just below tap P_4. A trap is situated between the main body of the pump and tap P_3 to prevent air being swept into the pump by the flowing mercury.

The CO_2 fraction was transferred to the cell simply by allowing the cold finger to warm up to room temperature and filling the cell in a single action of the mercury level. The CO fraction was transferred to the cell by successive exposures of the part of the section below tap P_2 to the main body of the pump and then transferring the portion of CO in the main body to the cell. The volume of the tube containing the silica gel and the volume between taps P_1 and P_2 were kept to a minimum as these constituted dead spaces. Three cycles are sufficient to transfer over 99% of the CO to the cell. Once the cell is filled it may be removed from the pump and placed in the counting assembly for analysis of carbon-14 content. All the taps and connections in the Töpler pump section were lubricated with high-vacuum silicone grease since mineral greases would give rise to high, erratic background counts if swept into the scintillation cell owing to their scintillating properties.

The scintillation cell and associated monitoring assembly were supplied by Panax Equipment Ltd. The cell was designed to fit into a standard lead castle, type SC-LP, which housed a 6097 SP photomultiplier tube. The electronic equipment consisted of a Dekatron scaler, type D 657C, and a pre-amplifier, type 4250H. A check on the performance of the electronic equipment and the photo-multiplier was provided by a sealed liquid scintillator reference source, type CR-35. With working conditions of 1500 V. H.T., 12 V. discriminator bias and a pre-amplifier gain of X200 the tube noise was of the order of 20 c.p.m. and the cell backgrounds were of the order of 40 c.p.m. The efficiencies of counting of the cells varied from 25% to 60% depending on the individual cell and the condition of its scintillator coating.

FIGURE 25

ELECTRODE ASSEMBLIES USED WITH CARBON-14 SAMPLES

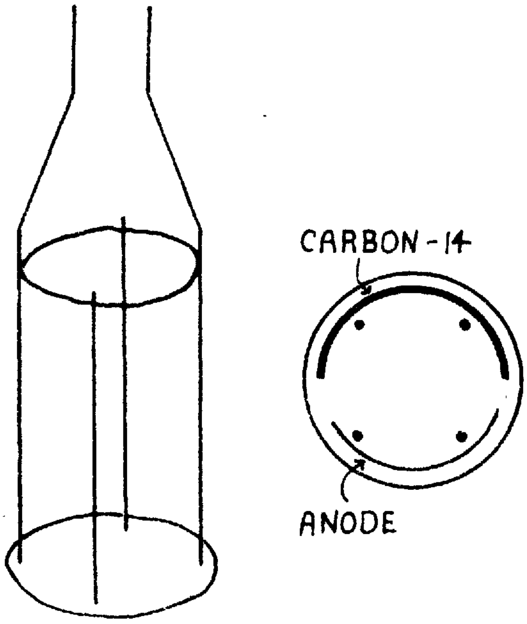
CARBON-14
ANODE

TYPE 'A'

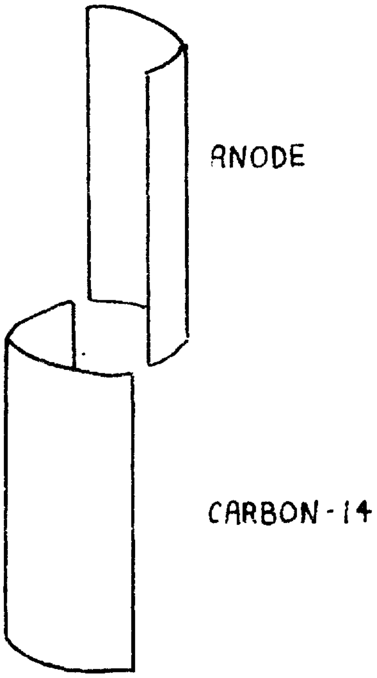
ANODE
CARBON-14

TYPE 'B'

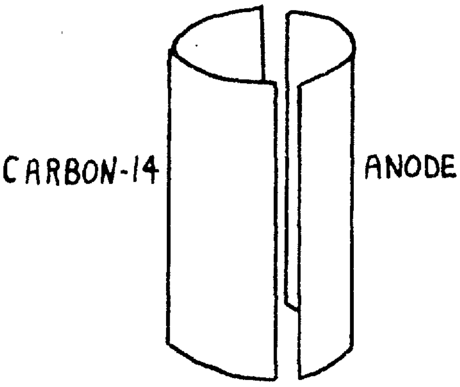
CARBON-14
ANODE

TYPE 'C'

CHAPTER 8

EXPERIMENTS WITH CARBON-14

A. Carbon-14 on Silica

8.1. Carbon-14 Sample

The carbon-14 sample used in this set of experiments was prepared by Mr. R.S. Sach of AERE, Harwell - the method of preparation being described in reference 51. The carbon-14 was deposited onto a semi-cylindrical silica backing of radius 1.6 cms., length 8.0 cms. and thickness 0.2 cms. by cracking carbon-14 labelled methane at 1100°C. This method of deposition resulted in the formation of a uniform film of pyrolytic carbon with the same specific activity as the initial methane of approximately 40 µC/mM. The total activity of the film was of the order of 12 µC. The use of an insulating material, such as silica, as a backing resulted in the sample having a high electrical resistance.

8.2.1. Static experiments at 0, 15 and 20 volts

The electrode assembly used in the first series of experiments is shown in figure 25 as the type A assembly. The carbon-14 sample was strapped to an 18 s.w.g. stainless steel wire support cage together with an aluminium foil anode - the filament being situated in the centre of the assembly. With this type of electrode assembly the carbon was always at the same potential as the anode.

Runs were performed in a static system of CO_2 at an initial pressure of 60 μHg. The required accelerating potential was applied between the filament and the anode and then the filament was switched on for a known period of time with the current being measured at regular intervals. The runs at zero volts were performed by connecting the anode to one side of the filament.

At the end of each reaction the resultant gas mixture was analysed for fractions condensible and non-condensible at $77^{o}K$ before being transferred to the gas scintillation cell for measurement of the carbon-14 content of the gas phase.

The gas scintillation cell used in this series of experiments had an efficiency of approximately 10% and gave a background count of 30±3 counts per minute.

The same filament was used throughout this series of experiments.

8.2.2. Results

The results obtained are given in table 13 of the appendix. In this table Pi refers to the initial CO_2 pressure and $PfCO_2$ and PfCO refer to the partial pressures of CO_2 and CO at the end of the reaction - all pressures being measured in microns of mercury. The last column

FIGURE 26

CARBON-14 ACTIVITY IN GAS AS FUNCTION OF MILLI-AMP MINUTES
STATIC CHARGES OF CO_2 - PRESSURE 60 μ Hg.

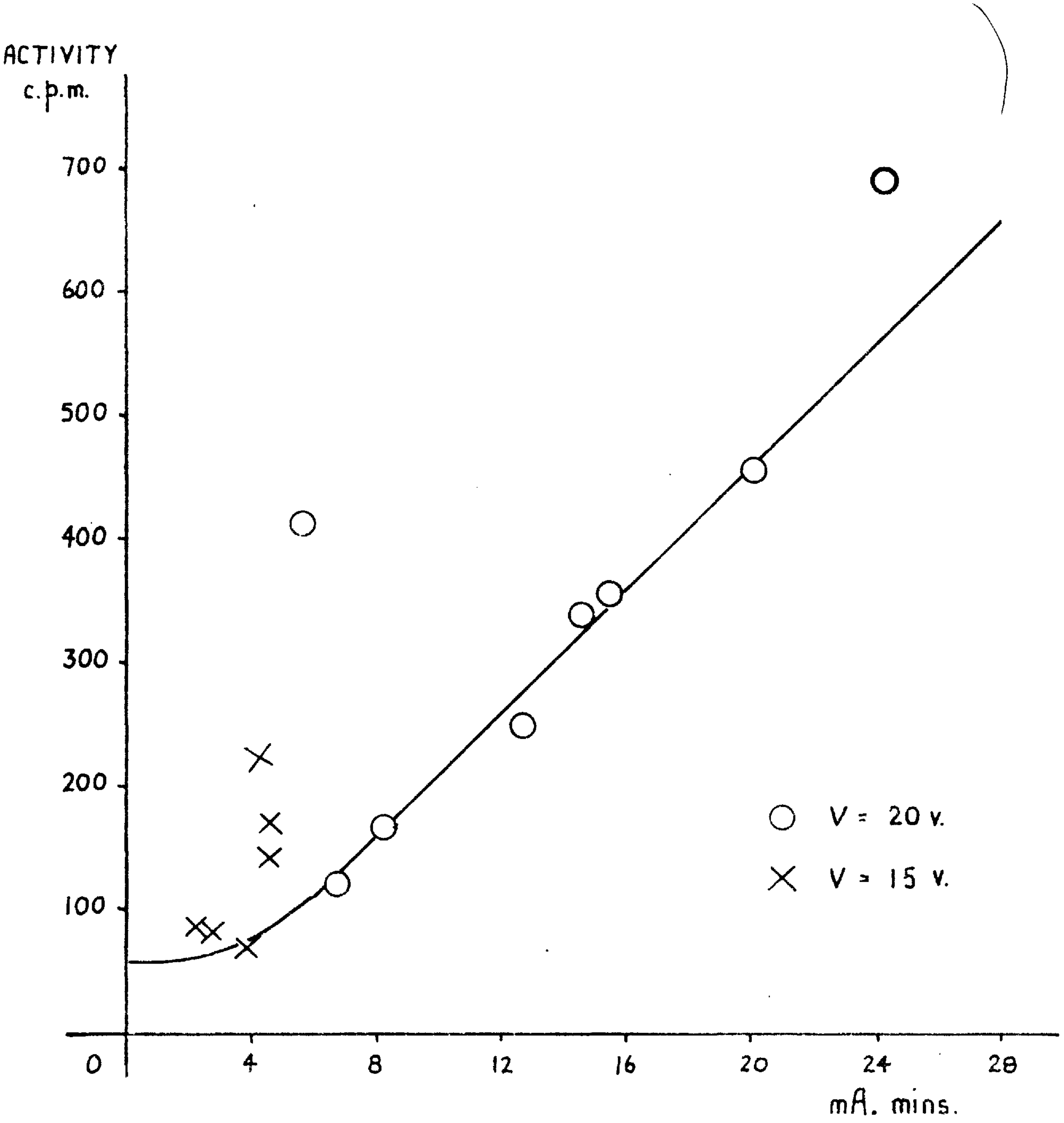

gives the carbon-14 activity in the gas phase measured in counts per minute. This activity includes the cell background count of 30±3 c.p.m.

From table 13 it can be seen that the runs performed with zero accelerating fields gave rise to small but significant activities in the gas phase. These activities might have arisen from the thermal decomposition of a surface oxide complex owing to the heating up of the surface during a run or, alternatively, from the thermal dissociation of carbon dioxide on striking the filament and the subsequent reaction of the oxygen atom with the carbon-14 surface.

The results obtained from the runs performed at 15 and 20 volts are reproduced in figure 26 as a plot of the carbon-14 activity in the gas phase as a function of milli-amp minutes. From this figure it can be seen that the majority of the runs performed at 20 volts gave a linear increase in the carbon-14 activity with increasing milliamp-minutes - thus demonstrating the effect of a radiolytic reaction taking place at this voltage. Run 109 gave a significantly higher reaction which is unexplained. From these runs it is apparent that the radiolytic reaction can best be detected in the range of 8 to 20 milli-amp minutes and currents in the region of 3 to 10 milli-amps. However, from the results obtained from the runs at 15 volts it is apparent that, with the electrode assembly used, the currents at low voltages are less than 1 milliamp. This entailed long reaction times and resulted in a large scatter in the few results obtained owing to the low activities produced and also to probable variations in the thermal effect from run to run. Therefore, no conclusions could be drawn from the results at 15 volts.

8.3. Effect of geometry

Owing to the carbon-14 activity detected after zero volt reactions the carbon sample was removed from the vicinity of the filament in order to prevent the carbon being heated up during the course of a run. The electrode assembly used is shown in figure 25 as the type B assembly. The carbon sample was suspended below the level of the filament and aluminium anode by two lengths of tungsten rod.

Runs were performed as described in section 8.2.1 and the results so obtained are given in table 14. For runs 141 to 146, inclusive, a bare aluminium anode was used either earthed (at the same potential as the filament) or at the same potential as the anode. It can be seen from the results of these runs that there was no significant reaction with the carbon surface even for reaction times of 10 minutes. This indicated that the species responsible for the carbon gasification were not reaching the sample.

In order to increase the concentration of reactive species by increasing the current in the system a carbon soot was deposited on the aluminium anode by burning napthalene in air. Although this did increase the current from 1 to 80 milli-amps there was still no carbon-14 activity in the gas phase - as the results of runs 148-150 show. During these runs an intense pale blue discharge occupied the space between the filament and anode but did not appear near the carbon-14 sample.

In view of these findings the electrode assembly finally employed is shown in figure 25 as the type C assembly. In this assembly the carbon-14 sample is at the same level as the aluminium anode but they are suspended independently so that their electrical conditions could be changed independently of each other.

8.4. Effect of surface condition

In the following series of experiments, performed in a static system of CO_2 at an initial pressure of 60 uHg, the type C electrode assembly was used with a napthalene carbon film deposited on the anode to increase the current. The carbon-14 sample was held at the same potential as the filament. The results obtained are given in table 15. The last column of this table gives the activity produced per milli-amp minute for each run.

Inspection of this last column shows that the first run of the series (run 167) gave by far the highest value. Prior to this run the carbon-14 sample had been exposed to the atmosphere for a period of approximately 5 weeks and this would have had a profound effect on the condition of the surface. The most unusual effect during this run was the appearance of an intense localised discharge on the sample. This discharge took the form of four or five very intense patches on the reverse side of the sample - each being approximately 5 mm. in diameter and similar in colour to the gas phase glow. The normal discharge in the inter-electrode space was fairly intense and uniformly distributed throughout the region. Since it was present in all the runs, it is probable that the increased activity in run 167 was due to the localised discharge.

Attempts to reproduce the condition of the surface prior to run 167 by exposing it to carbon dioxide and oxygen for long periods of time proved fruitless as table 15 shows.

The results of section 8.4 in which it was found that no reaction with the carbon-14 sample took place when it was removed from the vicinity of the discharge volume and of this section in which it was found that a much greater reaction took place when a localised discharge was present on the carbon-14 surface seem to indicate that the presence of the discharge is all important in the gasification reaction. This means that the reactive species must certainly be present in the discharge and should have been detected in the spectrographic work.

8.5.1. Flow experiments at 25 volts

Owing to the low activity produced by the low currents obtained in the static system, as noted in section 8.2.2, runs were performed in a flow system using the capillary bleed system described in section 7.3 to determine whether the carbon-14 sample could be used in experiments with lower energy electrons or not. The capillary tubing used had an internal diameter of 2.0 mm and a length of approximately 20 mm. This arrangement gave a flow rate numerically equal to the pressure in the reaction vessel - i.e. with a pressure of 60 μHg in the reaction vessel the flow rate was 60 μHg/min. In this series of experiments electrode assembly type C was used.

Prior to a run the reaction vessel, the capillary bleed, the Topler pump and scintillation cell were evacuated to a pressure below 10^{-2} μHg and then shut off from the pumps by closing taps T7 and T_{11}. The capillary tube was then connected to the reaction vessel by turning tap S_2 and carbon dioxide was admitted to the reaction vessel at such a rate that a pressure of approximately 60 μHg was maintained, measured on Pirani head P_1, with liquid nitrogen surrounding the trap of the capillary bleed section. The potential between the anode and filament was adjusted to 25 volts and the filament was switched for a period of 4.0 minutes with the current obtained being measured at regular intervals. At the end of the run the needle valve was closed and the capillary bleed section was isolated from the reaction vessel and the gas mixture in the reaction vessel was analysed for fractions condensible and non-condensible at 77°K. Following this the gas in the reaction vessel and the capillary bleed section was transferred to the gas scintillation cell for measurement of carbon-14 content. The scintillation cell used in this series of runs had an anthracene coating and had a background count of 37 ± 5 c.p.m. The efficiency of this cell measured with the $^{14}CO_2$ of known specific activity was 33%.

A constant reaction period of 4.0 minutes was used for all the runs to minimise any differences in thermal effects from run to run. The average current obtainable from the filament varied from run to run in the range from 3 to 10 milli-amps.

8.5.2. Results

Runs were performed with the carbon-14 sample

FIGURE 27

EFFECT OF ELECTRICAL CONDITION OF CARBON
FLOW SYSTEM OF CO_2 - CARBON-14 ON SILICA
ANODE POTENTIAL 25 VOLTS. - REACTION TIME 4·0 MINS.

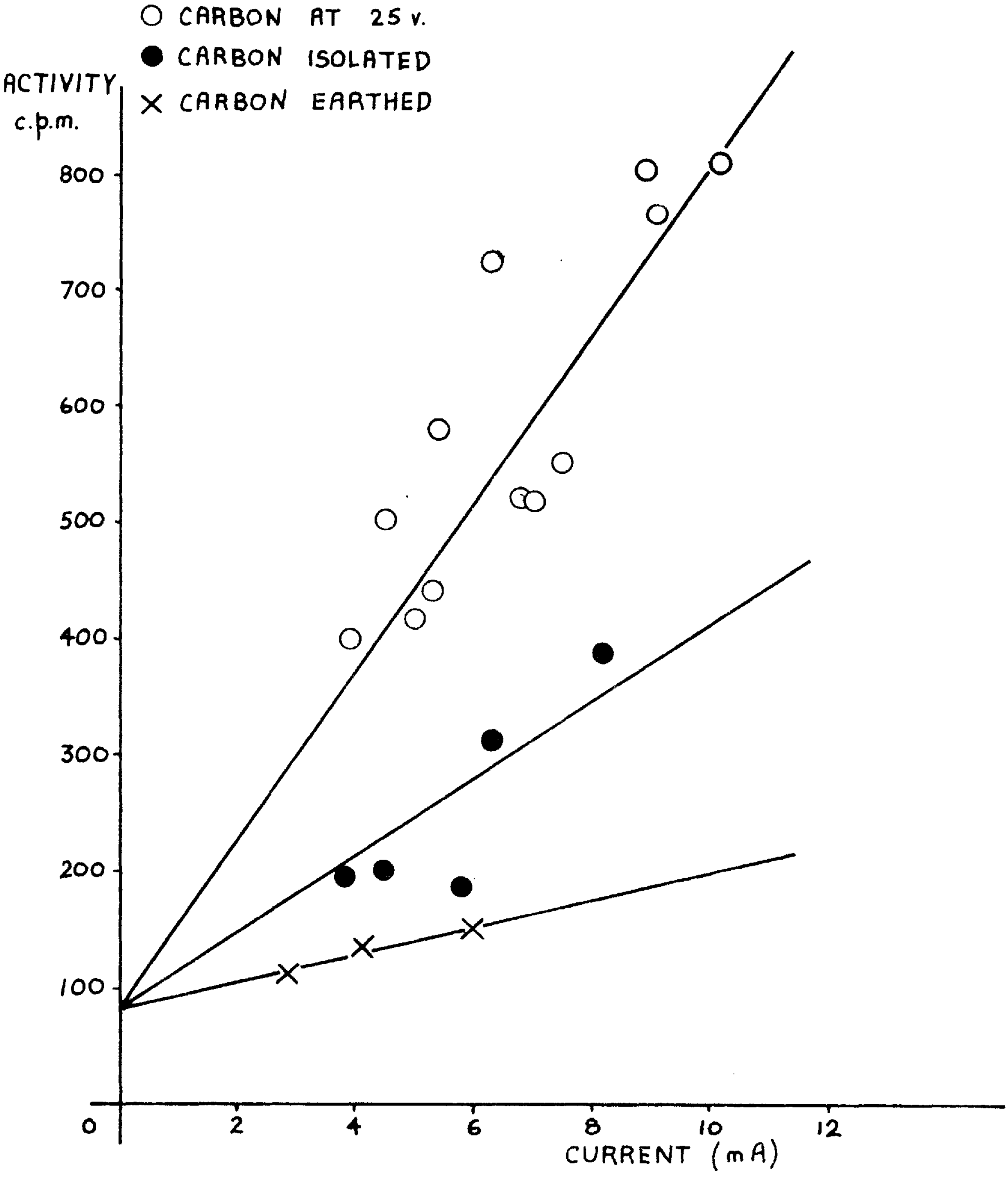

in one of the following three conditions:

a) at the same potential as the anode (25 volts);

b) at the same potential as the filament (earthed);

c) electrically isolated.

The results obtained are given in table 16 of the appendix. The second column of this table gives the flow pressure in the reaction vessel for each run, measured in uHg, and the fourth and fifth columns give the partial pressures of carbon dioxide and carbon monoxide in the reaction vessel at the end of the run. Plots of the measured carbon-14 activity, in counts per minute, as functions of the average currents obtainable during the course of the runs, measured in milli-amps, are reproduced in figure 27 and a plot of the carbon monoxide partial pressure as a function of the average current is reproduced in figure 28.

It can be seen from figure 27 that there is a significant difference between the runs performed with the carbon-14 in the different conditions described above. At first sight this is in direct contradiction with Claxton's results described in section 3.3 and in which it was shown that the rate of carbon gasification was independent of the electrical condition of the carbon surface. However, Claxton's results were obtained with currents greater than 100 milli-amps and the glow discharge was uniformly distri-

FIGURE 28

PARTIAL PRESSURE OF CO IN REACTION VESSEL
FLOW SYSTEM OF CO_2 CARBON-14 ON SILICA
ANODE POTENTIAL 25 VOLTS. REACTION TIME 4·0 MINS.

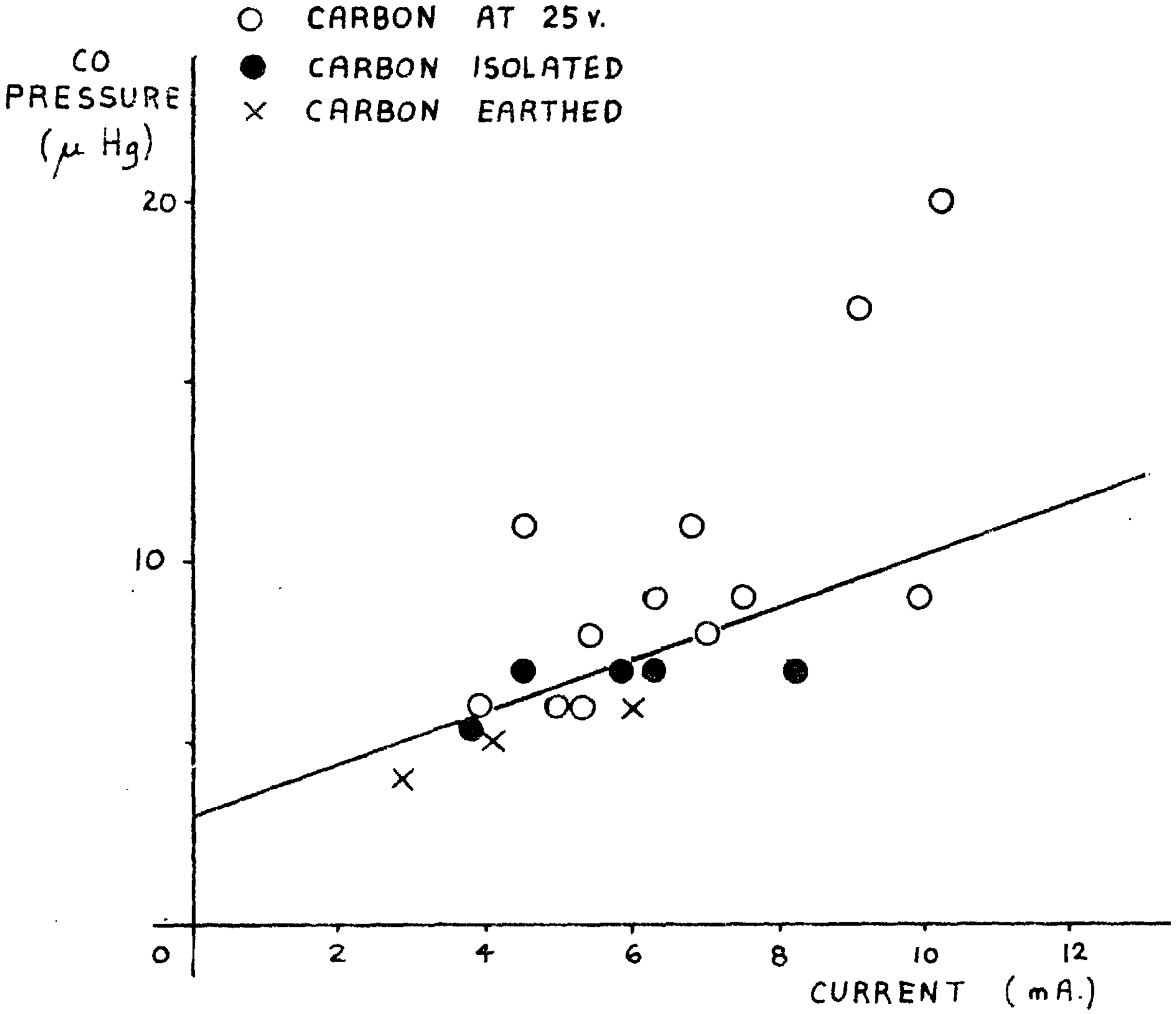

buted throughout the inter-electrode space no matter what the electrical condition of the carbon was. Under these conditions the discharge was very near the carbon surface and if the reactive species are formed by or present in the discharge the rate of carbon gasification would in fact be independent of the electrical condition of the carbon. In the experiments performed with the carbon-14 on silica sample, described here, the currents obtainable from the oxide cathode were always less than or equal to 10 milliamps and the form of the discharge was dependent on the electrical condition of the carbon. When the carbon was at the same potential as the anode the discharge was fairly faint and distributed uniformly throughout the inter-electrode space - under these conditions the rate of carbon gasification was greatest. When the carbon was either earthed or isolated the discharge was again fairly faint and confined to the region between the cathode and the aluminium anode and absent from the neighbourhood of the carbon-14 surface. In these cases the rate of carbon gasification was greater when the carbon was isolated than when it was earthed. The results do demonstrate that once outside the discharge region the reactive species must undergo a rapid de-activation process.

Inspection of figure 28 shows that the rate of carbon monoxide formation is approximately independent of the electrical condition of the carbon surface. The results obtained from the first four runs performed with the fresh oxide cathode gave significantly high value of the carbon monoxide pressure and may be explained by an enhanced reaction taking place between the carbon dioxide and oxide cathode.

The results obtained with 25 volt electrons did show that the count-rate expected at lower currents would be less than 200 counts per minute and therefore there would not be a sufficient range of reaction occurring in order to obtain reliable information on reactions occurring at lower voltages.

8.6. Distribution of carbon-14 in the gas phase

The last series of runs performed with the carbon-14 on silica sample served to measure the distribution of carbon-14 in the gas phase between carbon-14 dioxide and carbon-14 monoxide.

The runs were performed as described in section 8.5.1, using a flowing system of carbon dioxide and reaction times of 4.0 minutes. At the completion of each run the carbon dioxide fraction of the resultant gas was transferred to the gas scintillation cell for measurement of the carbon-14 content. After this counting, the cell was re-attached to the Töpler pump and the carbon monoxide

FIGURE 29

DISTRIBUTION OF CARBON-14 IN THE GAS PHASE

FLOW SYSTEM OF CO_2 CARBON-14 ON SILICA
ANODE POTENTIAL 25 v. REACTION TIME 4·0 MINS.

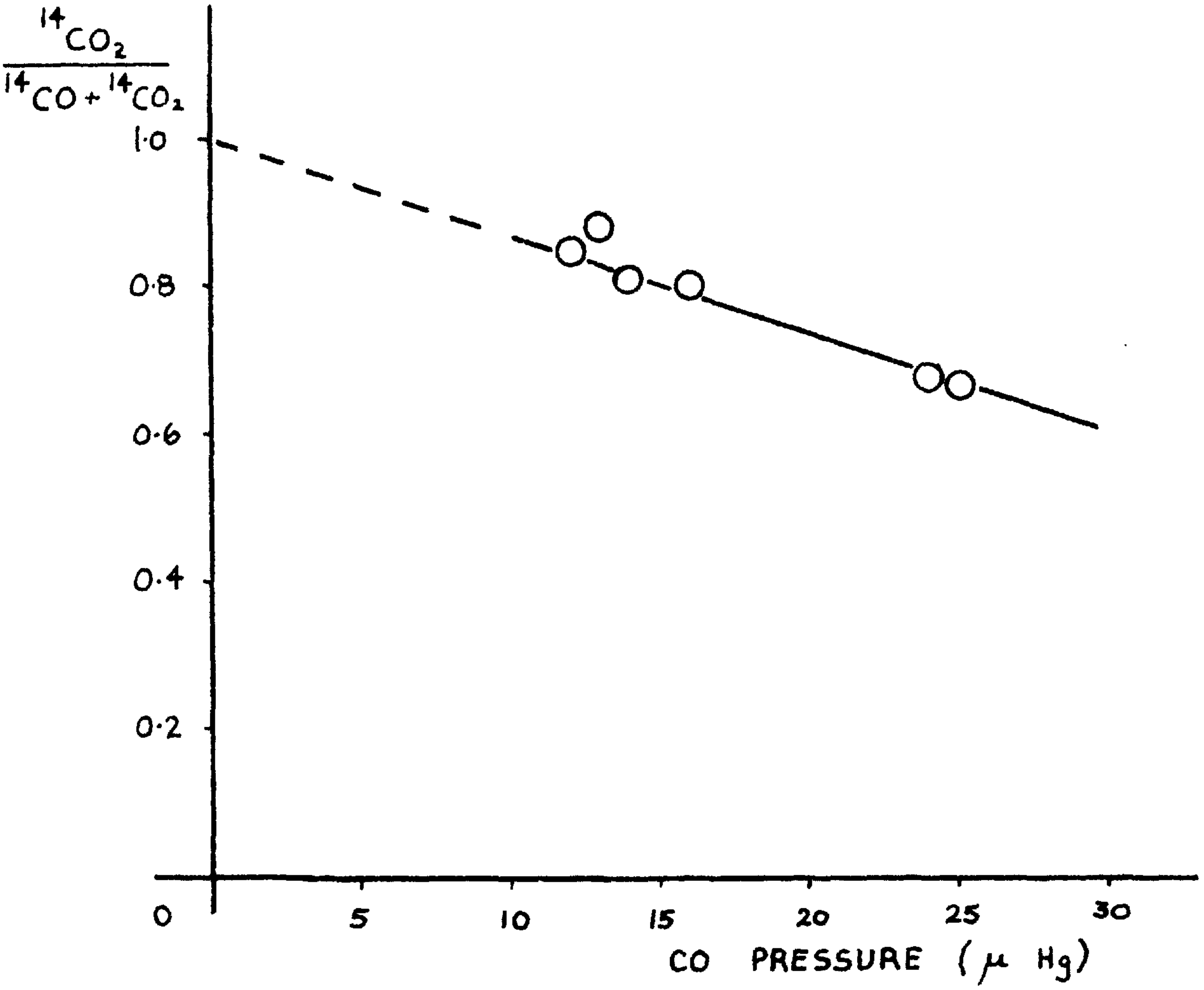

fraction was added to the carbon dioxide and the total carbon-14 content of the gas phase was measured.

The results obtained are given in table 17 of the appendix. The fourth and fifth columns of this table give the partial pressures of carbon dioxide and carbon monoxide in the reaction vessel at the end of a run with the capillary bleed section isolated from the remainder of the system. Figure 29 shows the fraction of activity appearing as ${}^{14}CO_2$ as a function of the resulting carbon monoxide partial pressure.

By inspection of figure 29 it can be seen that the fraction of carbon-14 activity appearing as carbon-14 dioxide decreases linearly with increasing carbon monoxide formation. By extrapolation of this line to low carbon monoxide pressures it would appear that at very low carbon monoxide pressure the carbon-14 appears solely as carbon dioxide. This may indicate that the carbon-14 is being gasified in the form of carbon dioxide and that the carbon-14 monoxide fraction is obtained by its subsequent radiolysis.

$$CO_2 \rightsquigarrow CO + O$$

$${}^{14}C(O) + O = {}^{14}CO_2$$

$${}^{14}CO_2 \rightsquigarrow {}^{14}CO + O \qquad \text{etc.}$$

8.7. Summary

Experiments have been performed with a carbon-14 film deposited onto a silica backing both in a static and a flowing system of carbon dioxide. In each case radiolytic reactions have been shown to take place only at currents greater than approximately 2 milli-amps. These currents were obtainable with accelerating voltages of 20 volts or over and therefore the sample could not be used to study radiolytic reactions at lower voltages.

The experiments performed in which the carbon sample was removed from the discharge region (section 8.3) and in which various electrical conditions were applied to the carbon sample (section 8.5) have demonstrated that the reactive species responsible for the carbon gasification are present in or near the discharge region only. Once outside this region they undergo a rapid deactivation process. This conclusion was substantiated further in section 8.4 where the presence of a localised discharge on the actual carbon surface led to an approximately four-fold increase in carbon-14 gasification.

It was demonstrated in section 8.6 that the majority of the carbon-14 gasified appeared in the gas phase as carbon dioxide.

B. Carbon-14 on Molybdenum

8.8. Carbon-14 sample

Owing to the very small currents obtained with the carbon-14 on silica sample at voltages less than 20 volts it was apparent that a carbon-14 film would need to be deposited onto a metal surface in order that the radiolytic reaction between carbon dioxide and carbon could be studied at lower voltages with the present apparatus.

This sample was prepared also by Mr. R.S. Sach of AERE, Harwell. Attempts to prepare the sample by cracking carbon-14 labelled methane directly onto a heated tungsten surface proved unsuccessful owing to the poor adhesion of the resulting graphite layer on the metal and also to some tungsten carbide formation. Therefore, the sample finally employed was prepared by cracking the methane onto a thin cellulose carbon filament heated to 1800°C and then evaporating the carbon-14 layer onto a molybdenum backing by increasing the temperature of the filament to a value in excess of 3000°C by flash heating. The specific activity of the resulting carbon-14 film was unknown but probably close to that of the initial methane, which was 4 curies per gram-mole. The molybdenum sheet had linear dimensions of approximately 7 x 5 cms. and was bent into a roughly semi-cylindrical shape.

8.9.1. Flow experiments

The carbon-14 on molybdenum sample was inserted into the reaction vessel as a type C electrode assembly (figure 25) with a fresh cathode and an aluminium anode. Experiments were performed as described in section 8.5.1 with pure carbon dioxide flow pressures of approximately 50 μHg. and with reaction times of 2.0 minutes.

Prior to each of the first few runs the electrodes were degassed by passing a large current between them for a short period of time while pumping at pressures below 5×10^{-2} μHg. This procedure gave very erratic carbon-14 activities in the gas phase during the subsequent runs. For the runs performed with zero accelerating fields the activities were of the order of 500 to 800 counts per minute.

Owing to this erratic behaviour the following series of runs were performed without this degassing treatment and therefore the condition of the carbon surface was not altered from run to run. This resulted in much more consistent results and, furthermore, the activities produced by the zero accelerating field runs were decreased to approximately 100 counts per minute. This effect demonstrates that the degassing treatment has a profound effect on the surface and makes it more reactive in the subsequent runs.

The object of this series of experiments was to study the radiation induced reaction between carbon dioxide and carbon at electron energies less than 25 eV. The appropriate accelerating potential was applied solely to the molybdenum electrode, leaving the aluminium anode electrically isolated. With this arrangement the electrons were accelerated in the region between the filament and carbon only; therefore, the volume in which the excited species were produced remained as independent of the electrode potential as possible. Furthermore, the currents measured would be those between the carbon and filament only. The reaction times were limited to 2.0 minutes to preserve the carbon-14 sample.

The gas scintillation cell used for this series of runs had an efficiency of approximately 55%.

8.9.2. Results

The results obtained from this series of runs are given in table 18 of the appendix. The second, third and fourth columns of this table give the applied voltage, the average current during the run and the flow pressure respectively. The carbon-14 activities produced in the gas phase are given in the fifth column, measured in counts per minute from the scintillation counter. It can be seen from the latter column that there was a slight variation in the activities produced in the zero accelerating field runs but this variation was consistent from day to day. The first run of any day always gave the highest activity and the subsequent runs led to a gradual decrease in this thermal activity.

FIGURE 30

REACTION RATE AS FUNCTION OF ELECTRON ENERGY

FLOW SYSTEM OF CO_2 CARBON-14 ON MOLYBDENUM

REACTION TIMES = 2·0 MINUTES

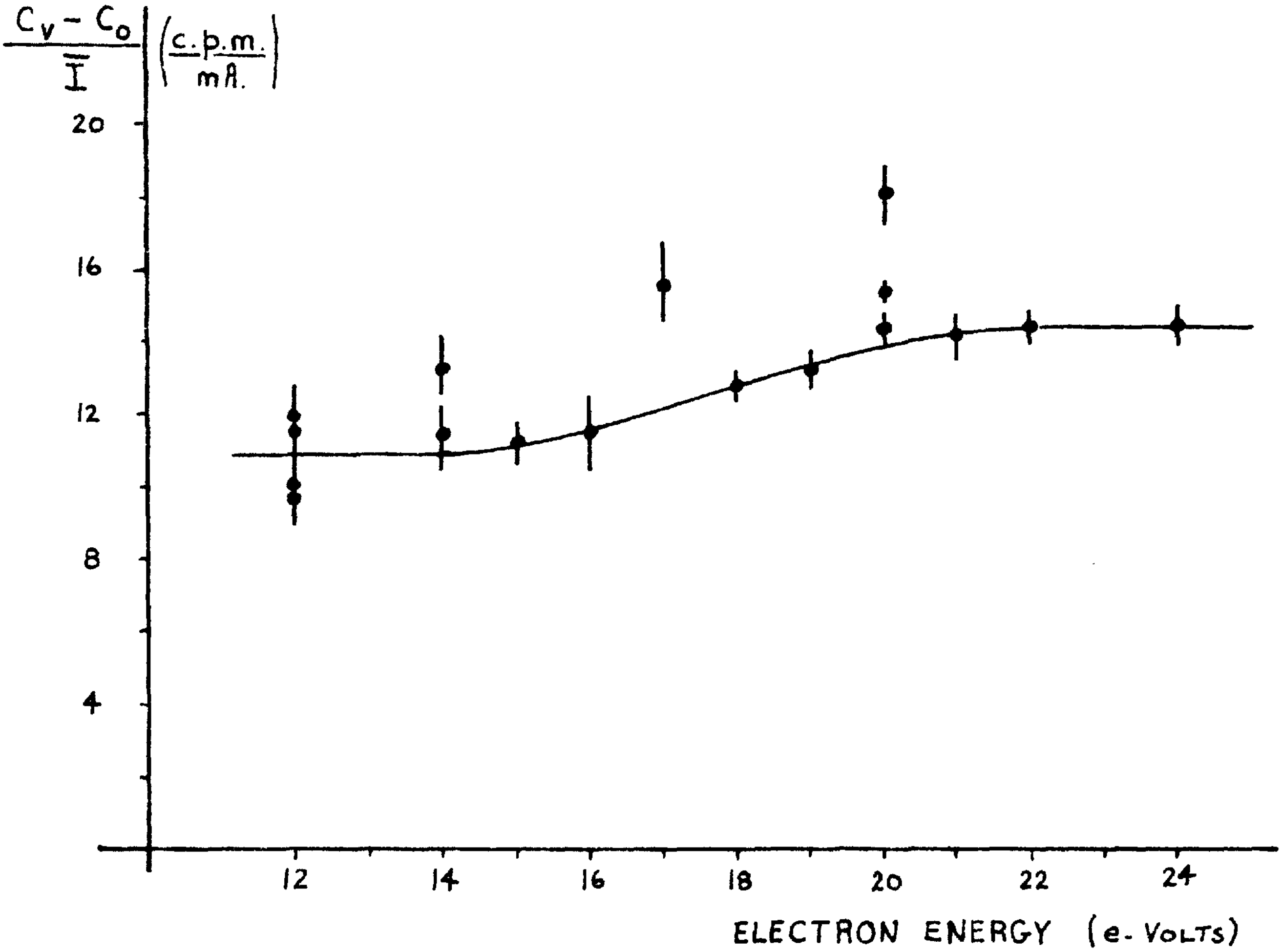

For the runs in which accelerating voltages of 12 volts or above were used the carbon-14 activities produced were always above the mean level of the thermal activities; this increase in activity will be due therefore to a radiolytic reaction. Owing to the variation in thermal activities and also owing to the different currents obtained in the runs the most appropriate measure of the radiolytic reaction is the excess carbon-14 activity over the thermal carbon-14 activity per unit average current. The last column of table 18 gives the values so obtained and they are plotted as a function of the electron energy in figure 30.

Prior to the performance of runs 385 to 390 the reaction vessel was exposed to the atmosphere for a short period of time. This fact may explain why the values of the radiation induced carbon-14 activity per unit average current obtained in runs 386, 388 and 390 were consistently higher than the others by a factor of 1.3 ± 0.1. This increased rate of carbon-14 gasification will probably have been caused by some change in the sample's surface.

By inspection of figure 30 it can be seen that the radiolytic reaction, measured in this way, is approximately constant at a value of 11 c.p.m./mA. from 12 to 14 eV and then gradually increases until it levels off at a value of 14.4 c.p.m./mA. at 21 eV and thereafter remains approximately constant, at least up to 24 eV.

The slight increase observed at 14 eV corresponds to the appearance potentials of the CO_2^+ and CO^+ ions - 13.8 and 14.1 eV respectively. These ions, together with their attendant secondary electrons, will make an appreciable contribution to the measured currents and therefore the representation of the cpm/mA given in table 18 will be somewhat misleading. A more realistic measure of the carbon gasification rate would be the carbon-14 activity produced per unit primary electron current. If such measurements were possible the values of the cpm/mA in table 18 and figure 30 would be increased for accelerating voltages above 14 volts. This would mean that the threshold obtained at approximately 14 eV would become more pronounced than actually shown although the levelling off at 21 eV would still be apparent.

Below 14 eV the reaction will be due to a neutral species which could be either atomic oxygen or excited carbon dioxide or carbon monoxide. Unfortunately, the lower voltage limit possible with this series of experiments was 12 volts and, therefore, lower thresholds for carbon gasification were impossible to obtain and, from these, absolute identification of the neutrally active species. Excited carbon monoxide can probably be ruled out from the results on the carbon monoxide studies described in chapter 5 in which it was found that carbon monoxide did not react with a carbon surface below 14 eV. The experiments performed with the carbon-14 on silica sample, summarised in section 8.5, led to the conclusion that the chemically active species seem to be present in appreciable quantities only in the discharge region. If this conclusion is correct it would be expected that the species would have been detected in the spectroscopic studies of chapter 6. From these studies it was concluded that there was no appreciable concentration of atomic oxygen present in the discharge and that the only excited species identified were those of CO_2, CO and CO^+. These findings may support the hypothesis that excited carbon dioxide is the species responsible for the radiation induced gasification of carbon rather than atomic oxygen. However, recent results by Feates and Sach[64] on the reaction of carbon dioxide and carbon-14 labelled graphite induced by vacuum ultra-violet radiation have shown that $O(^1D)$ and $O(^1S)$ atoms are capable of gasifying the graphite and, therefore, their presence cannot be ruled out in this work. This is especially so when one considers that these states of the atomic oxygen are metastable and will have a comparatively long life-time - long enough possibly for the majority of them to react with the carbon before being de-activated and so detected on the spectrograph.

The increase in gasification rate observed at approximately 14 eV is probably due to the appearance of a reactive ionic species. Owing to the thermal production of carbon monoxide by reaction with the filament there was always an appreciable concentration of this gas in the reaction vessel. The proximity of the ionisation potentials of carbon dioxide and carbon monoxide to each other makes it impossible to differentiate between the two ions. However, the results given in chapter 5 have shown that the carbon monoxide ion reacts with a carbon surface very easily and the only slight increase in carbon gasification may be due to small proportion of CO^+ ions present. The presence of carbon dioxide will mean that the ion exchange reaction $CO^+ + CO_2 = CO_2^+ + CO$ will reduce the CO^+ ion concentration even further. In table II of section 2.1 it was shown that the direct production of CO^+ ions by the reaction $CO_2 \rightsquigarrow CO^+ + O + e$ occurred at a threshold of 20.3 eV and it is interesting to note that it is at approximately this energy that the rate of carbon gasification begins to level off, as shown in figure 30, but no significance can be attached to this phenomenon.

An alternative explanation of the threshold at 14 eV may be the production of ions, followed by an ion-electron recombination reaction leading to the production of further excited neutral species.

$$CO_2 + e = CO_2^+ + 2e$$

$$CO_2^+ + e = CO_2^* = CO + O^{(*)}$$

Using this mechanism the levelling off of the reaction rate would correspond to the reaching of an equilibrium in the CO_2, CO_2^+ and electron concentrations in the gas phase.

It is apparent from the results discussed in this section that the majority of the excited species responsible for the gasification of carbon are electrically neutral and that the appearance of ions leads to an only slight increase in the rate of gasification.

8.10. Summary

Experiments have been performed with a carbon-14 labelled film deposited onto a molybdenum backing in a flowing system of carbon dioxide. The rate of carbon-14 gasification per unit average current has been measured as a function of the electron energy in the range of from 12 to 24 electron-volts.

It was found that the rate of carbon-14 gasification changed only slightly above the ionisation potentials of both carbon dioxide and carbon monoxide and it was concluded, therefore, that the gasification was produced primarily by electrically neutral species. Based on the evidence that the active species seem to be present in the region of the glow discharge only and the results from the spectroscopic study of the discharge it would seem that the neutral species is an excited carbon dioxide molecule although there is no conclusive evidence to reject atomic oxygen.

8.11. Comparison of carbon-14 and carbon soot results

Basically, two comparisons may be made between the runs performed with a carbon soot and those performed with the carbon-14 samples : comparison between the currents obtainable with the two types of carbon from an oxide coated cathode using the same accelerating voltage and comparison between the rate of carbon transport from the solid to the gas phase.

Using carbon samples, prepared by burning napthalene in air and depositing the soot onto an aluminium backing, the rate of carbon transport was determined by Claxton to be approximately 3×10^{-4} milli-grams per milliamp minute for electrons of 25 eV energy. This rate of carbon removal corresponds to an absolute activity of 2.2×10^{3} d.p.m./mA.min. of carbon-14 in the gas phase from the silica sample and of 2.2×10^{5} d.p.m./mA.min. of carbon-14 from the molybdenum sample. In fact, the rates of carbon-14 gasification observed with the two samples correspond to absolute disintegration rates of 60 and 14 d.p.m./mA.min. respectively.

Comparisons between the currents obtainable from oxide-coated cathodes when using the three types of carbon show a somewhat similar trend; much greater currents were obtainable under the same conditions with sooty carbon

FIGURE 31

CURRENT FROM FILAMENT AT 930°C IN FLOWING CO_2

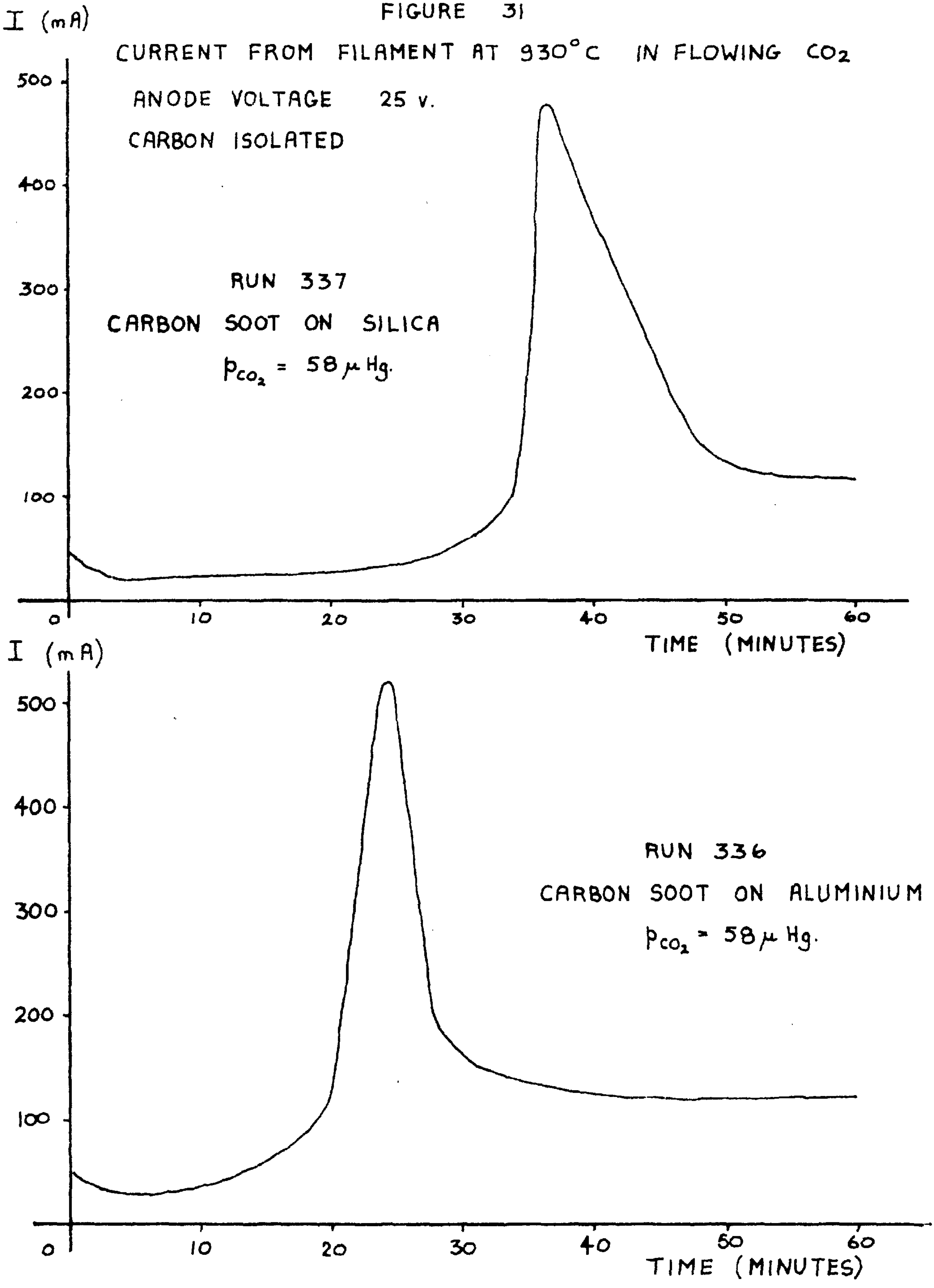

than with the carbon-14 on silica sample. Therefore, experiments were performed to determine whether this difference in currents could be attributed to the different types of backing or different types of carbon used.

In these experiments currents obtainable from a fresh oxide-coated cathode were measured in a flowing system of CO_2, at flow pressures of approximately 60 μHg, in the presence of sooty carbon deposited onto either a silica or an aluminium backing. In each case the carbon was electrically isolated from the anode and cathode. The results are illustrated in figure 31 and it can be seen in this figure that similar current characteristics were obtained with each type of backing. At the start of each run the current remained fairly low and a glow discharge was present in the region between the anode and cathode and absent from the vicinity of the carbon surface. After some time the glow discharge rapidly spread to the whole of the inter-electrode space and a sharp peak was observed in the current before it steadied down to a value of over 100 mA.

From these experiments it was concluded that the current was probably independent of the type of backing but depended on the type of carbon, being much greater with a sooty carbon than with a pyrolytic carbon. The reason or form of this dependence is unknown. Since the large currents are independent of the gas phase and the primary electron current from the filament is very small it would seem that some current multiplication process is taking place on the carbon surface itself. If this is the case, there may be some property of the surface, such as a work function, which controls this current multiplication and which is dependent on the form of the carbon.

The greatly increased reactivity of the sooty carbons as compared with the carbon-14 samples may be directly connected with these large currents, but again the reason is not understood at present. The pretreating of the carbon-14 on molybdenum sample, by passing a large current between the electrodes at pressures lower than 5×10^{-2} uHg, led to a five- to eight-fold increase in the subsequent runs when compared with the runs performed without this pre-treatment, and this effect does demonstrate that high currents do alter the reactivity to some extent.

Two further differences between the runs performed with sooty carbon and carbon-14 were as follows:-

1) In the runs performed with the sooty carbons the pressure flow rates were of the order of 600 μHg/min, whereas the flow rate of the capillary bleed apparatus used in the carbon-14 studies was only 60 μHg/min. This difference in flow rate will have a significant effect on the reaction rates but not enough to explain the great differences observed, especially between sooty carbon and the high specific activity carbon-14 on molybdenum sample.

2) A constant feature of work with oxide coated filaments is the contamination of electrodes by evaporation of material from the oxide surface. Such a process results in the formation of thin films of contaminant on the electrodes and was apparent in this work whenever the reaction vessel was dismantled. In the experiments with sooty carbons a fresh carbon film was prepared for each run and, therefore, they would not have had an accumulative effect on the carbon surface as in the case of the carbon-14 samples, which were used for several runs each. Furthermore, the high currents and high reaction rates obtained with the sooty carbon would probably lead to the rapid burn-off of the contaminant as it was deposited on the carbon surface. It would be instructive to study the effect of this contamination with a fresh carbon-14 sample to see whether there is an appreciable decrease in reactivity with time.

Thus it can be seen that there are some reasons why the carbon-14 samples should be less reactive than sooty carbon, but not to the extent found. It is probably that the sooty carbon is more reactive fundamentally and for the same reason gives much greater currents than pyrolytic carbon. More work would need to be done in this field before a constructive solution is found.

CHAPTER 9

GENERAL SUMMARY

9.1. Experimental Results

Experiments have been performed in a static system of carbon dioxide both in the presence and absence of carbon and it has been shown that when zero accelerating fields are used there is a rapid conversion of the carbon dioxide to carbon monoxide: this is presumably due to a chemical reaction with the free metals in the surface of the oxide coated cathode or to the thermal decomposition of the carbon dioxide molecules on striking the filament, which is heated to 900 - 1000°C. The heating up of the electrodes by the thermal radiation from the filament has been shown to produce no significant thermal reaction between the carbon dioxide and carbon.

Experiments have been carried out in a static system of carbon monoxide in which the rate of carbon monoxide decomposition has been measured as a function of the energy of bombarding electrons. In the presence of free carbon the threshold energy for decomposition to commence has been shown to be approximately 14 eV., while in its absence the threshold energy is increased to approximately 25 eV. In all cases where decomposition occurred the rate of decomposition was proportional to the pressure. Experiments in a flowing system of carbon monoxide have confirmed the upper threshold and have shown that it is also the threshold for the appearance of a pale blue glow discharge and the formation of carbonaceous deposits. Mercury vapour has been shown to have no significant effect on the carbon monoxide decomposition. From these results it has been concluded that carbon monoxide decomposes by an ionic reaction mechanism and that in the presence of free carbon the decomposition is catalysed on the carbon surface.

Spectrographic studies of the glow discharges produced in flowing carbon dioxide and carbon monoxide have shown that they are made up of the same band systems of CO_2, CO and CO^+. There was no evidence for the appearance of atomic oxygen in the discharge.

A carbon-14 tracer technique has been developed using a gas scintillation cell as a monitoring the carbon-14 which has greatly increased the sensitivity of the apparatus for experimenting of the gasification of carbon by the radiation induced reaction with carbon dioxide. Using a carbon-14 sample deposited onto a silica backing it has been shown that the chemically active species responsible for the carbon gasification are present in or near the discharge region only and that when this region is removed from the vicinity of the carbon surface little or no gasification occurs. From the results of the experiments performed with a carbon-14 sample deposited onto a molybdenum backing it was concluded that these species responsible for gasification are, in the main, electrically neutral and only a slight increase in the rate of gasification is observed when ionic species are present. The spectroscopic studies tend to favour excited carbon dioxide as the neutral species but there is no direct evidence to exclude atomic oxygen, especially when one considers the fact that the $O(^1D)$ and $O(^1S)$ states are metastable levels and will have comparitively long life-times.

It was found that sooty carbons gave far higher currents and reaction rates than the carbon-14 samples. Some of this increase was due to higher gas flow rates used and to less contamination of the sample surface by evaporation of material from the filament. However, it is considered that most of the increased reactivity and the high currents are due to some fundamental property of the carbon surface which is unknown at present.

9.2. Application to reactor conditions

A direct comparison between the results of the present studies and the effects liable to be encountered in a graphite moderated - carbon dioxide cooled nuclear reactor is made difficult by the completely different conditions employed in the two cases. In the present studies gases at pressures up to 60 µHg have been irradiated with electrons accelerated to energies in the range 12 to 30 eV. In reactors gas pressures up to 7 atmospheres are employed and the primary radiation consists of neutrons, gamma-rays and β-electrons.

These primary radiation particles will lose their energy to the surrounding medium in a variety of ways. The neutrons, since they are uncharged, do not produce ionisation directly in matter but interact almost exclusively with atomic nuclei, imparting to them kinetic energy of recoil. The recoiling nuclei, however, are capable of producing excitation and ionisation to the surrounding matter. Gamma-ray quanta of energies greater than 1 MeV will be absorbed in the vicinity of an atomic nucleus with the production of an electron-positron pair. The positron and electron will be slowed down by interaction with the medium and the positron will eventually combine with an electron giving out two 0.51 Mev gamma-rays in the process (so-called annihilation radiation). These gamma-rays and also any other quanta of energy less than 1 Mev will produce considerable ionisation by photo-electric and Compton scattering processes. The free electrons resulting from these processes will have considerable kinetic energy. Thus it can be seen that the interaction of all components of reactor radiation with the surrounding medium leads to the production of fast secondary electrons. This means that the type of radiation in nuclear reactors will be the same as in the present system, namely electrons, although the energies are completely different in the two cases.

When a fast secondary electron is slowed down to rest in a gas the total number of ion pairs produced is roughly proportional to the energy expended. When slowed down in carbon dioxide the energy expended per ion-pair formed is known to be approximately 32 eV. Since the ionisation potential is only 14 eV this means that excitation processes will also be present to a significant extent. From this one can see that energies involved in each electron-molecule interaction are the same no matter what the energy of the incident electron is.

For experiments performed with high energy radiation the chemical yields from radiation induced reactions are related to the energy absorbed by the experimental system and the term "G value" was introduced to denote the number of molecules changed for each 100 eV of energy absorbed. Thus G(X) refers to the number of molecules of a product X formed per 100 eV of energy absorbed and G(-Y) refers in the same way to the loss of a material Y that is destroyed on irradiation. In the graphite-carbon dioxide reaction it has been shown that the energy absorbed in the gas phase is by far the most important and the G values quoted for this reaction refer to 100 eV of energy absorbed by the gas phase. From the in-pile experiments it has been found that approximate values for the relevant G values are $G(-CO_2) = 5$, $G(-C) = 2.2$ and $G(CO) = 2.3$. From the $G(-CO_2)$ value it can be seen the average energy expended to cause the destruction of a carbon dioxide molecule is approximately 20 eV and again this is the same order of magnitude of energy for single electron-molecules interactions considered in the system reported here.

Perhaps the greatest difference in conditions between the two systems is the gas pressures used, 60 μHg here and up to 7 atmospheres in reactors. This very large difference in pressures will result in the excited species having very large life-times in the low pressure work. However, the carbon samples used here have a radius of approximately 1.6 cms. while the average pore radius in pile grade graphite is of the order of 10^{-4} cms. If one multiplies the radius of the volume of gas in the carbon by the gas pressure one obtains values of 0.1 and 0.5 cms. mmHg for the low pressure reaction vessel and the internal pores of pile grade graphite respectively. The relevance of these values is that they demonstrate that the number of collisions an active species would have to undergo in the gas phase before reaching the carbon surface is the same order of magnitude in the two cases and that the very large differences in life-times will become a not too serious handicap.

The above considerations demonstrate that it will not be unreasonable to make direct comparisons between the results in the low pressure work described here and those obtained for pore reactions occurring in the graphite moderator of a nuclear reactor.

The most significant comparison can be made from the results obtained with the carbon-14 on molybdenum sample in a flowing system of carbon dioxide in which it was found that neutral species play the greatest role in the gasification of carbon. The slight reactivity of ionised species would be expected to play an even smaller role in reactors owing to the absence of electrical clearing fields and, therefore, a greater chance of ion-electron recombination processes occurring. However, these recombination processes may be expected to lead to the production of further active neutral species and should not be ignored. In fact, it would be informative if a gaseous additive, whose ionisation potential was lower than carbon dioxide's, could be injected into the gas stream so that the CO_2^+ species could be de-ionised by an ion-exchange reaction rather than by recombination.

The problem in controlling the radiation induced reaction is one of preventing the neutral active species from reaching the carbon surface or if this is impossible treating the surface so that the species will not react with it. If oxygen atoms are the responsible species they could be de-activated to a large extent by the addition of an oxygen acceptor in the gas phase. In fact, in-pile experiments have shown that the addition of carbon monoxide does cause an appreciable reduction in the gasification but only for the superficial reaction - the in-pore reaction is affected by small quantities of carbon monoxide only ($\leq$ 500 v.p.m.). This difference in behaviour of the effect of carbon monoxide addition in the two reaction zones is not consistent with an oxygen-atom model and cannot be related in a simple manner to the existing picture of the reaction mechanism described in section 2.7. If excited carbon dioxide is the reactive species the control of the radiation induced reaction becomes more difficult. The excitation energy would need to be transferred to a quenching agent by a collision of the second kind; the quenching agent would have to be unreactive in itself to graphite and would possibly be difficult to discover.

The higher gas pressures and greater power densities of the Windscale Advanced Gas-cooled Reactors and the later civil stations result in there being higher natural carbon monoxide concentrations in the coolant gas system so that carbon monoxide radiolysis has become an important consideration. The results obtained in this study have demonstrated that the presence of a carbon surface affects the radiolysis to a very significant extent when low energy electrons are used. However, in the absence of free carbon the carbon monoxide decomposes readily at incident electron energies greater than 25 eV and it would be expected that this would be the predominant mode of decomposition in nuclear reactors. It has been concluded from the results that excited carbon monoxide ions are responsible for the gas phase radiolysis and, therefore, the reduction of this effect could be obtained by the introduction of charge transfer agents to the gas. As in the carbon dioxide case a search for a suitable agent may prove difficult for the carbon monoxide ion is highly excited. Once free carbon is present the results have shown that carbon monoxide ions in the ground state are capable of producing further decomposition - the reaction proceeding as a catalytic reaction on the carbon surface. However, this reaction can be controlled in the presence of carbon dioxide owing to the charge exchange reaction between the two gases $CO^+ + CO_2 = CO_2^+ + CO$.

The above discussion has demonstrated that the radiation induced gasification of carbon and the deposition of solids in the $CO_2/CO/C$ system could be reduced appreciably by the addition of suitable scavengers or quenching agents to the gas coolant system. The low pressure apparatus and carbon-14 tracer technique developed in this work might provide a suitable means for the search of such additives.

APPENDIX A - EXPERIMENTAL RESULTS

Table 1

RUN 45- Static charge of CO_2 - carbon present

Anode and carbon at the same potential as the filament.

Time (secs)	Total Time (mins)	CO_2 Pressure (μ Hg)	CO Pressure (μ Hg)	% CO
-	0.0	62	0.5	0.6
60	1.0	42	20	32.3
60	2.0	32	35	52.2
60	3.0	27	49	64.4
60	4.0	25	61	70.9
60	5.0	23	69	75.0
60	6.0	20	76	79.2
60	7.0	18	82	82.0
60	8.0	16	89	84.8
60	9.0	16	94	85.5
60	10.0	14	98	87.5

Table 2

RUN 44 - Static charge of CO_2 - carbon present

Anode and carbon at +10 volts w.r.t. filament

Time (secs)	Average Current (mA.)	Total mA.mins.	Total Time (mins)	CO_2 Pressure (μ Hg)	CO Pressure (μ Hg)	% CO
-	-	0.0	0.0	53	0.8	1.4
60	0.82	0.82	1.0	33	23	41.1
60	0.67	1.49	2.0	30	35	53.8
60	0.69	2.18	3.0	27	44	62.0
60	0.61	2.79	4.0	25	51	67.1
60	0.64	3.43	5.0	23	59	72.0
60	0.60	4.03	6.0	22	64	74.4
60	0.59	4.62	7.0	19	71	78.9
60	0.59	5.21	8.0	17	76	81.7
60	0.54	5.75	9.0	15	81	84.4
60	0.55	6.30	10.0	14	86	86.0
60	0.59	6.89	11.0	13	91	87.5
60	0.50	7.39	12.0	11	95	89.6
60	0.54	7.93	13.0	7	103	93.6
60	0.50	8.43	14.0	7	107	94.0
60	0.50	8.93	15.0	5	115	95.8

Table 3

RUN 43 - Static charge of CO_2 - carbon present

Anode and carbon at +12 volts w.r.t. filament

Time (secs)	Average Current (mA.)	Total mA.mins.	Total Time (mins)	CO_2 Pressure (μ Hg)	CO Pressure (μ Hg)	% CO
-	-	0.0	0.0	58	1	1.7
20	10.3	3.4	0.3	51	10.5	17.2
20	15.8	8.7	0.7	45	16	26.6
20	15.3	13.8	1.0	40	24	37.5
30	14.1	20.9	1.5	41	30	42.3
30	12.9	27.4	2.0	41	36	46.8
30	13.6	34.2	2.5	36	44	55.0
30	10.4	39.4	3.0	33	49	59.8
30	11.4	45.1	3.5	32	55	63.2
45	9.1	52.0	4.3	27	61	68.5
45	10.6	59.9	5.0	26	69	72.6
45	10.3	67.6	5.8	23	75	76.5
45	12.7	77.2	6.5	19	82	81.2
60	13.8	91.0	7.5	16	94	85.5
60	10.6	101.6	8.5	13	97	88.2

Table 4

RUN 46 - Static charge of CO_2 - carbon present

Anode and carbon at +25 volts w.r.t. filament

Time (secs)	Average Current (mA.)	Total mA.mins.	Total Time (mins)	CO_2 Pressure (μ Hg)	CO Pressure (μ Hg)	% CO
-	-	0.0	0.0	53	1	1.5
20	127.5	43.8	0.3	13	51	79.7
20	135.0	88.8	0.7	7	59	89.4
20	155.5	140.6	1.0	5	59	92.2
60	200.6	341.2	2.0	5	59	92.2
60	205.2	546.4	3.0	3	52	94.5
60	198.1	744.5	4.0	3	46	93.8
60	185.3	929.8	5.0	3.5	42	92.2
60	192.1	1121.9	6.0	2.5	39	93.3

Table 5

RUNS 50 & 51 - Static charges of CO_2 - carbon absent

Anode and electrode A_2 at +25 volts w.r.t. filament

Time (secs)	Average Current (mA.)	Total mA.mins.	Total Time (mins)	CO_2 Pressure (μ Hg)	CO Pressure (μ Hg)	% CO
a) Run 50						
-	-	0.0	0.0	67	0	0.0
30	8.3	4.2	0.5	37	15	28.8
30	6.2	7.3	1.0	31	21	40.4
60	4.5	11.8	2.0	22	34	60.7
60	3.1	14.9	3.0	16	41	71.9
60	2.6	17.5	4.0	12	50	80.6
60	1.8	19.3	5.0	10	55	84.6
60	1.4	20.7	6.0	9	61	87.1
180	2.1	27.0	9.0	7	77	91.7
b) Run 51						
-	-	0.0	0.0	52	0	0.0
15	38.5	9.6	0.3	30	14	31.8
15	26.8	16.3	0.5	26	19	42.2
30	28.2	30.4	1.0	20	27	57.4
30	25.3	43.1	1.5	18	32	64.0
30	26.1	56.2	2.0	14	39	73.6
60	27.6	83.8	3.0	11	49	81.7
60	24.2	108.0	4.0	8	57	87.7
60	26.1	134.1	5.0	5	65	92.9
60	19.3	153.4	6.0	4	71	94.7
60	26.8	180.2	7.0	4	80	95.2

Table 6

RUN 52 - Static charge of CO_2 - carbon absent

Anode and electrode A_2 at same potential as filament

Time (secs)	Total Time (mins)	CO_2 Pressure (μ Hg)	CO Pressure (μ Hg)	% CO
-	0.0	50	0.1	0.2
30	0.5	31	8	20.5
60	1.5	26.5	15.5	36.9
30	2.0	23.5	17.5	42.7
60	3.0	22	22	50.0
30	3.5	20	25	55.6
30	4.0	19	27	58.7
60	5.0	19	32	62.7
60	6.0	16	38	70.4
60	7.0	15	43	74.1

Table 7

RUN 53 - Static charge of CO_2 - carbon absent

Nickel strip in place of oxide-coated filament.

Anode and electrode A_2 at same potential as nickel strip.

Time (secs)	Total Time (mins)	CO_2 Pressure (µ Hg)	CO Pressure (µ Hg)	% CO
-	0.0	69	0.3	0.4
60	1.0	64	10	13.5
60	2.0	62	14	18.4
60	3.0	60	18.5	23.4
60	4.0	58	23	28.4
60	5.0	58	26	31.0
60	6.0	55	30	35.3
60	7.0	53	35	39.8
60	8.0	51	40	44.0
60	9.0	51	44	46.3
60	10.0	48	48	50.0

Table 8

Carbon weight-loss experiments

Flowing CO2 - carbon present

Run	Average Current (mA.)	Time (mins.)	mA.mins.	Flow Pressure (µ Hg)	Weight Change (mgms.)
a) Anode and carbon at same potential as filament					
60	-	60.0	-	64	-0.1
61	-	60.0	-	61	+0.2
62	-	90.0	-	63	-0.1
b) Anode and carbon at +25 volts w.r.t. filament					
65	185	30.0	5545	66	-0.9
66	105	30.0	3172	72	-1.4

Table 9

Static charges of CO Constant current = 5.0 milli-amps

$$p_{co} = p_o \exp.(-\alpha t)$$

α as a function of the electron accelerating voltage.

Run	Voltage	α min.$^{-1}$	$-\frac{\Delta CO_2}{\Delta CO}$	Heating Voltage
a) Carbon present - mercury vapour absent				
79	17.0	0.0245	0.53	3.8
80	18.0	0.0533	0.56	4.0
81	20.0	0.0783	-	3.8
77	24.0	0.0830	0.40	3.8
78	30.0	0.0919	0.43	3.8
b) Carbon present - mercury vapour present				
91	20.0	0.0530	-	-
90	24.0	0.0826	0.45	-
c) Carbon absent - mercury vapour present				
89b.	24.0	0.0000	-	6.9
85	26.0	0.0062	0.50	4.9
87	29.0	0.0283	0.38	4.4
89a.	30.0	0.0712	0.46	3.9
88	32.0	0.0797	0.38	3.9
86	34.0	0.0882	0.39	4.0

Table 10

Currents obtainable from an oxide-coated cathode at 850 °C. in a flow system of carbon monoxide both in the presence and absence of carbon. Carbon monoxide flow pressure 20 μ Hg.

Voltage	I_2 Carbon present (mA.)	I_1 Carbon absent (mA.)	$\frac{I_1}{I_2}$
20.0	120 ± 20	1.3 ± 0.1	0.011 ± 0.002
25.0	(300 ± 100)*	7.5 ± 0.5	0.025 ± 0.010
27.0 initial	750 ± 50	22 ± 1	0.029 ± 0.002
27.0 final	750 ± 50	280 ± 30	0.37 ± 0.03
30.0	400 ± 50	120 ± 40	0.30 ± 0.08

* The value of the current obtained at 25.0 volts in the presence of carbon is an assumed one based on currents obtained in the spectroscopic studies.

Table 11

Analysis of spectrum obtained with flowing CO (figure 17b)

Wavelength(A°)	I	Identification
2977.4	1	CO 3rd positive
3125.7	6	Hg line
3131.6	6	Hg line
3134.4	2	CO 3rd positive
3159.3	6	N_2 2nd positive
3246.9	1	CO_2
3253.9	1	CO_2
3264.6	1	CO_2
3269.9	1	CO_2
3284.3	1	CO_2
3305.7	3	CO 3rd positive
3341.4	1	Hg line
3371.3	10	N_2 2nd positive
3377.5	1	CO_2
3413.3	5	CO^+ comet-tail
3427.9	5	CO^+ comet-tail
3495.3	2	CO 3rd positive
3505.2	1	CO_2
3510.8	1	CO_2
3536.7	7	N_2 2nd positive
3545.9	2	CO_2
3576.9	10	N_2 2nd positive
3584.2	10	CO^+ comet-tail
3600.8	10	CO^+ comet-tail
3650.2	10	Hg line
3654.8	3	Hg line
3662.9	3	Hg line
3674.1	1	CO_2
3691.8	1	CO_2
3688.1	4	CO^+ comet-tail
3705.3	4	CO^+ comet-tail
3755.4	2	N_2 2nd positive
3777.8	10	CO^+ comet-tail
3795.8	10	CO^+ comet-tail
3804.9	10	N_2 2nd positive
3888.6	2	CO^+ comet-tail
3908.0	2	CO^+ comet-tail
3914.4	10	N_2^+ 1st negative
3997.3	10	CO^+ comet-tail
4017.7	10	CO^+ comet-tail
4046.6	5	Hg line
4077.8	3	Hg line
4108.1	1	Hg line
4123.6	8	CO Angstrom
4174.6	5	CO triplet
4188.4	3	CO triplet
4201.5	3	CO triplet
4227.2	3	CO triplet
4248.9	10	CO^+ comet-tail
4272.0	10	CO^+ comet-tail
4314.1	5	CO triplet
4328.7	5	CO triplet
4343.8	5	CO triplet
4358.5	8	Hg line
4378.9	4	CO^+ comet-tail
4403.3	4	CO^+ comet-tail
4444.7	1	CO triplet
4452.2	1	CO triplet

Table 11 (contd.)

Wavelength(A°)	I	Identification	Wavelength(A°)	I	Identification
4462.9	1	CO triplet	4917.2	2	Hg line
4478.8	1	CO triplet	4935.5	1	CO triplet
4510.9	10	CO Angstrom	4959.0	1	CO triplet
4524.0	5	CO triplet	4979.0	1	CO triplet
4539.4	8	CO^+ comet-tail	4996.7	1	CO triplet
4565.3	8	CO^+ comet-tail	5039.7	6	CO^+ comet-tail
4602.6	1	CO triplet	5072.1	6	CO^+ comet-tail
4683.4	6	CO^+ comet-tail	5198.2	6	CO Angstrom
4711.2	6	CO^+ comet-tail	5216.0	1	CO triplet
4747.5	2	CO triplet	5238.4	1	CO triplet
4764.8	2	CO triplet	5258.3	1	CO triplet
4787.0	5	CO triplet	5330.5	1	CO triplet
4806.7	2	CO triplet	5351.2	1	CO triplet
4835.3	8	CO Angstrom	5460.7	8	Hg line
4869.3	1	CO triplet	5461.4	3	CO^+ comet-tail
4879.5	2	CO^+ comet-tail	5499.9	3	CO^+ comet-tail
4910.9	2	CO^+ comet-tail	5610.2	2	CO Angstrom

Table 12

Analysis of spectrum obtained with flowing CO_2 (figure 18b)

Wavelength(A^{o})	I	Identification	Wavelength(A^{o})	I	Identification
2977.4	2	CO 3rd positive	3600.8	7	CO^+ comet-tail
3125.7	2	Hg line	3650.2	10	Hg line
3131.6	2	Hg line	3654.8	1	Hg line
3134.4	3	CO 3rd positive	3661.6	2	CO_2
3136.7	1	CO_2	3662.9	2	CO_2
3149.5	2	CO_2	3674.1	2	CO_2
3155.2	2	CO_2	3688.1	3	CO^+ comet-tail
3164.9	1	CO_2	3705.3	3	CO^+ comet-tail
3246.9	4	CO_2	3761.4	1	CO_2
3253.9	4	CO_2	3777.8	8	CO^+ comet-tail
3264.6	4	CO_2	3795.8	8	CO^+ comet-tail
3269.9	3	CO_2	3858.8	1	CO_2
3284.3	2	CO_2	3853.2	1	CO_2
3305.7	6	CO 3rd positive	3870.5	1	CO_2
3370.0	6	CO_2	3890.4	2	CO_2
3377.5	6	CO_2	3888.6	7	CO^+ comet-tail
3388.9	2	CO_2	3908.0	7	CO^+ comet-tail
3394.5	2	CO_2	3997.3	6	CO^+ comet-tail
3413.3	3	CO^+ comet-tail	4017.7	6	CO^+ comet-tail
3427.9	3	CO^+ comet-tail	4036.4	5	CO triplet
3493.3	5	CO 3rd positive	4046.5	5	Hg line
3503.2	4	CO_2	4077.8	4	Hg line
3510.8	4	CO_2	4108.1	4	Hg line
3533.8	4	CO_2	4123.6	5	CO Angstrom
3545.9	4	CO_2	4157	2	CO triplet
3551.4	3	CO_2	4174.6	3	CO triplet
3562.2	3	CO_2	4182.6	3	CO triplet
3565.5	3	CO_2	4201.5	5	CO triplet
3584.2	7	CO^+ comet-tail	4227.2	2	CO triplet

Table 12 (contd.)

Wavelength(A°)	I	Identification
4248.9	6	CO^+ comet-tail
4272.0	6	CO^+ comet-tail
4314.1	3	CO triplet
4328.7	3	CO triplet
4343.8	3	CO triplet
4358.3	4	Hg line
4378.9	2	CO^+ comet-tail
4393.1	2	CO Angstrom
4403.3	5	CO^+ comet-tail
4510.9	6	CO Angstrom
4518.0	4	CO^+ comet-tail
4539.4	3	CO^+ comet-tail
4565.8	3	CO^+ comet-tail
4571.0	2	CO triplet
4586.4	1	CO triplet
4602.6	1	CO triplet
4646.7	1	CO triplet
4680.3	2	CO triplet
4683.4	2	CO^+ comet-tail
4711.2	2	CO^+ comet-tail
4747.5	2	CO triplet
4764.8	2	CO triplet
4806.7	2	CO triplet
4835.3	10	CO Angstrom
4897.5	1	CO triplet
4917.2	1	CO triplet
4935.5	1	CO triplet
4959.0	1	CO triplet
4979.0	1	CO triplet
4996.9	1	CO triplet
5039.7	3	CO^+ comet-tail
5072.9	3	CO^+ comet-tail
5198.4	10	CO Angstrom
5460.7	7	Hg line

Table 13

Static charges of CO_2 - carbon-14 on silica

Anode and carbon at same potential

Cell background 30 ± 3 c.p.m.

Run	CO_2 Pressure (μ Hg)	Average Current (mA)	Time (mins)	mA.mins.	CO_2 Pressure (μ Hg)	CO Pressure (μ Hg)	Carbon-14 Activity (c.p.m.)
a) Anode and carbon at same potential as filament							
113	58	-	1.00	-	39	10 20%	128
115	58	-	1.00	-	43	7 14%	160
116	57	-	1.00	-	52	6	59
118	98	-	1.00	-	75	9 10%	42
120	68	-	1.00	-	57	8	55
121	65	-	5.00	-	41	15 27%	59
126	60	-	1.00	-	48	9	61
127	72	-	1.00	-	65	4	53
140	58	-	10.00	-	56	4 7%	53
b) Anode and carbon at +15 volts.							
122	62	0.77	3.00	2.3	42	13	88
123	62	0.77	5.00	3.9	43	12	70
132	67	0.46	10.00	4.6	41	19	172
133	64	0.15	17.00	2.6	40	12	85
134	68	0.21	20.00	4.2	61	11	228
135	59	0.22	20.00	4.4	48	8	148
c) Anode and carbon at +20 volts.							
105	58	4.2	2.00	8.3	36	15	166
106	60	6.8	1.00	6.8	35	15 30%	122
107	59	7.8	2.00	15.5	27	26 47%	357
108	59	17.5	0.83	14.6	31	24	340
109	64	3.8	1.50	5.7	41	13	411
112	57	40.3	0.55	24.3	25	25	692
119	66	25.3	0.50	12.7	44	18	251
124	60	11.0	1.83	20.1	30	36 55%	457

Table 14

Static charges of CO_2 - carbon-14 on silica

Carbon-14 removed from vicinity of filament

Anode voltage +20 volts

Cell background 30 ± 3 c.p.m.

Run	CO_2 Pressure (μ Hg)	Average Current (mA.)	Time (mins)	mA.mins.	CO_2 Pressure (μ Hg)	CO Pressure (μ Hg)	Carbon-14 Activity (c.p.m.)
141-1	66	0.41	2.00	0.8	51	9	34
142-1	64	0.98	2.00	2.0	51	6	29
143-1	61	0.97	5.00	4.9	50	12	29
144-1	64	1.20	10.00	12.0	46	13	37
145-2	64	1.16	5.00	5.8	49	9	35
146-2	63	1.14	10.00	11.4	49	11	41
148-3	60	33.5	1.00	33.5	21	38	43
149-4	60	81.7	1.00	81.7	17	64	42
150-3	30	87.3	1.00	87.3	8	50	48

The suffix on the run number denotes the condition of the carbon-14 sample as follows :

-1 carbon-14 at the same potential as the filament.

-2 carbon-14 at the same potential as the anode.

-3 carbon-14 at the same potential as the anode;
carbon soot deposited on the anode.

-4 carbon-14 at -6 volts w.r.t. anode;
carbon soot deposited on the anode.

Table 15

Static charges of CO_2 - carbon-14 on silica

Effect of surface condition on rate of carbon-14 gasification.

Anode voltage +20 volts.

Carbon at same potential as the filament.

Run	CO_2 Pressure (µ Hg)	Average Current (mA.)	Time (mins)	mA.mins.	CO_2 Pressure (µ Hg)	CO Pressure (µ Hg)	Carbon-14 Activity (c.p.m.)	$\frac{\text{c.p.m.}}{\text{mA.mins.}}$
167	61	160	1.00	160	9	96	1531	9.6
168	60	113	1.50	169	20	75	484	2.9
169	60	105	1.50	157	21	79	380	2.4
170	66	92	1.50	138	22	86	266	1.9
171	53	89	1.50	133	16	69	308	2.3
Stood in 26 mm Hg CO_2 for 17 hours.								
172	55	75	2.00	149	17	81	477	3.2
173	59	109	1.50	163	20	76	404	2.5
Stood in 760 mm Hg O_2 for 60 hours.								
174	61	49	3.00	147	40	95	191	1.3
175	64	122	1.00	122	43	50	230	1.9
176	59	52	3.00	156	17	81	541	3.5

Table 16

Flow system of CO_2 - carbon-14 on silica

Effect of electrical condition of carbon on the reaction rate.

Anode voltage +25 volts. Reaction times = 4.0 minutes.

Run	Flow Pressure (μ Hg)	Average Current (mA.)	CO_2 Pressure (μ Hg)	CO Pressure (μ Hg)	Carbon-14 Activity (c.p.m.)
a) Carbon-14 at the same potential as the anode (+25 v.)					
239	65	10.2	40	20	811
240	60	9.1	41	17	767
241	61	4.5	48	11	503
242	65	6.8	45	11	522
244	68	6.3	59	9	726
245	62	3.9	56	6	400
246	62	5.4	53	8	580
247	62	7.5	56	9	554
249	64	8.9	57	9	805
251	64	7.0	57	8	521
255	63	5.3	52	6	443
258	62	5.0	55	6	418
b) Carbon-14 at the same potential as the cathode (earthed)					
256	68	4.1	60	5	137
257	62	2.9	60	4	112
260	60	5.9	53	7	190
261	61	6.0	56	6	154
c) Carbon-14 electrically isolated from the anode and cathode					
248	63	4.5	54	7	201
250	63	3.8	58	5.5	196
252	61	5.8	56	7	187
253	62	8.2	54	7	392
254	62	6.3	50	7	316
d) Anode and carbon-14 at same potential as the cathode (thermal effect)					
243	63	0.0	55	5	96
259	63	0.0	59	3	113

Table 17

Flow system of CO_2 - carbon-14 on silica

Distribution of carbon-14 in the gas phase.

Anode and carbon-14 at +25 volts. Reaction times = 4.0 minutes.

Run	Flow Pressure (μ Hg)	Average Current (mA.)	CO_2 Pressure (μ Hg)	CO Pressure (μ Hg)	CO_2 Activity (c.p.m.)	Total Activity (c.p.m.)	$\frac{{}^{14}CO_2}{{}^{14}CO+{}^{14}CO_2}$
266	64	49.4	41	24	522	773	0.68
267	63	39.3	45	16	393	492	0.80
268	63	31.7	49	12	286	334	0.85
269	65	91.6	36	25	407	604	0.67
270	63	63.4	47	14	262	322	0.81
271	63	54.3	44	13	197	224	0.88

Table 18

Flow system of CO_2 Carbon-14 on molybdenum

Voltage applied to molybdenum only. Reaction times 2.0 mins.

Reaction rate as function of electron energy.

Run	Applied Voltage (volts)	Average Current (mA.)	Flow Pressure (μ Hg)	Carbon-14 Activity (c.p.m.)	$\frac{C_v - C_o}{\bar{I}}$
347	0	0	51	113	
348	0	0	54	98	
349	15	12.1	53	226	11.2 ± 0.5
350	0	0	52	92	
351	12	3.2	53	127	11.5 ± 0.6
352	0	0	52	110	
353	12	3.4	54	130	9.7 ± 1.5
354	0	0	52	89	
355	12	1.6	53	106	10.0 ± 2.5
356	0	0	55	91	
357	0	0	53	109	
358	0	0	52	95	
359	0	0	52	81	
360	12	2.1	52	107	11.9 ± 1.9
361	0	0	52	85	
362	10	0.55	52	76	--
363	0	0	52	79	
364	15	15.0	54	207	9.1 ± 0.3
365	0	0	52	76	
366	14	3.9	53	109	8.8 ± 1.2
367	0	0	53	73	
368	20	64.2	54	1064	15.4 ± 0.2
369	0	0	52	87	

Table 18 (contd.)

Run	Applied Voltage (volts)	Average Current (mA.)	Flow Pressure (μ Hg)	Carbon-14 Activity (c.p.m.)	$\frac{C_v - C_o}{\bar{I}}$
370	20	11.5	53	253	14.4 ± 0.4
371	0	0	52	87	
372	18	11.7	54	237	12.8 ± 0.4
373	0	0	52	71	
374	22	15.7	54	297	14.4 ± 0.4
375	0	0	52	70	
376	16	4.8	54	125	11.5 ± 1.1
377	0	0	54	72	
378	21	10.0	53	214	14.2 ± 0.5
379	0	0	53	73	
380	19	14.3	52	263	13.3 ± 0.4
381	0	0	52	68	
382	14	3.5	53	108	11.4 ± 1.1
383	0	0	52	70	
384	24	10.5	52	222	14.5 ± 0.5
385	0	0	52	62	
386	17	5.2	52	143	15.6 ± 0.8
387	0	0	52	57	
388	20	5.8	52	162	18.1 ± 1.0
389	0	0	53	59	
390	14	3.6	51	106	13.1 ± 1.0

APPENDIX B

Rate of reaction $CO_2 = CO + O$ on striking the heated filament.

From the kinetic theory, the number of gas molecules striking unit area in unit time is equal to $\frac{\bar{c}\, n}{4}$

where $\bar{c}$ = mean molecular velocity = $0.921 \sqrt{\overline{c^2}}$

n = number of molecules per unit volume

At 60 μ Hg. $n = 2.13 \times 10^{15}$ cms.$^{-3}$

At 0° C. $\sqrt{\overline{c^2}} = 3.96 \times 10^{4}$ cms. sec.$^{-1}$ for CO_2

Area of the filament = 2.0 cms.^{2}

Therefore, the no. of CO_2 molecules striking filament per second

$$= \frac{2 \times 2.13 \times 0.921 \times 3.96}{4} \times 10^{19}$$

$$= \underline{3.88 \times 10^{19} \text{ sec.}^{-1}}$$

The probability of the reaction $CO_2 = CO + O$ taking place when the molecule strikes the filament may be approximated to the value of the ratio $\frac{p_o}{p_{co_2}}$, where the values of the partial pressures are obtained from the equilibrium constant equation

$$\Delta F = -RT \log. K_p$$

Now $K_p = \frac{p_o \times p_{co}}{p_{co_2}} = \frac{p_o^2}{p_{co_2}}$ (pressures in ats.)

or, $p_o = \sqrt{760 \times 10^{-3} \times p_{co_2} \times K_p}$ (pressures in μHg.)

At 1300° C. $K_p = 3.27 \times 10^{-14}$

Therefore, when $p_{co_2} = 60$ μ Hg. , $p_o = 1.22 \times 10^{-3}$ μ Hg.

Hence the reaction probability = 2×10^{-5}

Using this value for the reaction probability the rate of decomposition of CO_2 molecules will be equal to 7.76×10^{14} sec.$^{-1}$

If we assume the reaction vessel to have a volume of 2 litres the rate of pressure decrease will be 0.73 μ Hg. min^{-1}

This is of the same order of magnitude as that encountered experimentally of 1.8 μ Hg. min^{-1} To this approximate calculation the following corrections may be made:

1) The r.m.s. velocity of the CO_2 molecules in the region of the filament will be that due to a temperature in excess of 0° C. and may be close to the temperature of the filament of 1000° C. .

2) The method of calculating the reaction probability used here is almost certainly at fault. However, the value obtained of 2×10^{-5} is close to that of 10^{-4} quoted by K. Laidler (The Chemical Kinetics of Excited States) for the transmission co-efficient of the reaction $CO(\,^1\Sigma) + O(\,^3P\,) = CO_2(\,^1\Sigma)$.

APPENDIX C -- REFERENCES

1. H.D.Smyth and E.C.G.Stueckelberg Phys. Rev. 36 472 (1930)
2. T.Kambara Proc. Phys. Soc. Japan 2 158 (1947)
3. R.E.Honig J. Chem. Phys. 16 105 (1948)
4. J.D.Morrison J. Chem. Phys. 19 1305 (1951)
5. J.L.Franklin and H.E.Lumpkin J. Am. Chem. Soc. 74 1023 (1952)
6. H.Wainfan,P.Walker and G.Weissler Phys. Rev. 99 542 (1955)
7. G.L.Weissler et al. J. Opt. Soc. Am. 49 338 (1959)
8. W.C.Price and Simpson Proc. Roy. Soc. 169A 501 (1938)
9. H.Sun and G.L.Weissler J. Chem. Phys. 23 1625 (1955)
10. Y.Tanaka,A.Jursa and F.le Blanc J Chem. Phys. 32 1199 (1960)
11. R.S.Mulliken J. Chem. Phys. 3 720 (1935)
12. H.Kallmann and B.Rosen Zeit. f. Phys. 58 52 (1929)
13. Hayawaka and Suguira T.Bull.Naniwa Univ. 3A 193 (1955)
14. J.C.Lorquet J. Chim. Phys. 57 1078 (1960)
15. S.Leifson J. Astrophys. 63 82 (1926)
16. T. Lyman Ultraviolettspektroscopie
17. A.Bonhoeffer and P.Harteck Grundlagen der Photochemie (1935)
18. A.G.Gaydon Spectroscopy and Combustion Theory p.190
19. E.Inn,K.Watanabe and M.Zelikoff J. Chem. Phys. 21 1648 (1953)
20. I.F.Weekes Third Symposium on Combustion p.520 (1949)
21. K.Wilde,B.Zwolinski and R.Parlin J. Am. Chem. Soc. 79 1323 (1957)
22. R.S.Mulliken J. Chem. Phys. 3 720 (1935)
23. T.Frabbes,F.Dell and S.Zlatarich J. Chem. Phys. 38 1939 (1963)
24. W.Groth Z. physik Chem. (Leipzig) B37 307 (1937)
25. H. Jucker and E.K.Rideal J. Chem. Soc. 1058 (1957)
26. B.Mahan J. Chem. Phys. 33 959 (1960)

27. J.O.Hirschfelder and H.S.Taylor J. Chem. Phys. 6 783 (1938)

28. P.Harteck and S.Dondes J. Chem. Phys. 23 902 (1955)

29. P.Harteck and S.Dondes J. Chem. Phys. 26 1734 (1957)

30. J.Sutton,M.Faraggi and M. Schmidt J. Chim. Phys. 57 643 (1960)

31. D.A.Dominey and T.F.Palmer Disc. Faraday Soc. 36 35 (1963)

32a) M.Anbar 2nd. Int. Conf. on Radiation Research (1962)

32b) P.Warneck J. Chem. Phys. 41 3435 (1964)

33. H.D.Hagstrum and J.K.Tate Phys. Rev. 59 354 (1941)

34. H.D.Hagstrum J. Chem. Phys. 23 1178 (1955)

35. C.R.Lagergren Dissertation Abstracts 16 770 (1956)

36. M.A.Fineman and A.W.Petrocelli J. Chem. Phys. 36 25 (1962)

37. A.G.Gaydon Dissociation Energies (Chapman Hall 1953)

38. L.M.Branscomb and S.J.Smith Phys. Rev. 98 1127 (1955)

39. H.D.Hagstrum J. Chem. Phys. 23 1178 (1958)

40. A.I.Cameron and R. Ramsey J. Chem. Soc. 93 966 (1908)

41. S.C.Lind and D.C.Bardwell J. Am. Chem. Soc. 47 2675 (1925)

42. W.R.Marsh and J.Wright AERE R4198 (1964)

43. A.R.Anderson et al. Proc. 2nd. U.N. International Conference on the Peaceful Uses of Atomic Energy - Volume 7,335-373 (1958)

44. J.Wright Proceedings of the US/UK meeting on the compatibility problems of gas-cooled reactors 1 148 (1960)

45. J.Wright AERE R.Chem.R.C/P65(1963)

46. P.C.Davidge and R.C.Marsh AERE R3706 (1961)

47. T.B.Copestake and N.S.Corney as reference 44 - page 76

48. M.Tomlinson and F.A.Walker AERE R3669 (1961)

49. H.E.F.Gow and W.R.Marsh AERE R3194 (1960)

50. F.S.Feates and R.J.Waites quoted in reference 45 page 50

51. R.S.Sach AERE R5721 (1961)

52. J.Wright reference 45 page 71

53a. K.T.Claxton Ph.D. Thesis - University of London (1962)

b. K.T.Claxton and R.F.Strickland-Constable Carbon 1 495 (1964)

54. G.Herrmann and O.Krieg Annalen der Physik 4 441 (1949)

55. A.Caress and E.K.Rideal Proc. Roy. Soc. 120A 370 (1928)

56. J.Bromley and R.F.Strickland-Constable Trans.Far.Soc. 56 1492 (1960)

57. R.W.B.Pearse and A.G.Gaydon The Identification of Molecular Spectra

58. S.C.Brown and W.W.Miller Rev. Sci. Inst. 18 496 (1947)

59. W.W.Miller Science 105 123 (1947)

60. D.G.Madley and R.F.Strickland-Constable The Analyst 78 122 (1953)

61. M.L.Eidinoff Analytical Chemistry 22 529 (1950)

62. D.R.Stranks J. Sci. Inst. 33 1 (1956)

63. P.S.Rudolph and S.C.Lind J. Chem. Phys. 33 705 (1960)

64. F.S.Feates and R.S.Sach Proc. 2nd. Industrial Carbon and Graphite Conference (1965)